# Understanding Microencapsulation and Performance of Composition-Equivalent PLGA Microspheres for 1-Month Controlled Release of Leuprolide

by

Jia Zhou

A dissertation submitted in partial fulfillment
of the requirements for the degree of
Doctor of Philosophy
(Pharmaceutical Sciences)
in the University of Michigan
2019

Doctoral Committee:

Professor Steven P. Schwendeman, Chair
Professor Gordon L. Amidon
Research Professor Gregory E. Amidon
Professor Zhan Chen

Jia Zhou

zhoujia@umich.edu

ORCID iD:  0000-0001-7168-5690

## DEDICATION

This dissertation is dedicated to my parents with my love.

## ACKNOWLEDGEMENTS

First, I would like to thank my advisor, Dr. Steven P. Schwendeman for his scientific guidance, financial support, and continuous encouragement. Since I joined his lab five years ago, he has encouraged me to develop critical thinking skills and leadership skills in research, which would be vital for my career development. I would also like to thank the rest of my dissertation committee, Dr. Gordon Amidon, Dr. Gregory Amidon, and Dr. Zhan Chen for their expertise and suggestions during my research. I am also thankful to Dr. Anna Schwendeman for her advice and insights.

I would to express my deepest gratitude to my parents. I appreciate their love and encouragement along the way. I know they will always stand with me with endless support and understanding. Having the love of my family made this accomplishment possible.

Next, I would like to thank FDA for the support of the research in the last three years. I am grateful to the ORS team, especially Dr. Yan Wang and Dr. Xiaohui (Jeff) Jiang, for their scientific inputs and guidance on the project. It was a unique and wonderful experience to work on a project with FDA.

I feel lucky to work in a great lab with such amazing lab members. I would like to thank Dr. Keiji Hirota for his collaboration and contribution in the project related to this dissertation. A special thank you to Karl Olsen for his help in and out of lab, kindness and continuous support. And to Rose Ackermann for the technical guidance. I would also like to thank Jenna Walker for her important contributions to the whole project, Dr. Nianqiu Shi for his help on the sampling,

Justin Hong for his help on taking SEM figures and Richard Schutzman for his help on the data analysis. To the current and former graduate students and post docs of Schwendeman group, thank you for giving me a great working environment that I will miss a lot: Dr. Morgan Giles, Dr. Amy Doty, Dr. Rae Sung Chang, Jason Albert, Dr. Avital Beig, Dr. Gergely Lautner, Sang Kim, Emily Morin and the rest of Anna lab members.

Finally, I would like to thank all my friends for being by my side during this journey. The experience in Ann Arbor is so memorable and enjoyable.

Go Blue!

## TABLE OF CONTENTS

## LIST OF TABLES

## LIST OF FIGURES

## ABSTRACT

Poly(lactic-co-glycolic acid) (PLGA) microspheres are the most commonly used and commercially successful long-acting release depots (LARs) for delivery of peptide drugs. However, the approval of generic versions of these products are slow. Due to the complexity of the manufacturing process, concerns about bioequivalence of generic complex drug products have been raised by the U.S. Food and Drug Administration (FDA). In order to address these challenges, this work aims to help fill in the knowledge gap between: (a) raw materials and manufacturing parameters, (b) critical quality attributes, and (c) release performance and mechanisms for PLGA LARs encapsulating the model drug, leuprolide.

The 1-month Lupron Depot® (LD) encapsulating water-soluble leuprolide in PLGA microspheres is the first injectable microsphere product launched in the US market. It is also a benchmark product upon which modern LAR products are often compared. Here, we describe the reverse engineering of the LD composition and important product attributes. Analyzed contents of the formulation and the determined PLGA characteristics matched well with the official values stated in the package insert and those found in the literature, respectively. The gelatin was identified as type B consistent with ~ 300 bloom. The 11-μm volume-median microspheres in the LD displayed very low content of residual moisture (< 0.5%) and methylene chloride (< 1 ppm).

Composition-equivalent PLGA microsphere formulations to the LD were prepared as a function of raw material and manufacturing variables. The following variables were adjusted at

constant theoretical loading of 16.4% leuprolide: polymer supplier/ polymerization type, gelatin supplier/ bloom number, polymer concentration, 1st homogenization speed and time, volume of primary water phase, 2nd homogenization time, volume of secondary water phase and stirring rate. The encapsulation efficiency (EE) of gelatin (101 ± 1%) was observed to be higher than the EE of leuprolide (42%- 63%). Desirable conditions of polymer concentration, homogenization time and volume of secondary water phase were critical to achieving high EE of leuprolide. The prepared formulations displayed a larger median particle size, a more porous surface, and higher residual solvents compared to the LD. The microspheres prepared with the identified LD raw materials possessed the same glass transition temperature as the LD. The leuprolide release kinetics of the formulations were also highly similar to the LD exhibiting zero-order kinetics after a ~20% initial burst release and displayed the same release versus mass loss kinetics.

The correlations between the process variables and emulsion size were established. The dimensionless Sauter mean diameter of primary emulsion droplet was proportional to the product of key dimensionless groups raised to appropriate power indices. A new dimensionless group (total surface energy/total energy input to fluid) was used to rationalize insertion of a proportionate time dependence in the scaling of the Sauter mean diameter. The increased viscosity of primary emulsion inhibited drug loss during microencapsulation while increased droplet size enhanced drug leakage to outer water phase. The Sauter mean diameter of secondary emulsion was also found proportional to the product of three dimensionless groups raised to appropriate power indices.

In summary, the rigorous approach of reverse engineering, characterization of composition-equivalent formulations and understanding of emulsion formation in the microencapsulation process described in this thesis could be useful for further development of

generic or new peptide loaded PLGA microspheres, and for guiding decisions on the influence of process variables on product physicochemical attributes and release performance.

# Chapter 1 Introduction

## 1.1 Poly(lactic-co-glycolic acid) (PLGA) formulations

### 1.1.1 Therapeutic proteins and peptides

Therapeutic peptides and proteins become promising drug candidates in clinical treatment and the market is growing rapidly [1–3]. However, the development and approval of protein/peptide-based formulations has been limited by the poor bioavailability of peptide by noninvasive administration routes, instability of proteins during long-term storage and short half-life of peptide in body circulation [4,5]. Efforts have been made to develop long-acting release (LAR) products to deliver peptide and protein continuously. The advantages of LAR products include increased stability and bioavailability, improved efficiency and enhanced patient compliance [4]. Most of the peptide formulations are delivered via invasive routes such as subcutaneous injections [4]. It is important and challenging to create safe and effective LAR formulations of peptides.

### 1.1.2 PLGA formulations for long-acting release

Polymer based LAR formulations have been widely used in peptide/protein delivery systems. Commonly used polymers include poly(lactic-co-glycolic acid) (PLGA) and poly(lactic acid) (PLA) [6,7]. PLGA represents the “gold standard” of biodegradable polymers [7] due to its well-known biocompatible/biodegradable properties and commercial availability. PLGA is the copolymer of monomers lactic acid (LA) and glycolic acid (GA) (Figure 1-1). When PLGA is exposed to aqueous environment, the degradation of PLGA initiates and hydrolyzes polymer

chains to the original monomers, LA and GA, both of which are the byproducts of a variety of metabolic pathways in body [8]. Therefore, PLGA is considered as biocompatible material *in vivo* in terms of the minimal systemic toxic degradation products after administration [9]. It has been widely studied in controlled release formulations and applied in several U.S. Food and Drug Administration (FDA)-approved products [6,10,11].

The polymers could be synthesized in two different ways: direct condensation (DC) of lactic and glycolic acids [12,13] and ring-opening (RO) polymerization of cyclic $_{D,L}$-lactide and glycolide [14,15]. The DC method produces PLGA, usually with low molecular weight [13,16], from acid monomers and can be performed in the absence of catalyst [13]. Those polymers are expected to contain more randomly distributed LA-GA, LA-LA and GA-GA bonds. The RO method produces polymers under mild conditions in the presence of a variety of catalysts [15] and most of the commercially available polymers are made by the RO method to readily obtain products with high molecular weight [17,18]. PLGA may contain small levels of residual monomers which may influence the *in vitro* release profile [19].

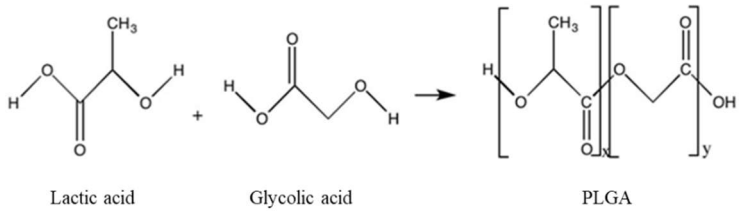


*Figure 1-1. Chemical structures of monomers and PLGA.*

### 1.1.3 Physicochemical properties and degradation of PLGA

The key physicochemical properties of PLGA (molecular weight, LA/GA ratio, polymer end-group, etc.) affect the crystallinity, capacity of water-uptake, and mechanical strength of the polymer and further determine the degradation rate of polymer [8,20] and release kinetics of drug from controlled release formulation [21,22]. Degradation of PLGA is the hydrolysis of its

ester linkages [23] leading to the decline of molecular weight of polymer and mass loss from polymer matrix [24]. The PLGA with higher molecular weight loses its mechanical strength slower than the one with lower molecular weight [24]. Polydispersity index (PDI) of the polymer is calculated by the ratio of weight average molecular weight (Mw) to number average molecular weight (Mn) describing the width of the molecular weight distribution. PLGA formulations with a lower PDI have shown a reduced initial burst release and sustained drug release [25]. Due to the stereochemistry of the asymmetric α-carbon atom, lactic acid has $_{D}$- and $_{L}$- form, and thus there are three different forms of polymer: poly($_{L}$-lactic acid), poly($_{D}$-lactic acid) and poly($_{D,L}$-lactic acid). All these forms may be applied in formulations [26] while $_{D,L}$-polymers are preferable because of the amorphous property and the fact that it helps facilitate a homogenous distribution of drug within the polymer matrix [27] and maintain the morphology of the product during storage [1]. The molar ratio of LA/GA determines the crystallinity, hydrolytic capacity and hydrolysis rate of PLGA [27]. Glycolic acid is more hydrophilic than lactic acid, and thus a higher content of GA facilitates the water uptake and increases the degradation rate of the polymer up to 50% GA content after which the polymer becomes crystalline [8]. The end-group of PLGA could be either free carboxylic acid or end-capped with esters and the latter form decreases the degradation rate of PLGA [24,28]. Glass transition temperature ($T_g$) of PLGA is generally reported to be higher than 37 °C [23,29] indicating the polymer is in the glassy state with rigid structure in nature and physiological conditions until hydration of the polymer. The $T_g$ is affected by the LA/GA ratio and Mw of the polymer and will be altered by the interaction between drug and polymer chains [1].

The cleavage of polymer chains takes place via erosion in two different ways: surface erosion and bulk erosion [30]. The rate of erosion and water penetration determine the type of

erosion [28]. If the rate of surface erosion is faster than the rate of water penetration, degradation proceeds from the surface of the polymer matrices and the interior polymers are assumed to be unchanged in dry state [7]. If the rate of water penetration is dominant, the cleavage will be initiated from the inside. The predominant form of erosion in PLGA is bulk erosion [28,31] because hydration is rapid and the hydrolysis of PLGA is faster than degradation products can leave the polymer [32].

## 1.2 **Microencapsulation methods for peptides/proteins**

Until 2016, there were fifteen PLGA/PLA based drug products in the US market and 11 of them were in microsphere dosage form [6]. The microsphere formulations are readily administered subcutaneously, intramuscularly or even orally [4,6,33]. Three methods mainly used to prepare PLGA microspheres include: double emulsion solvent evaporation, spray drying and phase separation-coacervation [7,11].

### 1.2.1 Solvent evaporation

Microencapsulation via solvent evaporation/extraction usually involves the formation of emulsions: single emulsion (e.g., oil-in-water (O/W) or oil-in-oil (O1/O2)), double emulsion (e.g., water-in-oil-in-water (W1/O/W2)) and solid-in-oil-in-water emulsion (S/O/W) [20,34]. Drug stability, solubility and solid-state properties determine the appropriate microencapsulation method to be used [20]. The critical steps for this method include formation of emulsion by two phases and solidification of microspheres by solvent removal [35].

Double emulsion solvent evaporation has the following steps: formation of the primary emulsion and secondary emulsion, and removal of organic solvent via appropriate process. To form the primary emulsion, an aqueous solution of hydrophilic drug is added to a solution of polymer dissolved in the water-immiscible organic solvent (e.g. methylene chloride (DCM)), and

then the mixture is emulsified by homogenizer, vortex or ultrasonication. DCM is the most commonly used solvent due to the high solubility for a wide range of polymers, immiscibility with water, low boiling point (~40 °C), high volatility and high evaporation rate [36]. Other solvents that could also be used include chloroform, ethyl acetate, and DCM-acetone [34]. The organic solvent used in the manufacturing process will affect the morphology, encapsulation efficiency and release profile of the prepared microspheres. Bilati *et al* [37] compared the effect of emulsification instruments on the particle size of emulsion. Simple benchtop vortex instruments produce coarse emulsion droplets with poor quality while sonication sharply decreases the droplet size even within a short time [37]. But ultrasonication may cause decline of the polymer molecular weight and accelerate the release kinetics [20]. To form the complex double emulsion system, an aqueous emulsifier is added to the primary emulsion. Polyvinyl alcohol (PVA) is the commonly used emulsifier to prevent aggregation of droplets. Then the double emulsion is transferred to an aqueous medium and stirred for hours to evaporate the solvent and harden the microspheres. The formed microspheres are washed by water to remove the excessive PVA solution/unloaded drug, and then lyophilized for storage. This method is applicable to temperature sensitive drugs. By carefully controlling the complex procedures, this method may produce microspheres with efficient encapsulation of water soluble drug with high yield [1,11]. But encapsulation efficiency of hydrophilic drug may be limited [7] due to the water-soluble drug leakage from polymer phase to the outer water phase [38].

### 1.2.2 Spray drying

Spray drying prepares microspheres by atomizing the emulsion into a stream of heated air, evaporating solvents and drying the particles in a short time. The first step is to create the atomization feed. It is usually a solution mixture of polymer and drug. For hydrophilic drugs, an

aqueous solution of drug is emulsified into the polymer dissolved organic solution to form a homogenous W/O emulsion. In some cases, temperature needs to be controlled to form a stable emulsion [39–41]. The second step consists of four phases [7,42,43]: a) atomization of liquid feed: the emulsion solution is transferred via a tubing at a certain speed into the atomizer. One of the most popular nozzles is two-fluid nozzle, which produces sprays by the disruptive action of a high velocity gas on a liquid stream at the exit of nozzle tip [44]; b) spray-air mixing: the sprayed droplets as well as the drying heated airflow enter the drying chamber. The mixing of air and atomized droplets allows for fast evaporation of the moisture [45]; c) solvent evaporation: the drying process involves heat transfer from the environment to the droplets and the mass transfer of vaporized moisture from droplets into the air [43]; d) dried particles separation: the particles will be collected by appropriate devices (e.g. cyclones). The air and the powder enter the cyclone tangentially, and the air will follow a strong vortex motion, forming a spiral pattern movement. It is hard for the particles with larger size or higher density to follow the air stream, so they will strike the glass wall and fall down into the collection vessel due to the centrifugal forces [43]. The obtained powder may have the similar residual moisture content as the particles attained by the lyophilization. The one-step process makes spray drying method easy to be scaled-up [46]. And due to the heated airflow in the drying, the residual organic solvents in the spray dried microspheres is lower than that in the particles made by solvent evaporation even without further drying processes [47].

The disadvantage of spray drying is the exposure of the materials to high temperature, which may cause the instability for heat-sensitive compounds. The denaturation and degradation of protein is time dependent process [48]. Although the temperature of inlet air flow is high, the contact time between sprayed droplets and the hot air is limited. When the droplets and airflow

pass through the chambers in the same direction, the heat will be absorbed by the droplets and the surface temperature will increase. However, the maximum temperature of the final particles theoretically will not beyond the outlet air temperature ($T_{out}$) [48]. And in practice, the actual temperature of the products is about 15 to 25 °C lower than the $T_{out}$ [49]. Therefore, it is feasible to apply the spray drying method to heat-sensitive agents, such as peptide and protein by careful temperature control. Other drawbacks of this method are unacceptable yield due to adhesion of the microspheres to the wall of the drying chamber and inability to atomize liquid with high viscosity. The example of marketed microspheres made by spray drying method is Suprecur® MP (long-acting biodegradable microparticles containing buserelin acetate).

### 1.2.3 Phase separation/Coacervation

The coacervation was introduced to pharmaceutical filed in 1960s [7] as a microencapsulation method by organic phase separation. The coacervation process consists of [50]: a) formation of W/O emulsion: dispersing hydrophilic drug aqueous solution into a polymer dissolved oil phase (e.g. DCM) to form W/O emulsion via suitable methods (e.g. homogenization and sonication); b) formation of coacervate: gradually adding coacervate agent (e.g. silicone oil) to induce phase separation; the DCM is extracted into the silicone oil phase and embryonic microspheres begin to precipitate; c) hardening: transferring the mixture into an incompatible medium (e.g. heptane) to harden the soft microspheres by removing the solvents; and d) rinsing, drying and particle collection: excess solvents will be removed and washed off by water. The microspheres are sieved, dried under suitable conditions. The PLGA works as the wall or coating polymer and the coacervate agent is regarded as a phase inducer. The phase separation is induced due to the incompatibility between the polymer and the coacervation agent [51]. The wall polymer need to deposit on the surface of the drug preferentially to achieve good

encapsulation [7]. The biggest problem in coacervation process is the agglomeration of microspheres. Parameters, such as stirring rate and temperature, need to be optimized to address this problem [8]. The example of marketed microspheres made by coacervation is Bydureon® (exenatide extended-release for injectable suspension) [50].

### 1.3 The effect of process variables on encapsulation by double emulsion solvent evaporation method

The procedures of solvent evaporation method are complicated and costly. The parameters need to be delicately controlled to ensure successful encapsulation of the drug [7]. Studies have been reported on the effect of key parameters on the formulation properties and release performance. *Polymer concentration* is one of the most critical encapsulation variables influencing emulsion viscosity, particle size, encapsulation efficiency (EE), hardening kinetics, porosity, and initial burst release [52]. Increasing the polymer concentration raises the viscosity of the organic phase and the difficulty to break up polymer solution to small droplets [53], which in turn, increases the particle size, i.e., the volume mean diameter of the microspheres [54–56] even though the number weight diameter may not be affected [56]. Meanwhile, concentrated polymer solution shortens the evaporation time of organic solvent [57], limiting the drug escape from the polymer matrix, thus increasing the EE of the drug [53,55]. Li *et al* [58] found decreasing the polymer concentration also decreased the homogeneity of drug distribution in the microspheres. When the polymer concentration is low, water tends to accumulate easily within the polymer matrix and form internal water pockets, and the microspheres are dried with bigger pores and higher internal porosity [55,56,58]. Increased viscosity of the organic phase also facilitates the formation of a compact polymer core [59], or tends to increase particle size

[53,56], reducing surface/volume ratio [55] and then decrease drug initial burst and even slow down the whole release process [53].

*W1/O phase volume ratio* is expected to influence EE, particle size, porosity, and initial burst. When the volume of primary water phase (W1) is increased (i.e., a high W1/O ratio), it causes coalescence of water droplets and a less stable primary emulsion [37], and the particle size of microspheres is increased [53,55,60]. Such an effect may become negligible when the volume of W1 is over a certain value [56]. Increasing the water volume in the primary emulsion results in larger pores within the polymer network structure and decreases the bulk density [53,56]. When the W1/O ratio is dramatically decreased, a smooth surface is observed in microspheres [57]. Explanations for this observation are: increased amount of DCM in the emulsion decreases the removal rate of organic solvent, and prevents the formation of porous skin by re-dissolving the formed pores [53]; and less water decreases the viscosity of emulsion and causes a faster water diffusion from inside to the outer water phase, finally leading to fewer pores on the surface [57]. The effect of W1/O ratio on the EE of drug is complex. On the one hand, lower W1/O ratio enables a good emulsification during the formation of primary emulsion, and such a delicate interface minimizes the drug loss during the secondary emulsification [57] and increases the EE [55,56]. On the other hand, a higher W1/O ratio produces larger microspheres with a higher EE of drug [37,60]. Since a higher W1/O ratio leads to a higher internal porosity of the microspheres, a higher initial burst is often observed in those formulations [53,55,56].

The homogenization condition to prepare the primary emulsion (*1$^{st}$ homogenization*) is critical to control the size of primary emulsion droplets, microsphere size, inner pore size distribution, and initial burst. Homogeneous and fine primary emulsion droplets with good

quality will inhibit the coalescence during the second emulsification and drug loss to the outer water phase, and finally result in higher EE [37]. Mao *et al* [55] found increasing 1st homogenization speed decreased internal porosity and significantly increased EE of drug in microspheres with slightly increased particle size and lower initial burst.

*O/W2 phase volume ratio* has been reported to affect particle size, solvent removal rate, porosity and release kinetics. When the second water phase volume is increased (low O/W2 ratio), there is faster solvent removal rate due to the sink condition facilitating dissolving DCM in the outer aqueous phase [58]. In this case, solidification of the outer region of the microspheres occurs quickly and a thick skin layer is formed, which impedes the solvent transfer and the solvent can be trapped inside. A higher residual solvent level will be detected in the formulation in this case [58]. When the ratio is controlled in an appropriate range, increased outer water phase volume reduces the emulsification efficiency and leads to increased particle size [55,60]. But when the water phase volume is too low, coalescence may happen due to the high concentration of particles [54]. Mao *et al* [55] observed slightly decreased internal porosity and increased initial burst due to the increased surface porosity when the volume of outer water phase was increased.

*Stir rate* has been shown to be a dominant factor that regulates the particle size [61]. When the mixing speed is increased, it will provide higher shear force [62] to break up the second emulsion into small droplets in the water phase and reduce the particle size of the microspheres [54,61,63]. The increased stirring rate may also give rise to more drug loss and low yield [63].

*Peptide/protein concentration/theoretical loading* is expected to have impact on porosity, EE and release kinetics. When the drug concentration is increased, the surface tension of the

primary emulsion is decreased, and bigger pores form in the microspheres. When theoretical drug loading is increased above a certain level, the EE might be reduced [61] due to the irregular shape and higher porosity of the microspheres prepared [64] and higher concentration gradient that causes more drug diffusion to outer water phase [55].

*Concentration of PVA solution* mainly affects particle size. PVA is the commonly used emulsifier during microencapsulation to prevent coalescence of soft droplets by decreasing the interfacial tension and steric hindrance of incoming droplets [65]. When the concentration of PVA is increased or the molecular weight of PVA is increased, it prevents the separation of nascent emulsion droplets and increases the particle size of the microspheres [55,66,67], and leads to the aggregation or coalescence of particles [68]. The PVA is produced by hydrolysis of polyvinyl acetate and the hydrolysis degree relates to the amount of hydroxyl groups in the polymer [69]. Biehn and Ernsberger [65] found the PVA with high viscosity and low degree of hydrolysis is optimal to increase the stability of emulsion.

### 1.4 **Initial burst release and release mechanism**

The drug release from PLGA microspheres follows a three-phase pattern including initial burst phase, lag-time and sustained release phase [70]. A phenomenon called “initial burst” is observed during the first 24 h of drug release, which is mainly due to the rapid release of loosely bounded drug from microspheres surface [70–72]. Wang *et al* [33] monitored the initial burst of octreotide loaded PLGA microspheres and provided other assumptions about the initial burst. The permeability of microspheres was found to continuously decrease during the first day of release and according to the level of permeability, three phases were proposed [33]: a) phase I (0-3 h): the initial release rate was high and sharply decreased after 30 min; the pore density at surface was increased; b) phase II (3-5.5 h): release rate increased gradually due to the increased

diffusion coefficient of peptide in the aqueous network; more drug was exposed to the pores and diffused from the pores inside microspheres; c) phase III (5.5-24 h): the surface porosity decreased; the release rate reduced gradually and approached zero at 24 h; a “skin” type structure was formed at the surface of the microspheres and the density was increased, which stopped the initial burst. The microspheres in this study was prepared by solvent evaporation method and the authors also indicated that the morphologies of microspheres prepared by other methods might be significantly different [33]. A lag time phase following the initial burst is often observed and it could be explained by the cessation of release after the closing of surface pores. During the lag period, water slowly penetrates the microspheres and the auto-catalysis takes place. Also the number of carboxylic acid end groups increases, lowering the pH in the microclimate [30,73]. These processes accelerate the erosion in polymer bulk, and then the drug release enters the third phase. The degradation products are accumulated in the microspheres. When the osmotic pressure inside the PLGA matrices reaches a threshold, the surface and bulk of the microspheres can be ruptured. The pore network allows for the release of monomers and oligomers [74]. Drug diffusion is also initiated and the peptide escapes from the microspheres via the aqueous channels [10]. Thus, the drug release rate is regulated by the rate of erosion and potentially rate of diffusion [10].

Multiple mechanisms are involved in the drug release from the microspheres including [75]: a) diffusion through pores: the water-soluble drugs could diffuse through the external pores and internal porous structures formed during the formation of microspheres and release to the external environment if the pore size is large enough and the pore network is continuous from drug phase to the surface of microspheres; polymer hydration will cause pore opening while polymer healing will close the pores; b) diffusion through polymer phase: polymer chains inside

of the microspheres forms a matrix barrier for drug release and the tortuosity will be reduced by the erosion and water uptake, creating less tortuous pathways for drug molecules [28]; c) osmotic pumping: water uptake upon exposure of microspheres to the release medium increases the osmotic pressure, creating new pores and driving the drug transport; d) erosion: degradation/erosion of polymer exposes the drug molecules to the surface of the microspheres [75,76]. Besides, the water absorption also causes a phenomenon called "swelling", which indicates the increased volume of microspheres and increased mobility of polymer chains. Meanwhile, the $T_g$ decreases, and the transition from glassy state to rubbery state takes place, which enhances the diffusion of drug within PLGA matrix [33,76].

### 1.5 **Lupron Depot®**

Leuprolide acetate is a nonapeptide with the amino acid sequence: 5-oxo-Pro-His-Trp-Ser-Tyr-D-Leu-Leu-Arg-Pro · acetate [77]. It is a synthetic analogue of gonadotrophin-releasing hormone (GnRH) (luteinizing hormone-releasing hormone (LH-RH)) and has higher affinity for GnRH receptors than the natural GnRH peptide [78]. So it is known as a super LH-RH agonist being able to inhibit the secretion of gonadotropin after continuous administration in therapeutics doses [2,78]. Leuprolide is usually used in the treatment for the hormone-dependent cancer or disorder, like breast and prostate cancer, endometriosis and uterine fibroids [78]. It has been a top LH-RH agonist holding a significant market share in the global peptide pharmaceutical market [79,80].

Leuprolide is orally inactive and usually administered subcutaneously or intramuscularly with a half-life of ~3-4 h [78,81]. Due to the inconvenience of frequent administration, efforts have been made on the development of PLGA/PLA based products for controlled release of leuprolide. Currently, such products available on US market include Lupron Depot, Lupron

Depot-PED, Lupron, Eligard and Lupaneta Pack [6]. Lupron Depot® (LD, leuprolide acetate for depot suspension) is a group of PLGA/PLA microsphere products loaded with leuprolide acetate for 1-, 3-, 4-, 6-month administration [82].

### 1.5.1 Features of PLGA in the formulation

From the patent and literature [83,84], we can assume the 1-month LD uses the PLGA produced by Wako Pure Chemical Industries, Ltd. (Tokyo, Japan) using direct condensation method. During the development of LD, the originator, Takeda Pharmaceutical Company Ltd. [54] analyzed the effect of some significant features of PLGA (e.g. Mw, LA/GA ratio, end-capping and residual water-soluble acid number) on the microencapsulation of leuprolide. In the 1-month depot formulation, PLGA (LA/GA ratio = 75/25) with average molecular weight of 14000 was selected to achieve a desirable release performance and stability [1]. A contributing mechanism (which will be discussed later) of high EE of leuprolide in these microspheres is believed to be the interactions between the carboxylic acid of PLGA and amino acid residues of peptide [1]. The employment of acid-end group PLGA provides a large number of acidic residues that promotes the ionic interactions.

### 1.5.2 Excipients

The 1-month LD microspheres encapsulate 10% of leuprolide and 1.7% of purified gelatin [77]. Gelatin was regarded as drug retaining substance [85] which may generate considerable viscosity and form a solid matrix [1]. The inventors claimed adding the gelatin significantly increased the EE of peptide [54]. However, it was later found that the cooling of the primary emulsion increased the viscosity of the emulsion, and the same high EE of peptide could be obtained even in the absence of gelatin [86]. So in describing the critical condition to achieve a high EE of leuprolide in microspheres the LD inventors stated: “unless there is an increase in

the inner phase viscosity, encapsulation efficiency will not be elevated even in the case of inner phase with higher concentration of gelatin" [54]. Gelatin was not used in 3,4 and 6- month Lupron Depot® [77] and removed from the 1-month product in Japan. D-Mannitol (15%) was added to the microspheres to prevent aggregation during lyophilization and storage [1].

### 1.5.3 Manufacturing procedures for LD product

Microencapsulation of leuprolide in LD was achieved by using a double emulsion solvent evaporation method invented and improved by Okada *et al* [54,85], Yamamoto *et al* [87], Kamei *et al* [88] and Igari *et al* [89]. Briefly, an aqueous solution containing leuprolide and gelatin was warmed to 60 to 70°C and emulsified in a DCM solution dissolving PLGA to form a W1/O emulsion, which was then cooled to 10 to 20 °C. This emulsion was emulsified in an aqueous PVA solution to form the W1/O/W2 emulsion. The secondary emulsion was stirred at room temperature to evaporate organic solvent. The solidified microspheres were dispersed in water and then centrifuged to wash off unloaded drug and PVA. D-mannitol powder was added to the recovered microspheres before lyophilization. The suspension was freeze-dried under reduced pressure to collect the microspheres powder [87–89].

### 1.5.4 Encapsulation mechanisms for LD microspheres

The basic amino acids (arginine and histidine) in the leuprolide interacted with the carboxylic acids of PLGA (pKa ~ 3.5) [90] during microencapsulation. The interaction has been proved by a chemical shift of arginyl and histidyl residues of leuprolide in the primary emulsion to lower magnetic field in NMR spectroscopy [91]. If the deprotonation of the polymer end group is disrupted by introducing acids to the water phase, the EE of peptide will be reduced due to the inhibition of the peptide-polymer interaction [1]. Okada *et al* [83] proposed a micelle-like structure for microspheres with leuprolide distributing throughout the polymer matrix and

forming a rigid drug core. The alkyl chains in the polymer formed a hydrophobic barrier that could prevent drug escape.

The release of leuprolide from LD is mainly controlled by the degradation of polymer [83]. When the leuprolide loading increased from 0 to 8%, the corresponding $T_g$ of the microspheres was also elevated [1,84], indicating increased leuprolide loading contributes to the ionic interaction. However, increasing water-soluble drug loading within the polymer phase will also give rise to more aqueous channels that limit high EE and accelerate initial burst [84]. Thus, the loading of leuprolide needs to be regulated to ensure a desirable EE and release behavior. For example, an appropriate loading of leuprolide in 3-month PLA microspheres was suggested to be 12% [84].

### 1.6 **Mechanistic understanding of microencapsulation**

As described in previous section (1.3), the manufacturing variables will affect the physicochemical properties and quality of emulsion, and subsequently regulate the attributes of microspheres. However, the current emulsion-based microencapsulation process is based on trial and error and has batch-to-batch variation and scale-up difficulties [92,93]. Quantitative experiments and correlations have been developed to improve the understanding of how the process variables influence the product attributes.

The formation of emulsion is the dispersion of two immiscible liquid phases. The key manufacturing parameters in the droplet formation include: style, geometry and process variables of mixing device [62,94] and physicochemical properties of dispersed phase and continuous phase [95,96]. The common mixing devices are impeller/static mixer, rotor-stator mixer and ultrasonicator [62]. The high-shear rotor-stator mixers have been widely used in the emulsification process. The rotor-stator mixer has a stator with the rotor rotating at high speed

inside. The stators usually have holes or slots where the fluid flows through. The relationships between the geometry, rotor speed, and the energy dissipation have been studied [94,97–100]. The first step is to link the energy dissipation rate to geometry and rotor speed [94]. For the dimensional analysis, Atiemo-Obeng [101] indicated that the definition of power number ($P_O$) and Reynolds number ($Re$) for rotor-stator mixer could be the same as those for conventional stirred tanks. The turbulent power could be described using the primary length scale, impeller (rotor) diameter. The power number ($P_O$) is

$$P_O = \frac{P}{\rho \omega^3 D^5} \tag{1-1}$$

where $P$ is the power, $\rho$ is the liquid density, $\omega$ is impeller speed and $D$ is rotor diameter. The Reynolds number is

$$Re = \frac{\rho \omega D^2}{\mu} = \frac{\omega D^2}{v} \tag{1-2}$$

where $\mu$ is the fluid dynamic viscosity. In the full turbulent regime ($Re$ is above ~$10^4$), the $P_O$ is constant of Reynolds number [94] but dependent on the geometry of rotor-stator, and in the range of 2 to 6 [101]. When impeller type and thickness, and turbulent flow conditions are assumed to be constant, $P_O$ becomes nearly constant [102]. The concept developed by Kolmogorov has been widely used to describe the turbulent eddies [95,103]. The Kolmogorov length scale ($\delta_K$) is expressed as:

$$\delta_K = (\frac{v^3}{\varepsilon})^{1/4} \tag{1-3}$$

where ε is the local energy dissipation rate per unit mass of fluid. For isotropic turbulence, ε could be expressed as the energy loss rate from mixer to the fluid divided by the mass of fluid ($\rho V$) [52,93]:

$$\varepsilon = \frac{\rho\omega^3 D^5 P_O}{\rho V} = \frac{\omega^3 D^5 P_O}{V} \tag{1-4}$$

Then the $\delta_K$ is:

$$\delta_K = \left(\frac{V\mu^3}{\omega^3 D^5 \rho^3 P_O}\right)^{1/4} \tag{1-5}$$

Droplet size ($d$) and viscosity ($\mu$) are the two key characteristic properties to describe the emulsion and these values have be reported to be correlated to [96,97,104–106]: continuous phase viscosity ($\mu_c$) and density ($\rho_c$), dispersed phase viscosity ($\mu_d$) and density ($\rho_d$), dispersed phase volume fraction (Φ), interfacial tension (σ), rotor speed ($\omega$), and mixing time/pass times ($t$). Sauter mean diameter ($d_{3,2}$) defined as the ratio of third and second moments of a particle size distribution, has been used to study the effect of processing variables on the physical properties of emulsion [95]. Based on the values of $\delta_K$, droplet size, and the viscosity of the solution, different correlations to predict mean particle size from dimensionless groups have been studied and summarized by Calabrese [92], Leng [107] and Hall *et al* [95,96]. Rotor stator mixers usually produce droplets with the diameter ($d$) the order of $\delta_K$ and smaller ($\delta_K > d$) [92], and if the stress on droplet is inertial, the following correlation exists [92]:

$$\frac{d_{3,2}}{D} \propto (WeRe)^{-\frac{1}{3}} \tag{1-6}$$

where $We$ is the Weber number and defined as

$$We = \rho\omega^2 D^3/\sigma \tag{1-7}$$

When $\delta_K >> d$, the correlations is [92]:

$$\frac{d_{3,2}}{D} \propto (WeRe^4)^{-\frac{1}{7}} \tag{1-8}$$

If the droplets are broken by turbulent viscous stress, the relationship becomes [92]:

$$\frac{d_{3,2}}{D} \propto (We^{-1}Re^{1/2}) \tag{1-9}$$

Hall *et al* [95] found that the rotor speed ($\omega$) and dispersed phase viscosity ($\mu_d$) have more significant influence on the droplet size compared to the other parameters (e.g., Φ and $\frac{\mu_d}{\mu_c}$) in an O/W emulsion prepared by in-line Silverson rotor-stator mixer. But when the $\mu_d$ is above a certain value, the droplet size is independent of the dispersed phase viscosity [95,108]. Pai [105] indicated that in the O/W system, the viscosity ratio ($\frac{\mu_d}{\mu_c}$) is usually high and deformation of droplets might not happen. Studies on the kinetics of droplet size during emulsification reported that the mean droplet size ($d$) is exponentially correlated with ultrasonication time [106,109,110] and a general equation to describe size decays as a function of time ($t$) is expressed as [106]:

$$d = y_0 + Ae^{\frac{(t-t_0)}{\tau}} \tag{1-10}$$

where $y_0$ is the saturation diameter, $\tau$ is the characteristic decay time, $t_0$ is the first time when a mean droplet size is detected, and the corresponding size value is ($y_0 + A$). Before time $t_0$, it is assumed that two immiscible phases are in a heterogeneous system [106].

The viscosity of a suspension of solid spheres could be predicted by Einstein equation [111,112]:

$$\frac{\mu}{\mu_c} = 1 + 2.5\Phi \tag{1-11}$$

Taylor [113] derived an equation for emulsions with small concentration of dispersed phase:

$$\frac{\mu}{\mu_c} = 1 + (\frac{\mu_c + 2.5\mu_d}{\mu_c + \mu_d})\Phi \tag{1-12}$$

Krieger and Dougherty [114] proposed an alternative empirical model for a high concentration of dispersed phase and when the Φ is low:

$$\frac{\mu}{\mu_c} = 1 + (\frac{\mu_d}{\mu_c} - 1)\Phi \quad (1\text{-}13)$$

## 1.7 **Research Scope and Impact**

PLGA LARs have gained commercial success and some of them could be good candidates serving as reference drugs for the generic product filing. However, complex and aseptic unit processes and specialized instrument could cause difficulties to scale up with low yields, and ultimately a high cost of goods. Changes in raw materials and manufacturing conditions may cause different attributes and release performance resulting in batch failure and/or changes to safety and efficacy. Studies are needed to fill in the knowledge gap between raw materials/manufacturing parameters and products attributes/release performance/mechanisms in composition-equivalent formulations. The resulting approach is expected to facilitate the development of new and generic peptide loaded microsphere products.

## 1.8 **Thesis Overview**

The preceding introduction discusses the difficulties that might impede the development of generic peptide loaded PLGA products and the key parameters involved in the solvent evaporation method. The one-month Lupron Depot® was selected as model drug product since it is a benchmark product upon which modern long-acting release products are often compared. Despite expiration of patent coverage, no generic product for the LD has been approved in the USA. The overall goal of this project is to understand how raw materials and variables in manufacturing processes will affect the attributes, release performance and mechanisms of composition-equivalent formulations relative to the Lupron Depot. Ultimately, the results described here could help on the development of new and generic peptide loaded microsphere

products and may offer an aid in FDA regulation development for generic drug of LARs in the future. This thesis consists of 5 chapters describing key concepts to address these concerns.

Chapter 2 describes reverse engineering of the 1-month Lupron Depot®. Analytical methods for analyzing the components of the LD, including its diluent, were developed, and the specific composition was identified and quantified. The results are consistent with the values reported in the drug label and literature. The gelatin was identified as Type B with Bloom 300. Attributes including particle size distribution, residual water and solvent levels, $T_g$, and in vitro release demonstrate the unique features of this product.

Chapter 3 focus on the development of composition-equivalent PLGA formulations for 1-month controlled release leuprolide as a function of manufacturing variables/raw materials. The effect of those variables on product attributes and release performance *in vitro* were studied. This section shows the composition, $T_g$, and in vitro release kinetics of the microspheres loaded with leuprolide can be largely replicated on the bench scale. The loading efficiency of leuprolide is lower than that of gelatin. Changes in initial burst release often mirrored changes in drug loading/encapsulation efficiency. Changing manufacturing variables centered at a standard formulation did not strongly affect release behavior *in vitro*.

Chapter 4 develops a mechanistic understanding of microencapsulation. Particularly, this section seeks to understand how to use the input manufacturing variables to predict characteristics of emulsion by mathematical correlations. Nondimensional correlations were established based on the literature, Buckingham Π theory and creation of a new dimensionless group (surface energy/energy input to fluid) to derive relationships between emulsion droplet size and manufacturing variables. The correlations between the process variables with emulsion viscosity and droplet size were identified and further linked to the results of EE in Chapter 3.

The conclusions of this research and potential future applications are discussed in Chapter 5. Chapter 2 was published in AAPS Journal in 2018. Chapters 3 and 4 are in preparation for publication.

# Chapter 2 Reverse engineering the 1-month Lupron Depot®[1]

## 2.1 **Abstract**

The 1-month Lupron Depot® (LD) encapsulating water-soluble leuprolide in poly(lactic-co-glycolic acid) (PLGA) microspheres is a benchmark product upon which modern long-acting release products are often compared. Despite expiration of patent coverage, no generic product for the LD has been approved in the USA, likely due to the complexity of components and manufacturing processes involved in the product. Here, we describe the reverse engineering of the LD composition and important product attributes. Specific attributes analyzed for microspheres were as follows: leuprolide content by three methods; gelatin content, type, and molecular weight distribution; PLGA content, lactic acid/glycolic acid ratio, and molecular weight distribution; mannitol content; *in vitro* drug release; residual solvent and moisture content; particle size distribution and morphology; and glass transition temperature. For the diluent, composition, viscosity, and specific gravity were analyzed. Analyzed contents of the formulation and the determined PLGA characteristics matched well with the official numbers stated in the package insert and those found in literature, respectively. The gelatin was identified as type B consistent with ~ 300 bloom. The 11-μm volume-median microspheres in the LD slowly released the drug *in vitro* in a zero-order manner after ~ 23% initial burst release. Very

[1] Adapted by permission from Springer Customer Service Centre GmbH: Springer Nature The AAPS Journal, Reverse Engineering the 1-Month Lupron Depot®, Jia Zhou, Keiji Hirota, Rose Ackermann, Jennifer Walker, Yan Wang, Stephanie Choi, Anna Schwendeman and Steven P. Schwendeman, 2018

low content of residual moisture (< 0.5%) and methylene chloride (< 1 ppm) in the product indicates in-water drying is capable of removing solvents to extremely low levels during manufacturing. The rigorous approach of reverse engineering described here may be useful for development of generic leuprolide-PLGA microspheres as well as other new and generic PLGA microsphere formulations.

## 2.2 **Introduction**

The 1-month Lupron Depot® (LD) is a poly(lactic-co-glycolic acid) (PLGA) microsphere product, which encapsulates and slowly releases leuprolide acetate, to reduce injection frequency relative to daily injections of soluble peptide for treatment of hormone-sensitive prostate cancer, breast cancer, endometriosis, and uterine fibroids [1,2]. Since its launch in the USA in 1989, the LD has become a benchmark product with which modern long-acting release (LAR) PLGA products are often compared. Annual market sales of LD in the USA was $580 million in 2014 [115], making it an attractive candidate for generic competition. Despite expiration of patent coverage, no generic product for the LD has been approved in the USA. Three- and six-month LD formulations are also commercialized, which are also of interest for generic development.

For injectable PLA/PLGA-based drug products, the proposed generic product should be qualitatively (Q1) and quantitatively (Q2) the same as the reference listed drug (RLD) to be considered for approval in an Abbreviated New Drug Application (ANDA) according to the 505(j) pathway [116]. The extensive list of ingredients of LD is expected to pose challenges to generic product development [1,77]. Referring to publications of LD and the package insert [77], the 7.5 mg LD for 1-month administration formulation is prefilled in a dual-chamber syringe for better usability. The powder filled in the front chamber (chamber 1) contains microspheres loaded with leuprolide and gelatin (7.5 mg leuprolide acetate, 1.3 mg gelatin and 66.2 mg

PLGA) and 13.2 mg D-mannitol. The injection diluent filled in the second chamber (chamber 2) is composed of 5 mg carboxymethylcellulose sodium (Na-CMC), 50 mg mannitol, 1 mg polysorbate 80, water for injection (USP), and glacial acetic acid to control pH (USP) [77]. Before administration, the microspheres will be mixed with the diluent thoroughly until a homogeneous suspension forms [77].

As an initial step in the generic drug development, the relevant analytical methods need to be established to determine the composition of the RLD. The characteristic properties of active and inactive ingredients are also of interest for the potential use in the selection of manufacturing materials for generic drug product development. For example, comprehensive characterization of PLGA is required in the generic application of polymer-based products [54]. The key properties of PLGA, including lactic acid/glycolic acid (LA/GA) ratio, molecular weight distribution and polymer end-group identity, all could affect the release mechanism and release rate of the drug from the microspheres. In addition, the PLGA synthesis method and presence or absence of specific catalyst could also potentially affect product performance. During the manufacturing process of microspheres, the PLGA polymer could potentially degrade resulting in changes in the formulated product, which may cause failure in an equivalence test. Another complex ingredient in the case of LD is gelatin. Gelatin was originally added to the leuprolide solution to increase encapsulation efficiency in the manufacturing of microspheres [54]. Later it was found that increasing the viscosity of the primary emulsion by cooling was the key step to achieve high encapsulation efficiency of leuprolide in the microspheres [1,86]. Gelatin is a mixture of proteins and peptides derived from collagen in animal tissues and bones. Gelatins are derived most commonly from bovine and porcine sources as type A or B, according to acid or

base hydrolysis, and possess a gel strength indicated by bloom number [117]. However, the specific gelatin product used in the LD formulation is not disclosed to the best of our knowledge.

We describe the reverse engineering of the 1-month LD injection system to (a) determine the identity and quantity of specific components of this formulation, (b) characterize key aspects of the formulation critical to performance of the product, and (c) establish chemical assays that are useful to accomplish the above. By improving our understanding of the LD, the barrier to increasing the number of PLGA products can be reduced, especially to those pursuing generic PLGA products for leuprolide.

## 2.3 **Materials and Methods**

### 2.3.1 Chemicals and Reagents

The 7.5 mg leuprolide dose for one-month administration Lupron Depot® (LD, AbbVie Inc., North Chicago, IL, USA) was employed for reverse engineering the product composition. The LD products were purchased from the pharmacy department at the University of Michigan Health System. Leuprolide acetate with purity more than 98% by high-performance liquid chromatography (HPLC) analysis was purchased from Soho-Yiming Pharmaceuticals Co. Ltd. (Shanghai, China). This leuprolide acetate was detected by UV absorbance at 280 nm of wavelength on ultra-performance liquid chromatography (UPLC) and confirmed to be within 100.55 ± 2.16 % (mean ± SEM, n=3) of the USP standard (USP 36 NF 31; catalog number: 1358503; lot: I0M442) in the range of 0-600 μg/mL. Gelatin products used in this paper include: type B gelatin derived from porcine skin with bloom number 300 (beMatrix™ Low Endotoxin Gelatin LS-W) and type B gelatin derived from bovine bone with bloom number 250 were purchased from Nitta Gelatin Inc. (Osaka, Japan); type A gelatin derived from porcine skin with bloom number 300 and type B gelatin derived from bovine skin with bloom numbers 75 and 225

were purchased from Sigma-Aldrich (St. Louis, MO, USA). Hereafter, the gelatins are designated by "company name; type; bloom number". The AccQ•Tag Chemistry kit was purchased from Waters (Waters Corporation, Milford, MA, USA). All solvents used were HPLC grade and were purchased from Fisher Scientific. Wako 7515 PLGA polymer (catalog No. 823-11966) was purchased from Wako Pure Chemical Industries, Ltd. (Tokyo, Japan).

### 2.3.2 Determination of leuprolide acetate loading

Two extraction methods were employed to determine the leuprolide content in the LD formulations. A single extraction method (Method 1) was published by LD originator, Takeda Pharmaceutical Company Ltd [21,54] where methylene chloride (DCM) was used to dissolve PLGA microspheres and 1/30 M sodium phosphate buffer at pH 6.0 was used to extract leuprolide acetate into the aqueous phase. Approximately 5 mg of formulation was weighed accurately and 10 mL of DCM and 20 mL of phosphate buffer (pH 6.0) was added. The supernatant of the aqueous phase was obtained after mixing the solution vigorously for 5 min and subsequent centrifugation (2000 g, 5 min) at room temperature.

In Method 2, 5 mg of the LD formulation was dissolved in 750 μL DCM and then leuprolide acetate was extracted with 750 μL of 50 mM sodium acetate buffer at pH 4.0 [118,119]. In order to extract leuprolide from the organic phase, this extraction process was repeated for 5 times [118] and then with 50 mM sodium acetate buffer pH 4.0 containing 1 M sodium chloride (11 total extractions) [119]. Between each extraction, the supernatant was collected by centrifugation at 6000 g for 4 min at room temperature.

In both methods, the content of leuprolide acetate in the aqueous phase was determined by UPLC. The UPLC system consisted of an Acquity Quaternary Solvent Manager, Sample Manager-FTN, Column Manager and TUV Detector (Waters, Milford, MA, USA). The

separation of leuprolide was carried out with an Acquity UPLC BEH C18 column (1.7 μm, 2.1 x 100 mm, Waters, Milford, MA, USA) and a gradient elution of acetonitrile with 0.1% TFA (solvent A) and water with 0.1% TFA (solvent B) at a flow rate of 0.5 mL/min as follows: 0 min (25% A), 2 min (35% A), and 2.5 min (25% A), followed by 1 min recovery with initial conditions. The concentration of leuprolide was detected by UV absorbance at 280 nm of wavelength and its peak appeared around a retention time of 2.4 min. Three batches of LD with different lot numbers were used and the experiment was performed in triplicate.

Amino acid analysis was used as the third method (Method 3) to determine the content of leuprolide acetate in LD. Leuprolide contains 9 amino acids and tyrosine (Tyr) and histidine (His) are the specific amino acids that do not exist in the gelatin [1,117]. Histidine was used to determine the content of leuprolide. About 25 mg of LD formulations or 5 mg of leuprolide acetate were weighed into hydrolysis tubes and 1.0 mL of 6 N constant boiling HCl (Fisher Chemical, Fair Lawn, NJ, USA) was added. The tubes were purged under nitrogen, sealed under light vacuum, and incubated at 110 °C for 24 h. After incubation, the solution was frozen with liquid nitrogen and lyophilized under vacuum at room temperature. Then, 400 μL of 20 mM HCl was added into each tube to reconstitute the samples. Standard solutions of leuprolide acetate were prepared by dilution of the hydrolyzed leuprolide samples. Derivatization and analysis were performed by using Waters AccQ•Tag Chemistry kit. Briefly, hydrolyzed amino acids were derivatized using the borate buffer (<5% sodium tetraborate in water) with the Waters AccQ•Fluor reagent (6-aminoquinolyl-N-hydroxysuccinimidyl carbamate). Norleucine was added to the samples during the derivatization and used as the internal standard. The derivatized samples were separated by reverse phase UPLC using a C18 column (AccQ•Tag Ultra C18, 1.7 μm (Millipore Corporation, Milford, MA, USA)) and a gradient elution of solvent A (5%

solution of Waters AccQ•Tag Eluent A concentrate (19 wt% sodium acetate, 6-7 wt% phosphoric acid and 1-2% wt% triethylamine)) and solvent B (2% formic acid in acetonitrile solution) at a flow rate of 0.5 mL/min as follows: 0 min (99.9% A), 1 min (98.5% A), 11.5 min (78% A), 13.5 min (40% A) and 15 min (99.9% A), followed by a 2 min recovery with initial conditions. The urea derivatives yielded during the derivatization were detected by fluorescence (excitation-emission, 250-395 nm). Three batches of LD with different lot numbers were used and the experiment was performed in triplicate.

### 2.3.3 Characterization of the gelatin in the LD formulation

#### *2.3.3.1 Determination of gelatin type*

Ion exchange chromatography was employed to differentiate the pI difference between type A and B gelatin in order to identify the gelatin type in the LD formulation. To extract gelatin from the LD formulation, the formulation powder was first suspended in ice-cold water to dissolve and remove the D-mannitol from the sample. Ice-cold water was used to inhibit degradation of PLGA. The suspended microspheres were collected using a nylon membrane filter with 0.20-μm pores under vacuum and then washed with another 5 mL of $ddH_2O$ to rinse off mannitol bound to the microspheres. Then, the microspheres were transferred into a pre-weighed 2-mL tube and dried at room temperature under vacuum until the weight of the sample remained constant. The dried mannitol-free microspheres (i.e., microspheres without mannitol) were dissolved in 5 mL of DCM and 10 mL of $ddH_2O$ was added. The mixture was heated to 60 °C and mixed well to extract gelatin and leuprolide into the aqueous phase. After centrifugation at 2000 g for 5 min at 40 °C with slow brake, 8 mL of the aqueous phase was collected and replaced with the same volume of $ddH_2O$. The extraction was repeated one more time and then the extract was collected after lyophilization of the aqueous solution.

Since the extract contained leuprolide as well as gelatin, leuprolide was removed by using a centrifugal filter unit (Amicon Ultra-15, 10 KDa cutoff, EMD Millipore Corp., Darmstadt, Germany) to avoid the interference in the ion exchange chromatography. Briefly, the extract was reconstituted with 15 mL of 6 M acetic acid and transferred into the molecular cut-off filter device, followed by centrifugation at 5000 g for 40 min at 30 °C. Then, 12 mL of 6 M acetic acid was added to the concentrated extract and the separation was repeated one more time. To remove the acetic acid in the purified samples, 11 mL of 10 mM sodium chloride solution pre-warmed at 50 °C was added to the tube. The excessive solution was removed by centrifugation at 5000 g for 30 min at 40 °C. This replacement process was performed twice. The purified gelatin extracts remaining on the upper layer of the filter tubes was collected after lyophilization. The dried extracts were reconstituted with dd$H_2O$ to make the final concentration of gelatin around 2 mg/mL and heated to 60 °C for 15-20 min with several times of vortexing, and immediately applied to ion-exchange HPLC. Three batches of LD with different lot numbers were used. Type A and type B gelatins were dissolved in 6 M acetic acid, applied to a molecular cut-off filter device and processed in the same manner and used as reference samples. Concentrations of all gelatin samples were 2 mg/mL.

The type of gelatin was analyzed by cation ion-exchange HPLC installed with a TSKgel SP-NPR column (Tosoh Bioscience LLC, King of Prussia, PA) and a gradient elution of solvent A (10 mM citric acid buffer at pH 3), solvent B (20 mM sodium phosphate buffer at pH 11.5) and solvent C (1 M NaCl) at a flow rate of 1 mL/min as follows: 0 min (74:26, A:B), 2 min (53:47, A:B), 5.5 min (24:76, A:B), 12 min (100% B) and 14.5 min (100% C) followed by recovery with initial conditions for 3 min; the column temperature was 50 °C. The wavelength of UV detection was 220 nm. After each run, acetic acid was used to wash the needle and dd$H_2O$

was used to clean the residues on the column. A blank control was injected between samples to confirm there was no cross over contamination.

*2.3.3.2 Molecular weight (Mw) of gelatin*

The gel strength of gelatin is typically determined by a texture analyzer and described by bloom number. Briefly, 6.67% gelatin water solution is prepared in a specified 150 mL standard bloom jar. After chilling, the rigidity of the gel is measured as the force required to depress a standard probe with a diameter of 0.5 inch to a depth of 4 mm into the gel [117]. However, due to the limited quantity (1.3 mg) of gelatin in each syringe, preparing such a gelatin test solution is not a reasonable cost. As bloom number is related to molecular weight of gelatin [117], the distribution of gelatin molecular weight was studied instead of the bloom test, which requires extensive amount of sample to perform the assay. To determine the Mw, gelatin was extracted from the LD and purified as described in the gelatin typing section. Three batches of LD with different lot numbers were used. Three commercial gelatins with different bloom numbers (Nitta B 300, Nitta B 250 and Sigma B 75) were loaded in the microspheres as described below and extracted and purified in the same way. Extracted and purified gelatin was reconstituted with dd$H_2O$ at 2 mg/mL and 10 μL of the samples were injected to UPLC installed with a TSKgel UP-SW3000 column (Tosoh Bioscience LLC, King of Prussia, PA, USA). The mobile phase was composed of 0.1 M potassium dihydrogen phosphate buffer and 0.1 M disodium monohydrogen phosphate buffer (1:1, v:v) and the flow rate was set to 0.2 mL/min. The column temperature was 30 °C and the sample temperature was 40 °C. The wavelength of UV detection was 230 nm. Protein standards (Gel Filtration Markers Kit, Sigma-Aldrich, St. Louis, MO, USA) were used as molecular weight markers. The standard mixture contained carbonic anhydrase, albumin, alcohol

dehydrogenase, β-amylase, apoferritin and thyroglobulin. The molecular weight of the standard mixture ranged from 29,000 to 700,000 Da.

*2.3.3.3 Preparation of PLGA microspheres for gelatin analysis*

Gelatin and leuprolide acetate were loaded into PLGA microspheres by solvent evaporation method. PLGA (600 mg) was dissolved in 1 mL DCM. Gelatin (10 mg) and leuprolide acetate (68 mg) were dissolved in 150 μL dd$H_2O$ at 60 °C. The water phase and the oil phase were mixed and then emulsified using a VirTis Tempest $IQ^2$ homogenizer (SP Scientific Inc., Warminster, PA, USA) at speed 15000 rpm for 4 min to form a W1/O emulsion. The obtained W1/O emulsion was cooled to 18 °C to increase the viscosity of the emulsion. Then, 4 mL aqueous 0.25% polyvinyl alcohol (PVA) (EG-40P) (Soarus L.L.C., Arlington Heights, IL, USA) solution was added to the W1/O emulsion and the mixture was homogenized at 12000 rpm for 4 min. After homogenization, a W1/O/W2 emulsion was obtained. The W1/O/W2 emulsion was transferred into 200 mL 0.25% PVA solution and stirred with an overhead stir-tester (Glas-Col G.K.H. stir-Tester and Model HST20 stirrer, Terre Haute, Indiana, USA) at 700 rpm for 3 h to evaporate the methylene chloride and solidify the oil phase. The suspensions were rinsed with at least 1 L of water to wash off the unencapsulated drug and PVA. The microspheres were passed through a 90-μm opening sieve to remove the large microspheres and collected by centrifugation at 4000 rpm for 5 min. The microspheres were freeze-dried under vacuum for 48 h.

*2.3.3.4 Determination of content of gelatin by amino acid analysis*

Amino acid analysis was performed in the same way as described in the Determination of Leuprolide Acetate Loading section. Standard solutions of gelatin were prepared by dilution of the hydrolyzed Nitta B 300 gelatin samples. Gelatin has several specific amino acids such as

alanine (Ala), asparagine and aspartic acid (Asx), hydroxylproline (OH-Pro) and valine (Val), which do not exist in the nonapeptide sequence of leuprolide [1,117]. The second abundant amino acid in the gelatin, alanine, was used to determine the gelatin content in the LD formulation. Poor reproducibility was found when using glycine, the most abundant amino acid in the gelatin, likely because of poor peak separation. Three batches of LD with different lot numbers were used and the experiment was performed in triplicate.

### 2.3.4 Characterization of the polymer in the LD formulation

#### *2.3.4.1 Determination of the PLGA weight average molecular weight (Mw), number average molecular weight (Mn), and polydispersity index (PDI)*

As the cryoprotectant in the LD, D-mannitol is insoluble in tetrahydrofuran (THF) and it was removed as described in gelatin typing section. Then, mannitol-free LD microspheres were dissolved in dehydrated THF at 4 mg/mL. As the presence of moisture/water can induce degradation of the polymer, THF was dehydrated by 3Å molecular sieves (Sigma-Aldrich, St. Louis, MO, USA). The samples were subjected to gel-permeation chromatography (GPC) installed with two styragel columns (HR 1 and HR 5E columns, Waters, Milford, MA, USA) and a refractive index detector (2414 refractive index detector, Waters, Milford, MA, USA). Polystyrene standards with Mw ranging from 1,000 Da to 50,000 Da were dissolved in the dehydrated THF. Mw, Mn and PDI of PLGA were calculated by Breeze software (Waters, Milford, MA, USA).

#### *2.3.4.2 Quantitative NMR analysis to determine PLGA content and lactic acid (LA) to glycolic acid (GA) ratio*

Quantitative $^{1}$H NMR (qNMR) (Varian, Inc., Palo Alto, CA, USA) was used to determine the ratio of lactic acid and glycolic acid as well as the content of PLGA by using dimethyl

terephthalate (DMT) as an internal standard [120]. The mannitol in the LD formulations was removed as described in gelatin typing section. The mannitol-free LD microspheres were dissolved in $CDCl_3$ at 15-20 mg/mL with DMT at 1.0-2.0 mg/mL and subjected to NMR analysis. From the area of the peaks, the masses of LA and GA in PLGA were determined using the following equation [120],

$$M_s = M_{IS} \cdot \frac{Mw_s}{Mw_{IS}} \cdot \frac{nH_{IS}}{nH_s} \cdot \frac{P_{IS}}{P_s} \cdot \frac{A_s}{A_{IS}} \quad (2\text{-}1)$$

where "s" designates LA or GA in polymer and "IS" represents the internal standard; $M_s$ and $M_{IS}$ are the masses, $Mw_s$ and $Mw_{IS}$ are the molecular weights in g/mol; $P_s$ and $P_{IS}$ are the purities; $nH_s$ and $nH_{IS}$ are the numbers of protons that contribute to the peak signals used for integration; and $A_s$ and $A_{IS}$ are the peak areas for the selected peaks [120]. It is noted that $P_s$ was set at 100% because the purity of PLGA to manufacture LD was undisclosed.

*2.3.4.3 Determination of acid number of PLGA*

The number of free carboxylic acid end group in PLGA was determined by organic phase titration [31]. Approximately 10 mg of LD was dissolved in 5 mL of dehydrated acetone/tetrahydrofuran (1:1, v:v) mixture. Phenolphthalein methanol solution (0.1 wt%) was added as an indicator. The solution was immediately titrated with 0.01 M methanolic potassium hydroxide to a stable pink end point. The acid number of PLGA was calculated using the following equation:

$$Acid\ number\ [mg\ KOH/\ g\ PLGA] = \frac{(Volume\ of\ sample\ [mL]) \times (N_{KOH}) \times (Mw_{KOH})}{(Weight\ of\ PLGA\ [g])} \quad (2\text{-}2)$$

2.3.5 Characterization of the diluent

*2.3.5.1 Determination of pH of diluent in the LD formulation*

The pH of diluent was determined by a pH meter (430 pH Meter, Corning, Inc. Corning, NY, USA) equipped with a microelectrode (MI-410, Microelectrodes, Inc., Bedford, NH, USA). The pH meter was calibrated using standard solutions at pHs 4 and 7 at room temperature.

*2.3.5.2 Determination of water content of diluent*

The diluent is supposed to contain 5 mg (0.5%) Na-CMC, 50 mg (5%) D-mannitol, 1 mg (0.1%) polysorbate 80 in water for injection (1 mL injection diluent for a 7.5 mg dose of the drug), and glacial acetic acid (USP) to control pH [1,77]. The water content was estimated by the weight difference before and after drying of diluent. Approximately 300 μL of the diluent was added to pre-weighed vials and the weight of diluent was recorded. After the diluent was dried at reduced pressure at 60 °C for 48 h, the weight of sample was recorded. In order to confirm the weights of the samples remained constant and the water has been completely removed, the samples were further dried under the same conditions for an additional 2 h and the weight was measured again. This step was repeated for one more time to determine the final weight of the samples.

*2.3.5.3 Determination of D-mannitol content in the LD formulation and in diluent*

The content of D-mannitol was determined using a D-mannitol colorimetric assay kit (Sigma-Aldrich, St. Louis, MO, USA). D-mannitol was converted to D-fructose by mannitol dehydrogenase in the presence of NAD. This reaction produces NADH and the concentration of NADH could be determined by UV absorbance at 450 nm of wavelength. Approximately 1 mg of LD formulation was added to 2 mL tubes. The formulation was suspended in 1.5 mL of dd$H_2O$ and then centrifuged at 8000 g for 5 min. Then, 10 μL of the supernatant was added to the 96-well plate using a pipette pre-calibrated by a balance. To determine the content of

mannitol in diluent, approximately 20 mg of the diluent was diluted 500 times with dd$H_2O$ and 10 μL of the samples were added to the 96-well plate by a pre-calibrated pipette. The assay buffer and reaction mixture solution were added according to the instructions in the assay kit. After the incubation at 37 °C, the plate stood for another 30 min until the air bubbles disappeared. The concentration of mannitol was determined by UV absorbance at 450 nm of wavelength (SpectraMax M3, Molecular Devices, Sunnyvale, CA, USA).

*2.3.5.4 Determination of viscosity and specific gravity of diluent*

The viscosity of the diluent in LD was determined by an Anton-Paar rolling-ball viscometer Lovis 2000 M/ME, which measures the rolling time of a ball through liquid according to Hoeppler's falling ball principle [121]. The mimic diluent was prepared by adding Tween 80, Na-CMC (high viscosity or low viscosity, Sigma-Aldrich, St. Louis, MO, USA) and mannitol at the same ratio as the composition in diluent.

Specific gravity was measured using a 1 mL pycnometer. The pycnometer was pre-weighed and filled with the diluent in LD. Then the pycnometer was placed in a thermostatic bath with temperature controlled at 25 °C. After the temperature of the solution was equilibrated, excess volume of the solution expelled from the top of the pycnometer was absorbed with Kimwipes (Kimberly-Clark Professional, Roswell, GA, USA). The weight of the filled solution was recorded to determine the specific gravity using the density of water at 4 °C (density = 1 g/mL).

*2.3.5.5 Determination of Tween 80 content in diluent*

To determine the content of Tween 80 in the diluent, *bis*-ANS (4,4’ -dianilino-1,1’ -binaphthyl-5,5’ -disulfonic acid, di-potassium salt) was used as a fluorescence probe. This fluorescence probe is almost non-fluorescent initially, and the fluorescence increases when it

reacts with the hydrophobic group in Tween 80 [122]. Briefly, 50 μL of diluent was mixed with 950 μL water and then 55 μL of 1 mM *bis*-ANS solution was added. Then, the mixture was vortexed for 5 s and shaken at 220 rpm for 5 min, followed by no agitation to equilibrate for 25 min. The stock standard solution of Tween 80 (Thermo Fisher Scientific Inc., Waltham, MA, USA) was prepared in dd$H_2O$ with the presence of Na-CMC and mannitol at the same ratio as the composition in LD diluent and it was further diluted to make serial standard solutions that fell within the range of 30-100 ppm. Two hundred μL of the mixture was loaded to Costar 96-well plates (black bottom polystyrene) and the concentration of Tween 80 was determined by fluorescence (excitation-emission, 380-500 nm) (SpectraMax M3, Molecular Devices, Sunnyvale, CA, USA).

### 2.3.6 Characterization of product attributes

#### *2.3.6.1 Particle size distribution*

The median diameter of the microspheres was determined using a Malvern Mastersizer 2000 (Malvern Instruments Ltd., Worcestershire, UK). About 30-40 mg of LD formulation was suspended in 1 mL of diluent and vortexed vigorously before added to the instrument sample dispersion unit. Three measurements were performed per sample at a stirring speed of 2500 rpm and sampling time of 15 s.

#### *2.3.6.2 Surface morphology*

The surface morphology of microspheres was examined using a Hitachi S3200N scanning electron microscope (SEM) (Hitachi, Tokyo, Japan). The LD microspheres were fixed on a brass stub using double-sided carbon adhesive tape and the samples were prepared electrically conductive by coating with a thin layer of gold for 120 s at 40 W under vacuum [123]. Images were taken at an excitation voltage of 10.0 kV.

*2.3.6.3 Glass transition temperature*

The $T_g$ of LD was determined with a modulated differential scanning calorimeter (mDSC) (TA Instruments, New Castle, DE, USA). LD microspheres (3-5 mg) were crimped in DSC aluminum pans. Temperatures were ramped between -20 °C and 90 °C at 3°/min. All samples were subjected to a heat/cool/heat cycle. The results were analyzed by using TA TRIOS software and $T_g$ was taken as the midpoint of the reversing heat event.

*2.3.6.4 Residual moisture*

Residual water content in microspheres from the LD was determined by Karl Fischer (KF) titration. Eighty mg of LD was weighed into a vial and sealed with a septum cap. Anhydrous dimethyl sulfoxide (DMSO) was added to make the final concentration at 10 mg/ml and the sample was sonicated for 10 minutes before injected into the KF for titration. The moisture in the blank DMSO was also determined.

*2.3.6.5 Residual solvent*

Residual solvent (methylene chloride) in Lupron Depot® was determined by a Trace 1310 gas chromatograph (GC) (Thermo Fisher Scientific Inc., Waltham, MA, USA). The LD microspheres were added into a glass vial containing anhydrous DMSO to make the final concentration at ~10 mg/ mL and the vial was sealed. The samples were applied to the GC by two different methods: headspace and liquid injections. For headspace injection, the GC conditions were as follows: nitrogen gas was used as the carrier solvent at a flow of 25 mL/min; air flow was 350 mL/min and hydrogen flow was 35 mL/min; the front detector temperature was 240°C and the front inlet pressure was a constant flow at 2 mL/min. Each sample was agitated for 20 min at 80°C and 1 mL of the headspace sample was injected into the front inlet with the temperature of 140°C, split flow of 40.0 ml/min, and a split ratio of 20. The GC column

temperature was initially set at 40°C for 15 min, then increased at 10°C/min to 240°C and held at 240°C for 2 min. For liquid injection, the GC conditions were as follows: nitrogen gas was used as the carrier solvent at a flow of 33 mL/min; air flow was 450 mL/min and hydrogen flow was 34 mL/min; the front detector temperature was 220°C and the front inlet pressure was a constant flow at 12 mL/min. The injection volume was 1 μL and the inlet operation was in splitless mode with temperature at 200°C. The GC column temperature was initially set at 40°C for 1 min, increased at 5°C/min to 65°C and then increased at 100°C/min to 190°C. A standard curve was prepared by adding methylene chloride to DMSO at 1, 10, 50, 100, 250, and 500 ppm.

*2.3.6.6 Release kinetics*

Drug release of microspheres was carried out using a sample-and-separate method in release medium PBST (phosphate buffered saline (PBS) + 0.02% Tween 80 + 0.02% $NaN_3$, pH 7.4). Microspheres (~10 mg) were suspended in 1 mL of medium and shaken mildly at 37 ºC. At each time point (1, 3, 7 days and weekly thereafter), the medium was completely collected after centrifugation at 8000 rpm for 5 min and replaced with fresh PBST buffer. The concentration of leuprolide in the supernatant was determined by UPLC as described in the section of determination of leuprolide acetate content.

2.3.7 Statistical Analysis

Statistical analyses were carried out using GraphPad Prism 7.04 software. One sample t test was used to compare the measured values to the officially labeled numbers. The level of significance was established at the 95% confidence interval ($\alpha = 0.05$).

## 2.4 **Results and Discussion**

### 2.4.1 Characterization of LD microspheres

*2.4.1.1 Leuprolide acetate content*

Leuprolide acetate content in the one-month LD was determined by 3 different methods, as shown in Figure 2-1. Method 1, as performed by the originator of the LD, indicated 8.31 ± 0.05 wt% (mean ± SEM, n=3) of leuprolide acetate in the LD. However, cationic leuprolide is capable of binding to negatively charged terminal chains of PLGA even in the DCM phase [118]. Note that the acetate counterion of leuprolide is less acidic than the end group of PLGA [124] and is therefore expected to deprotonate the polymer end group to some extent. Hence, method 2 with multiple extractions of leuprolide acetate was performed, giving 8.95 ± 0.31 wt% (mean ± SEM, n=3) as the leuprolide acetate content. As expected, method 2 increased the recovery of leuprolide by 0.6 wt% more than method 1. In method 3, the leuprolide content was determined by the concentration of amino acid in the samples, which should not be affected by the interaction between the peptide and polymer that exists in the extraction method. The peak area ratios of histidine (retention time = 8.15 min) to the internal standard, norleucine (retention time =12.7 min), were used to determine the concentration of leuprolide based on the standard curve. The measured value, 8.89 ± 0.13 wt% (mean ± SEM, n=3), was slightly higher than the result in method 1 and comparable to that of method 2. All three methods provided reasonable measured values which were not significantly different (t test, $p>0.05$) from the officially reported value 8.5 wt% in the package insert of LD [77]. The leuprolide acetate standard solutions used in this study were compared to the USP leuprolide acetate standard solutions on three different days and were confirmed to be within 100.5 ± 2.2 % (mean ± SEM, n=3) of the USP standard by UPLC in the concentration range of 0-600 μg/mL.

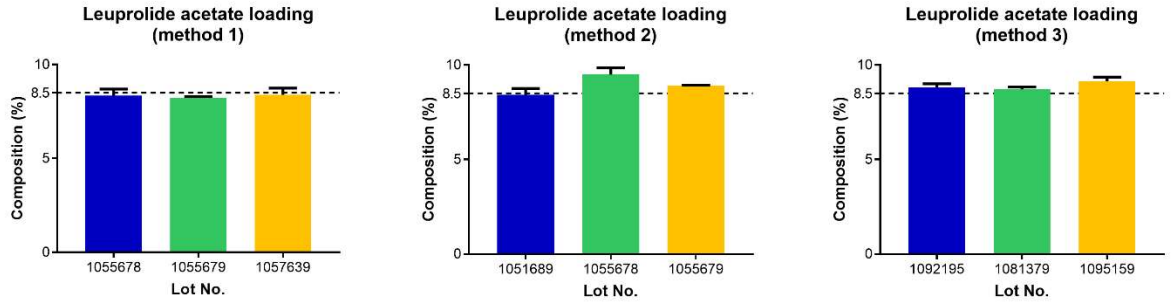


*Figure 2-1. Leuprolide content in LD formulations determined by two different extraction methods. All values present as mean ± SEM (n=3). The dash lines indicate the official LD loading.*

### *2.4.1.2 Gelatin type*

Figure 2-2 displays representative ionic exchange chromatographs of gelatin samples. Pure type A and B gelatin was differentiated based on their major peaks, which appeared at retention times around 13.5 min (Figure 2-2H) and 4.2 min (Figure 2-2F-G), respectively. The extracted gelatin from three different batches of LD shown in Figure 2-2B-D exhibited major peaks at roughly the same retention time as that of type B gelatin, which were far from that of type A gelatin. Therefore, the gelatin loaded in the LD was identified as type B.

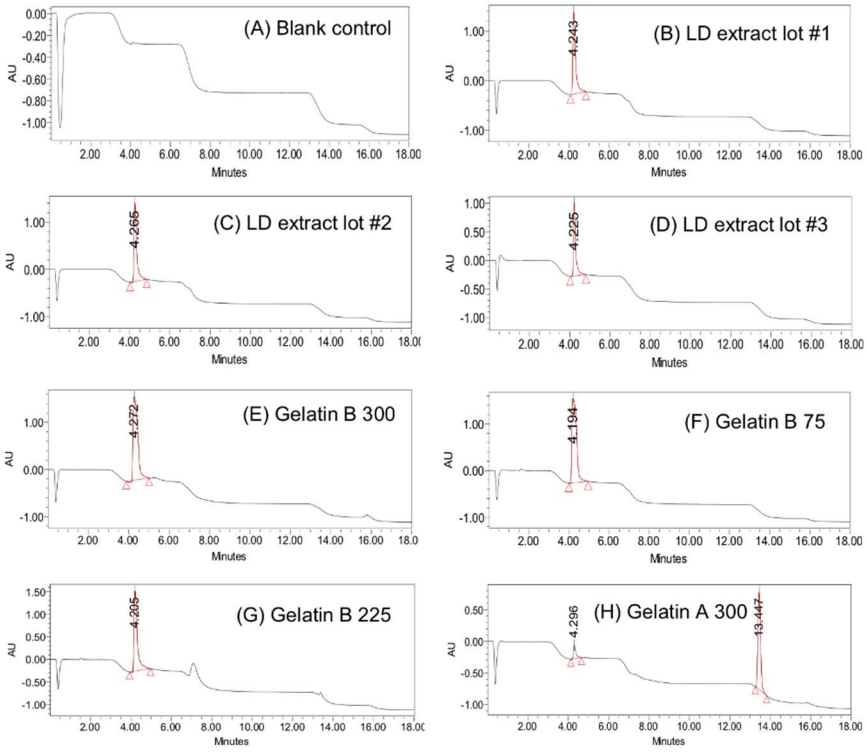


*Figure 2-2. Ion exchange chromatograms of (A) blank control, (B) LD extract lot #1, (C) LD extract lot #2, (D) LD extract lot #3, (E) type B gelatin with bloom number 300 from Nitta gelatin Inc., (F) type B gelatin from Sigma-Aldrich with bloom number 75, (G) type B gelatin from Sigma-Aldrich with bloom number 225 and (H) type A gelatin from Sigma-Aldrich with bloom number 300. Note that negligible peaks are present in type A gelatin sample potentially due to the impurity in the product.*

### *2.4.1.3 Molecular weight of gelatin*

The representative chromatography of extracted gelatin from LD is shown in Figure 2-3A. As the retention time of peaks are related to the molecular weight, the peaks were fractioned into 8 sections (Figure 2-3A&B) based on the molecular weight standards. The percentages of the area of peak were obtained to plot the Mw distributions of gelatin samples (Figure 2-3C). In Figure 2-3C, Nitta type B gelatins of bloom numbers 300 and 250, Sigma type B gelatins of bloom numbers 75 and 225 and Sigma type A gelatin 300 bloom were dissolved in acetic acid and collected after being applied to molecular cut-off filter device before UPLC analysis in the same way as the purification process of extracted gelatin from LD. Considering

the potential degradation of gelatin during dissolving, encapsulation and extraction, we dissolved and loaded various gelatins into the PLGA microspheres using polymer produced by Wako and leuprolide acetate according to the W/O/W method. Then we performed the extraction and purification process in the same way as described above for the LD. Three gelatins with relatively high, medium and low bloom numbers were studied in this experiment and the Mw distributions are designated as *extracted Nitta B 300*, *extracted Nitta B 250* and *extracted Sigma B 75* in Figure 3C. Compared to the gelatin samples without the encapsulation process, all of the extracted gelatins showed higher levels of lower Mw fractions indicating of gelatin hydrolysis during microspheres preparation. The extracted Nitta B 300 showed very similar Mw distributions to the extract from the LD (Figure 3C). To further confirm Nitta B 300 is comparable to the gelatin in LD in terms of their Mw distribution, we prepared three batches of microspheres loaded with Nitta B 300 gelatin and performed the extraction, purification and Mw analysis as described above. The Mw distributions of extracted Nitta B 300 gelatin were compared to the extracts from three different batches of LD in Figure 2-3D. From the results regarding peaks shape and Mw fractions, it is reasonable to conclude that the LD was encapsulated with high Mw gelatin (i.e., Bloom 300). Combined with the result from the gelatin typing section, the properties of Nitta B 300 gelatin matched the gelatin used in the LD. Furthermore, Nitta B 300 is manufactured with low endotoxin, suitable for injection and was used in publications [54] from the LD inventor. Therefore, Nitta B 300 gelatin was used as the reference gelatin in the measurement of gelatin content and identified as the probable source of gelatin in the LD.

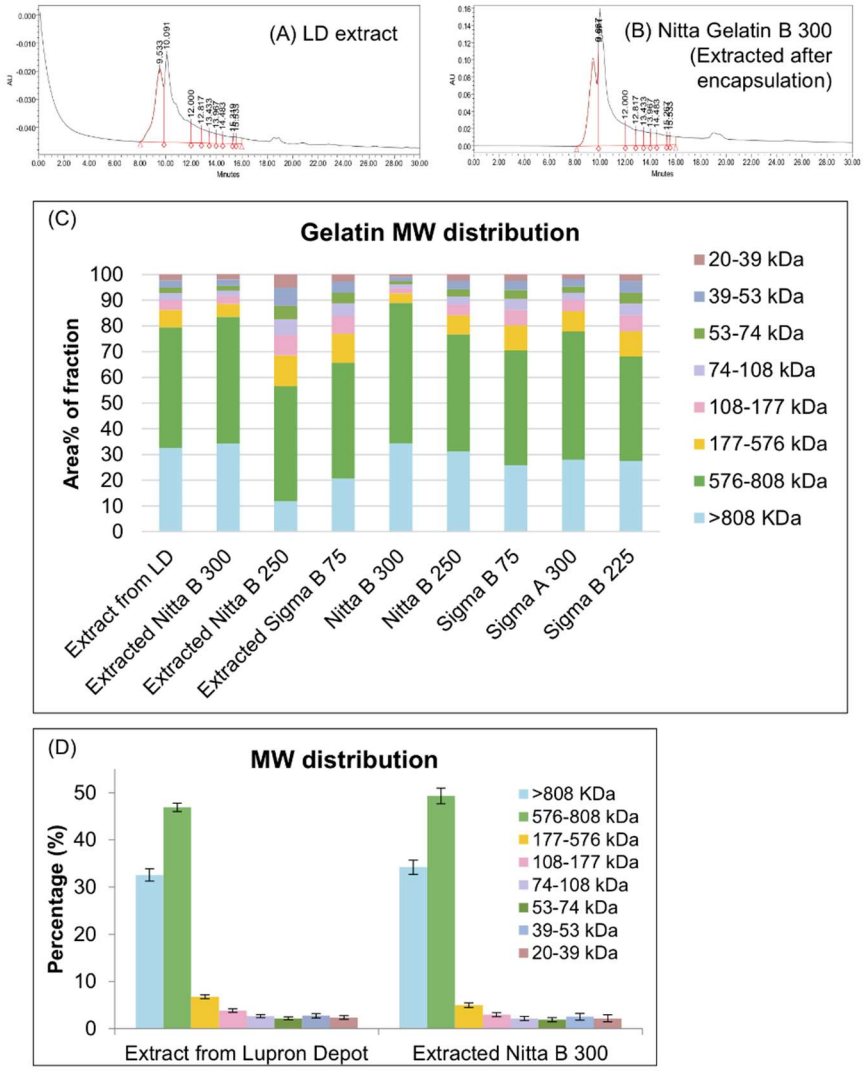


*Figure 2-3. GPC chromatograms of (A) extract from the LD and (B) extracted Nitta gelatin B after PLGA encapsulation; Mw distributions of different gelatin products (C); and comparison of the Mw distributions between extract from the LD and extracted Nitta B 300 (D) (the bars indicate mean ± SEM, n=3). * Extracted gelatin samples were taken after PLGA encapsulation.*

### *2.4.1.4 Gelatin content*

The peak area ratios of alanine (retention time =10.05 min) to the internal standard (retention time =12.7 min) were used to determine the concentration of gelatin based on the standard curve. The average content of gelatin in the LD samples was determined as 1.55 ± 0.08 wt% (mean ± SEM, n=3) (Figure 2-4), which was not significantly different (t test, $p>0.05$) from the labeled content of 1.5% gelatin.

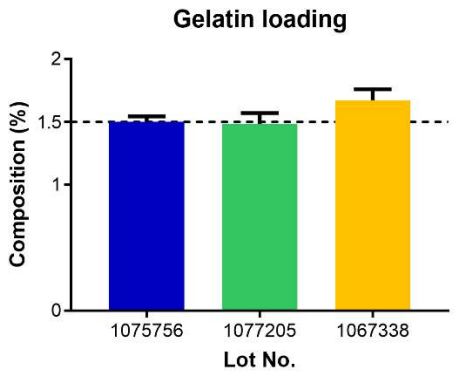


*Figure 2-4. Gelatin content in the LD. All values represent mean ± SEM (n=3). The dash line indicates the official LD loading.*

### *2.4.1.5 Molecular weight of PLGA*

PLGA is a biodegradable polymer by hydrolysis of ester bonds and the Mw of the PLGA is an important attribute to control the duration and kinetics of drug release [21]. Weight averaged molecular weight (Mw) and number averaged molecular weight (Mn) of LD was determined as approx. 13.0 kDa and 8.7 kDa, respectively with a PDI of 1.5 (Figure 2-5). The LD 7.5 mg is reported to be composed of PLGA with an LA/GA ratio, 75:25; Mw, 12.1 to 14 kDa [21,22]; and a ratio of Mw to Mn (PDI) of 1.81 [21]. However, these characteristic numbers are related to the raw polymer before encapsulating leuprolide with gelatin by double emulsion solvent evaporation technique and Mw, Mn, and PDI could potentially be affected during the formulation process. Therefore, the results reflect the numbers of the PLGA in the finished product and were in reasonable ranges for Mw and Mn [21]. The PDI obtained in this study was slightly lower than the published one.

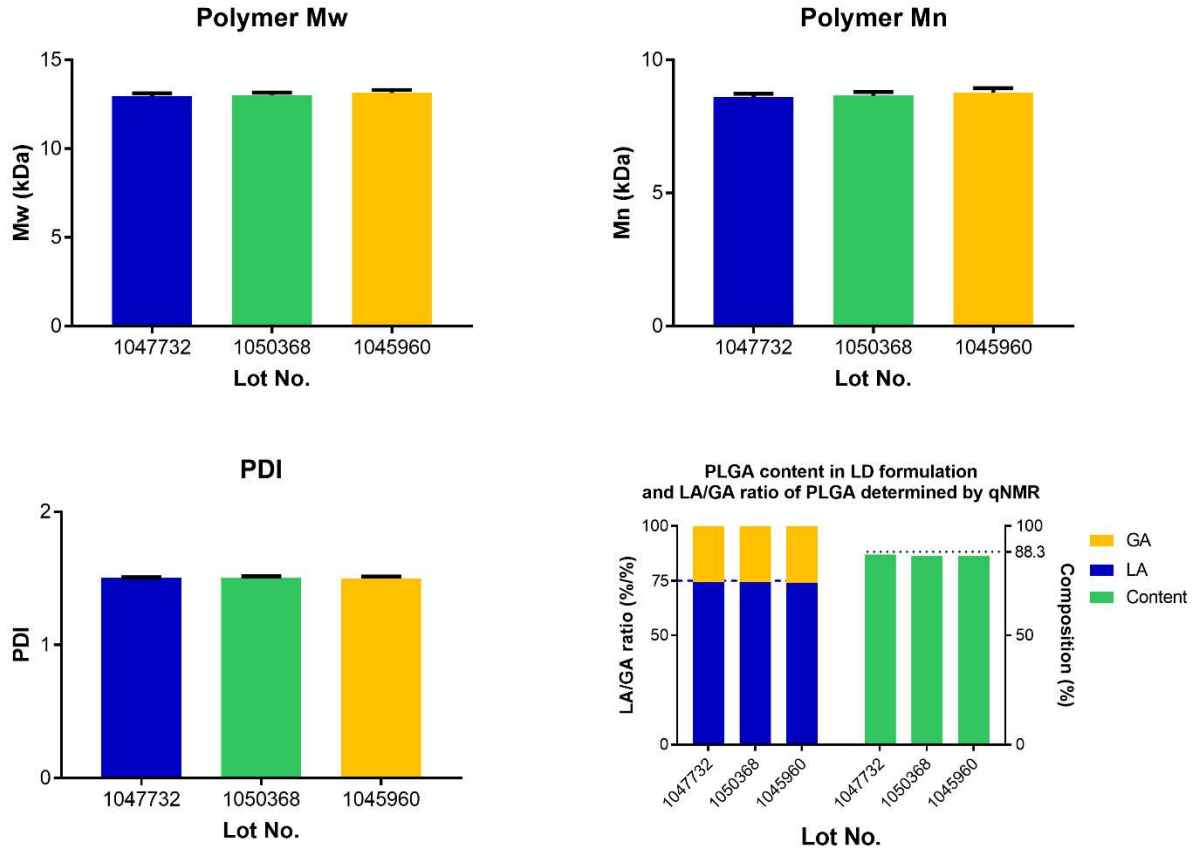


*Figure 2-5. Characterization of PLGA in the LD formulations. The values of Mw, Mn and PDI represent mean ± SEM (n=3). The dash lines indicate the official values.*

### *2.4.1.6 LA/GA ratio and content of PLGA*

LA/GA ratio is another attribute of PLGA to control the duration of release. The PLGA ester bonds (pairs of GA-GA, LA-LA and GA-LA or LA-GA) containing GA is less stable than the bonds with LA, and thus a higher content of glycolic acid facilitates the water uptake and increases the rate of degradation of the polymer [8]. As the release progress depends on the degradation of PLGA ester bonds, the composition of monomer changes over time of release, typically resulting in an increase in LA/GA ratio [124].

Figure 2-6 displays a representative NMR. The LA/GA ratio was determined from the proton signals generated by methyl ($–CH_3$) and CH groups of GA and methylene ($–CH_2$) groups of LA. The initial LA/GA ratio was found to be 74.3/25.7, which closely corresponded to the

expected values of 75/25 [1,22]. Additionally, the content of PLGA was determined by the sum of the masses of LA and GA calculated by equation (1). As summarized in Figure 2-5, it was found that the content of PLGA was 87.0 ± 0.3% (mean ± SEM, n=3), which is quite close to the officially reported PLGA mass 88.3% [77].

| | Range | Normalized | Absolute |
|---|---|---|---|
| 1 | 8.32 .. 7.88 | 0.64 | 27993.75 |
| 2 | 5.39 .. 5.06 | 2.90 | 126034.78 |
| 3 | 4.97 .. 4.55 | 2.00 | 86971.15 |
| 4 | 4.13 .. 3.76 | 0.97 | 41991.20 |
| 5 | 1.68 .. 1.44 | 8.83 | 384166.28 |

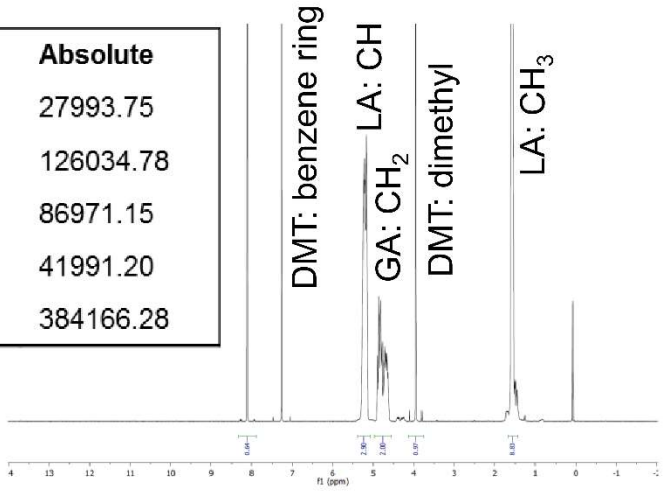


*Figure 2-6. 1H NMR spectrum of PLGA from the LD with internal standard dimethyl terephthalate (DMT).*

*2.4.1.7 Acid number of PLGA*

The acid number represents the number of free carboxylic acid functionalities in the PLGA at the terminal of the polymer chain and is essential to evaluate whether end group is a carboxylic acid or an aliphatic ester. PLGA is insoluble in aqueous phase so titration was performed in acetone/tetrahydrofuran solution using methanolic KOH.

The acid number of PLGA in a single lot of the LD 3.75 mg dose formulation was determined as 12.9 mg KOH/g PLGA. In the polymers with similar molecular weight, the polymer with a carboxylic acid end group always has higher acid number compared to the polymer with an ester-capped group [125]. Schrier and DeLuca [125] studied the acid numbers of different Resomer® polymer products (manufactured by Boehringer-Ingleheim (Ingleheim, Germany)) with and without ester end-capping, and showed that for the polymers with free acid

end and with molecular weight in the range of 8 – 12.5 kDa (RG 501H, 502H and 752H), the acid numbers were above 14 mg KOH/g PLGA while the ester end-capping forms had acid numbers below 2 mg KOH/g PLGA. The polymer Resomer® RG 752H has comparable molecular weight (Mw 13kDa) to the polymer used in LD and the acid number was reported as 14.3 mg KOH/g PLGA [125]. The high value of the acid number obtained in this study indicates the PLGA is the acid end-group polymer instead of ester end-group polymer, consistent with the innovators' publications and patents.

*2.4.1.8 D-mannitol content in LD formulation*

After encapsulation, D-mannitol was added to the microspheres to prevent aggregation during freeze drying process and to help resuspension of the microspheres before administration [1]. As shown in Figure 2-7, the measured content of D-mannitol mixed with microspheres was 15.63 ± 0.43 wt% (mean ± SEM, n=3), which was not significantly different (t test, $p>0.05$) from the expected number, 15 wt% [77].

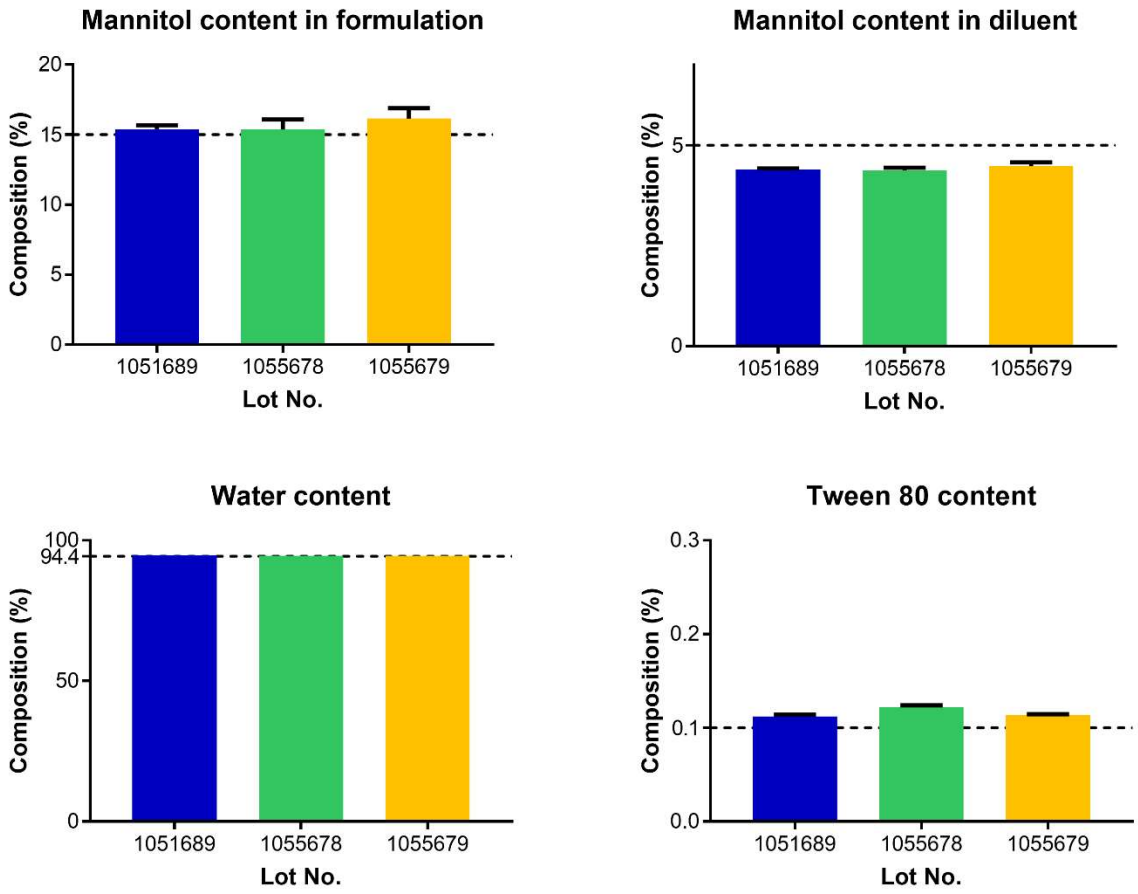


*Figure 2-7. Contents of D-mannitol in the LD formulation and diluent, and water and tween 80 in the diluent. All values represent mean ± SEM (n=3 for D-mannitol content in the formulation, water content and tween 80 content; n=4 for D-mannitol content in the diluent). The dash lines indicate the official LD compositions*

## 2.4.2 Characterization of the diluent

### *2.4.2.1 pH, water content and D-mannitol of diluent*

The diluent of a LD kit displayed a pH of 6.0-7.0. The content of water in the diluent was estimated as 94.55 ± 0.01 wt% (mean ± SEM, n=3) (Figure 2-7) and the results showed close values relative to the official content 94.4 wt%. The content of D-mannitol in the LD diluent was determined as 4.42 ± 0.07 wt% (mean ± SEM, n=3) (Figure 2-7). The value is close to but slightly lower than the official content of 5 wt%.

### *2.4.2.2 Characterization of viscosity and specific gravity*

It is considered that Na-CMC should be added to increase the viscosity of the diluent for maintaining the suspension of PLGA microspheres and for accurate injection. As characteristics of Na-CMC vary depending on Mw and viscosity, the diluent was initially subjected to microviscometry to identify the relative viscosity of Na-CMC. As a result, the viscosity of diluent was determined as 2.99 ± 0.06 cP (mean ± SEM, n=3) and the simulated diluent containing low viscosity Na-CMC and all the other ingredients at the same quantity as the commercial diluent showed a similar value of 3.31 ± 0.03 cP (mean ± SEM, n=3). The specific gravity of the LD diluent was determined to be 1.02.

*2.4.2.3 Tween 80 content*

The critical micellar concentration (c.m.c.) of Tween 80 is 13-15 ppm [126,127] and the formation of Tween 80 micelles may affect the interaction between the hydrophobic group in Tween 80 and the fluorescence probe used in the assay. The presence of Na-CMC and mannitol may also affect the formation of Tween 80 micelles and the generated fluorescence. Several studies were performed to avoid those influences in the measurement of Tween 80 content in LD. The results are not shown in this paper, but some key conclusions are summarized as below: 1) Serial solutions of Na-CMC and mannitol were prepared in the absence of Tween 80 and showed negligible fluorescence; 2) the standard Tween 80 solutions with the presence of Na-CMC and mannitol need to be prepared in the high concentration range (30-100 ppm) to achieve desirable linearity ($R^2$=0.99). The injection diluent from the LD was diluted to the concentration that fell within this range to generate reliable results. The content of Tween 80 in the diluent was determined as 0.116 ± 0.003 wt% (mean ± SEM, n=3) which was close to the official content of 0.1 wt% (Figure 2-7).

2.4.3 Characterization of product attributes

The particle size distribution of LD (Figure 2-8) was narrow with a volume median diameter of 11.4 ± 0.5 μm (mean ± SEM, n=3) (d (v, 0.5)). Ten percent of the volume distribution was below 3.8 ± 0.2 μm (mean ± SEM, n=3) (d (v, 0.1)) and 90% of the volume distribution was below 30.0 ± 0.6 μm (mean ± SEM, n=3) (d (v, 0.9)). These results were supported by the SEM micrographs. As seen in Figure 2-9, the LD formulations were spherical microspheres mixed with mannitol and the majority of the microspheres were < 20 μm. The $T_g$ of LD was measured as 48.6 ± 0.1 °C (mean ± SEM, n=3). Note that the presence of leuprolide has been reported to increase $T_g$ of the microspheres as a result of the peptide-polymer interaction [1,118]. The water content of the LD was determined by Karl Fischer titration as 0.44 ± 0.10% (mean ± SEM, n=3), indicating careful drying of the product. Very surprisingly, the residual content of methylene chloride determined by two different GC methods was < 1 ppm. Clearly the in-water drying protocol is capable of achieving low levels of organic solvent in the final microspheres manufactured on a large scale. Lastly, as seen in Figure 2-10, the cumulative release of LD in PBST lasted for 7 weeks with a 22.8 ± 0.4% initial burst on day one followed by a zero-order release after day three. The release curves after day one were fit using linear regression and the time to 50% release ($t_{50}$) was calculated to be 12.3 ± 0.2 days. Overall, these data are consistent with the existing literature [1,84] on the LD and a carefully formulated and manufactured product.

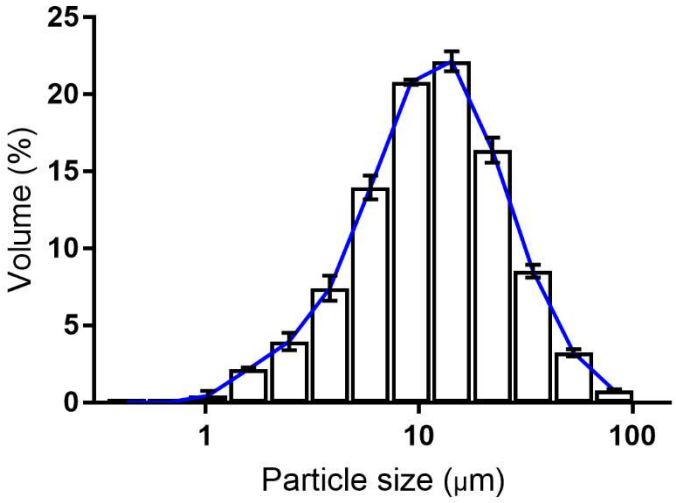


*Figure 2-8. Particle size distribution of the LD microspheres. The columns indicate mean ± SEM (n=3).*

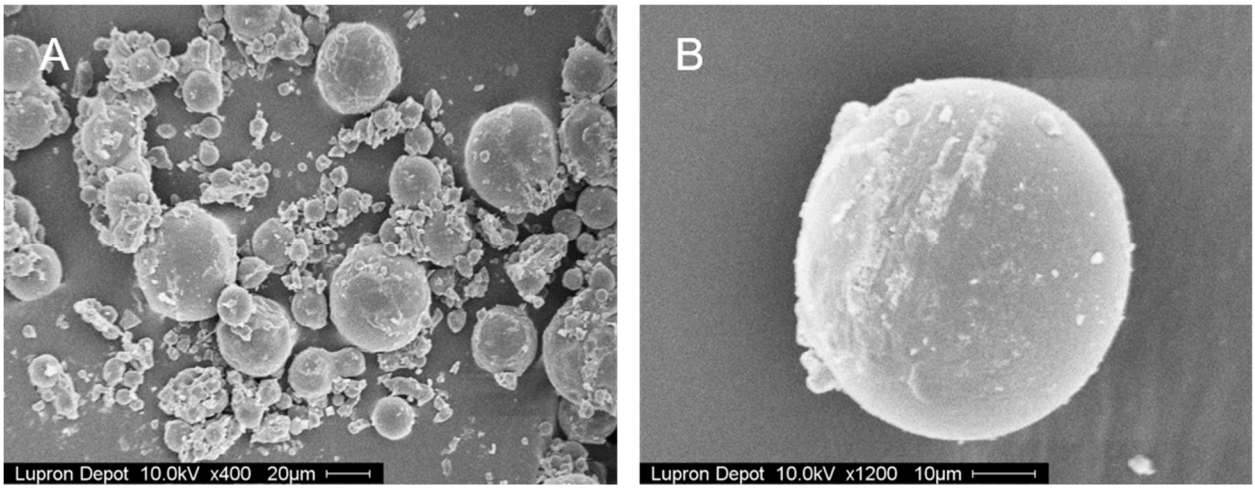


*Figure 2-9. SEM micrographs of LD formulation.*

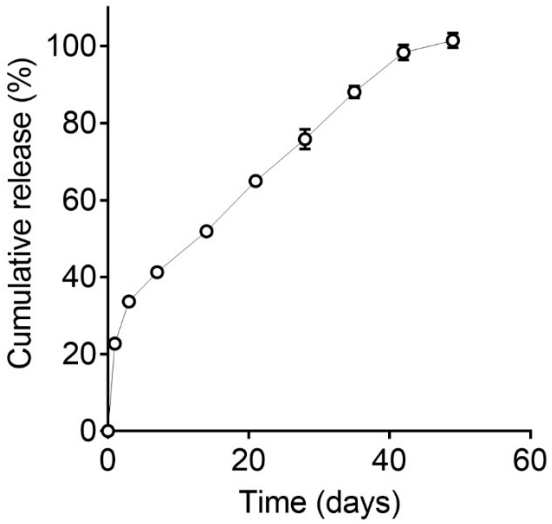


*Figure 2-10. In vitro release of LD formulation. Data represent mean ± SEM (n=5). Error bars not plotted when smaller than symbols.*

Comparing and contrasting our data with those previously reported, mostly from the LD manufacturer, Takeda Chemical Industries, Ltd. (Osaka, Japan), we find excellent agreement and some new insights. The comparison between the published values and measured values are summarized in Table S 2-1. The determination of composition of chamber 1 provided reasonable measured values, which were not significantly different from the labeled values. The measured values of the composition of diluent was also close to the labeled values and the accuracy might be affected by the complexity of the diluent. The specific gelatin used in the formulation was identified in this report. The Mw of the polymer in the product was close to the reported Mw of raw polymer [1,21,22] indicating no significant degradation occurred during the manufacturing. The viscosity of the diluent was determined and was similar to the simulated diluent. The particle size distribution and SEM micrographs indicated the LD microspheres were fine and small particles, which matched the brief descriptions in the literature [1]. The $T_g$ of the LD formulation showed a higher value compared to the raw polymer due to the interaction between peptide and polymer chains and relatively high drug loading (10%) [1,84]. The inventors stated the residual

DCM in the formulation was below 100 ppm [1] and our observation indicated this value was below 1 ppm. Ogawa *et al* [128] studied the release of leuprolide from PLGA by using rotating bottle method and phosphate buffer (pH 7) containing 0.05% Tween 80, and concluded the release kinetics followed zero-order release over 4 weeks by measuring peptide remaining in the microspheres. In this study, we used a sample-and-separate method and microspheres were incubated in PBST and shaken mildly. We observed a slightly faster initial release and a zero-order release after day three. The release was more than 80% after day 35 and complete after day 49.

## 2.5 **Conclusions**

Analytical methods for analyzing the specific components of the 1-month Lupron Depot®, including its diluent, have been developed, and the ingredients have been identified and quantified. The results are consistent with the values reported in the drug label and literature, although we found the LD content by rigorous amino acid analysis and multiple extraction protocols slightly higher than listed in the drug label but not statistically significant. The most complex aspect of the analysis is the evaluation of gelatin in the LD, which may undergo hydrolysis during preparation of microspheres and extraction from drug product. The gelatin appears to be Type B with Bloom 300. Attributes including particle size distribution, residual water and solvent levels, $T_g$, and *in vitro* release demonstrate the unique features of this product. The analysis described here will be useful for further development of generic leuprolide microspheres and also could be applied for reverse engineering analysis of other PLGA-based long acting release products.

## 2.6 **Acknowledgments**

This research was funded by FDA contract HHSF223201510170C A0001 BAA. This paper reflects the views of the authors and should not be construed to represent FDA's views or policies. We gratefully thank Jason Romberg from Anton Paar USA Inc. helped with the determination of viscosity of the injection diluent.

## 2.7 **Supplementary material**

*Table S 2-1. Summary and comparison of measured values to published values.*

| | Ingredient | Character variance | Measured values (Mean ± SEM, n=3-5) | Published values | Reference(s) |
|---|---|---|---|---|---|
| **Chamber 1 (microspheres mixed with mannitol)** | Leuprolide | Content (%) | 8.31 ± 0.05 (Method 1) | 8.5 | [1,77] |
| | | | 8.95 ± 0.31 (Method 2) | | |
| | | | 8.89 ± 0.13 (Method 3) | | |
| | Purified gelatin | Content (%) | 1.55 ± 0.08 | 1.47 | [1,77] |
| | | Type | Type B | - | - |
| | | Mw | Bloom number 300 | - | - |
| | DL-lactic/glycolic acid copolymer | L/G ratio | 74.3/25.7 | 75/25 | [1,54] |
| | | Content (%) | 86.5 ± 0.3 | 75.06 (88.27% in mannitol-free microspheres) | [1,54,77] |
| | | Mw (kDa) | 13.04 ± 0.06 | 12-14 (raw polymer) | [1,22,54] |
| | D-Mannitol | Content (%) | 15.6 ± 0.5 | 14.97 | [1,77] |
| **Chamber 2 (diluent)** | Carboxymethylcellulose sodium (Na CMC) | Viscosity | 2.99 ± 0.06 mPa·s Low viscosity Na CMC | - | - |
| | D-Mannitol | Content (%) | 4.42 ± 0.07 | 5 | [1,77] |
| | Polysorbate 80 | Content (%) | 0.116 ± 0.003 | 0.1 | [1,77] |
| | Water | Content (%) | 94.55 ± 0.01 | 94.4 | [1,77] |
| **Product attributes** | | Particle size | 11.4 ± 0.5 μm | 20-30 μm | [1] |
| | | $T_g$ (°C) | 48.6 ± 0.1 | $T_g$ (42-47 °C) of the microspheres increased as the | [1,84] |

| | | | | |
|---|---|---|---|---|
| | | (Leuprolide loading in mannitol-free microspheres is 10%) | peptide loading (0-8%) was increased. | |
| | Residual solvent | <1 ppm | <100 ppm | [1] |
| | Residual moisture | 0.44 ± 0.10% | - | - |
| **Cumulative release** | Methods | Sample-and-separate method | Rotating bottle method | [128] |
| | Initial burst on day 1 (%) | 22.8 ± 0.4 | - | - |
| | Time to 50% release ($t_{50}$) (days) | 12.3 ± 0.2 | 16.6 | [128] |

# Chapter 3 Effect of manufacturing variables and raw materials on the composition-equivalent formulations

## 3.1 Abstract

The 1-month Lupron Depot® (LD) is a poly(lactic-co-glycolic acid) (PLGA) microsphere product encapsulating 10% water-soluble leuprolide acetate. Despite expiration of patent coverage, no generic product for the LD has been approved in the US, likely due to the complexity of manufacturing processes involved in the LD formulation. Here we describe the development of composition-equivalent PLGA microsphere formulations to the LD as a function of raw material and manufacturing variables, and their influence on the product physicochemical attributes and release performance. The following variables were adjusted at constant theoretical loading of 16.4% leuprolide to achieve the desired 10% loading of peptide: polymer supplier/ polymerization type, gelatin supplier/ bloom number, polymer concentration, 1st homogenization speed and time, volume of primary water phase, 2nd homogenization time, volume of secondary water phase and stirring rate. The loading and encapsulation efficiency (EE) of leuprolide and gelatin were determined to identify composition-equivalent formulations within specification ± 10% of the LD. Key properties of the formulations (e.g., morphology, particle size distribution, glass transition temperature ($T_g$), residual moisture and solvent, and porosity) were characterized to determine the effect of manufacturing variables on the product attributes. The EE of gelatin across all formulations prepared (101 ± 1%) was observed to be much higher than the EE of leuprolide (57 ± 1%). Desirable conditions of polymer concentration, 2nd homogenization time

and volume of 2nd water phase are key to achieving high EE of leuprolide although very high EE (>70%) was not achievable owing to the inability to emulsify primary emulsion with very high viscosity. The leuprolide release kinetics of the formulations were highly similar to the LD in a zero-order manner after ~20% initial burst release, indicating a critical role of the composition on peptide release in this case. The characterization of composition-equivalent formulations described here could be useful for further development of generic leuprolide PLGA microspheres, and for guiding decisions on the influence of process variables on product physicochemical attributes and release performance.

## 3.2 **Introduction**

Polymer based long acting release (LAR) formulations have been widely used in peptide/protein delivery systems to increase bioavailability and reduce dosing frequency. Commonly used biodegradable and biocompatible polymers include poly(lactic-co-glycolic acid) (PLGA) and poly(lactic acid) (PLA) [6,7]. Several PLGA/PLA based microsphere products have gained commercial success and some of them could be good candidates serving as reference drugs for the generic product filing. However, the intricate preparation process may impede the development of PLGA-based generic drug products and increase the difficulties of regulation by U.S. Food and Drug Administration (FDA). Moreover, the composition-equivalent formulations developed under different manufacturing conditions may have different attributes and release performance, which may further influence the drug bioavailability, and in turn drug safety and efficacy. Despite of the investigation of effect of variables on some of the product properties, the relationship between raw materials/manufacturing parameters and products attributes/release performance from the scope of composition-equivalent formulations is not fully studied.

Lupron Depot® (LD) is a group of PLGA/PLA based LARs loaded with water-soluble nonapeptide, leuprolide acetate, for 1-, 3-, 4-, 6-month administration [82]. As a highly active luteinizing hormone-releasing hormone (LH-RH) agonist, leuprolide is able to inhibit the secretion of gonadotropin after continuous administration in therapeutics doses [2,78]. Hence leuprolide is used in the treatment for the hormone sensitive cancer or disorder, like breast and prostate cancer, and endometriosis [78]. It has been a top LH-RH agonist [79] holding a significant market share in the global peptide pharmaceutical market for decades [80]. Despite expiration of patent coverage, no generic product for the LD has been approved in the US. The one-month Lupron Depot® is the PLGA microspheres product launched on US market in 1989 designed for monthly delivery of leuprolide. The LD consists of PLGA microspheres loaded with leuprolide and gelatin (7.5 mg leuprolide acetate, 1.3 mg gelatin and 66.2 mg PLGA), which are prepared by double emulsion solvent evaporation method. D-mannitol (13.2 mg) is added before lyophilization to prevent aggregation of microspheres [1,54]. Therefore, to mimic the LD product one must consider both the complexity of the manufacturing process and an extensive list of product ingredients [6].

In the previous work, we reverse engineered the LD to establish the relevant analytical methods and determine the raw materials, composition, characteristic properties and release kinetics of LD [129]. Based on the published literatures (including multiple patents) and our reverse engineering results, we identified the raw materials of inactive ingredients used in preparation of LD microspheres as Wako 7515 PLGA polymer produced by direct condensation (DC) method [84,130] and beMatrix™ Low Endotoxin type B gelatin with bloom number 300 produced by Nitta Gelatin Inc. First, those raw materials were used in preliminary pilot studies with the manufacturing variables regulated to establish a ‘standard’ condition that could produce

microspheres with desirable attributes and performance (e.g. equivalent loading as LD, high EE, spherical shape, suitable particle size, low initial burst release, and continuous long-term *in vitro* release). Then, a formulation table was established by creating multiple levels of the variables in the standard conditions and different formulations were generated by changing one variable a time from the standard condition. An equivalent PLGA synthesized by ring-opening (RO) polymerization of cyclic $_{D,L}$-lactide and glycolide and various type B gelatins with different bloom numbers were employed to study the influence of raw materials on the leuprolide/PLGA formulations. Finally, sameness, key product attributes and release performance were studied to determine the causes of the possible differences between composition-equivalent formulations and reference product.

We describe the development of composition-equivalent PLGA microsphere formulations to the 1-month LD. The characterization of composition-equivalent formulations described here could be useful for further development of generic or new LAR microsphere products, and for guiding decisions on the influence of manufacturing process variables on product attributes and release performance.

## 3.3 **Materials and Methods**

### 3.3.1 Chemicals and reagents

Leuprolide acetate with purity more than 99% by high-performance liquid chromatography (HPLC) analysis was purchased from Bachem Americas Inc. (Torrance, CA, USA). This leuprolide acetate was detected by UV absorbance at 280 nm of wavelength on ultra-performance liquid chromatography (UPLC) and confirmed to be within 101 ± 3 % (mean ± SEM, n=3) of the USP standard (USP 36 NF 31; catalog number: 1358503; lot: I0M442) in the range of 0-600 μg/mL. Type B gelatin derived from porcine skin with bloom number 300

(beMatrix™ Low Endotoxin Gelatin LS-W) was purchased from Nitta Gelatin Inc. (Osaka, Japan). Type B gelatins derived from bovine skin with bloom numbers 75 and 225 were purchased from Sigma-Aldrich (St. Louis, MO, USA). Wako 7515 PLGA polymer was purchased from Wako Pure Chemical Industries, Ltd. (Tokyo, Japan). Resomer® 752H polymer was purchased from Sigma-Aldrich (St. Louis, MO, USA). Polyvinyl alcohol (PVA) (GOHSENOL™ EG-40P) was purchased from Soarus L.L.C. (Arlington Heights, IL, USA). The AccQ•Tag Chemistry kit was purchased from Waters (Waters Corporation, Milford, MA, USA). The 7.5 mg leuprolide dose for one-month administration Lupron Depot® (LD, AbbVie Inc., North Chicago, IL, USA) was purchased from the Hospital Pharmacy at University of Michigan Health System. All solvents used were HPLC grade and were purchased from Fisher Scientific.

### 3.3.2 Preparation of PLGA microspheres loaded with leuprolide

Leuprolide acetate and gelatin were loaded into PLGA microspheres by solvent evaporation method. The raw materials used in the LD were identified in the previous reverse engineering studies [129] and published references by the originators [1,22,54]. Particularly, the polymer produced by Wako Pure Chemical Industries, Ltd. (Tokyo, Japan) by direct condensation method with average molecular weight of 14000 and LA/GA ratio of 75/25, and type B gelatin derived from porcine skin with bloom number 300 (beMatrix™ Low Endotoxin Gelatin LS-W, Nitta Gelatin Inc., Osaka, Japan) were employed in the procedure. Pilot studies were conducted to establish a ‘standard’ condition that could produce microspheres with desirable attributes and performance (e.g. equivalent loading as LD, high EE, spherical shape, suitable particle size, low initial burst release, continuous long-term release, etc.). The standard condition consisted of dissolving Wako PLGA (500 mg) in 1 mL methylene chloride (DCM). Gelatin (bloom number 300) (10.6 mg) and leuprolide acetate (100 mg) were dissolved in 120

μL dd$H_2O$ at 60 °C. The oil phase was transferred to the water phase and immediately vortexed for 20 s followed by emulsification using a VirTis Tempest $IQ^2$ homogenizer (SP Scientific Inc., Warminster, PA, USA) at speed 10000 rpm for 2 min to form a W1/O emulsion. The obtained W1/O emulsion was cooled in an ice bath for 2 min to increase the viscosity of the primary emulsion. Two mL aqueous 0.25% PVA solution was mixed with the cooled primary emulsion by vortex for 20 s and homogenization at 15000 rpm for 30 s to form the secondary emulsion, i.e. a W1/O/W2 emulsion. The W1/O/W2 emulsion was transferred into 200 mL 0.25% PVA solution and stirred with an overhead stirrer (IKA Eurostar 60 Digital Constant-Speed Mixer, IKA Works, Inc., Staufen im Breisgau, Germany) at 750 rpm for 3 h to evaporate the DCM and solidify the polymer phase. The microsphere suspensions were passed through a 75-μm opening sieve and washed with at least 1 L of water to rinse off the unencapsulated drug and PVA, and remove the large microspheres. The microspheres were collected by centrifugation at 4000 rpm for 7 min at 4 °C and then mixed with a suitable amount of D-mannitol. The microspheres were freeze-dried under vacuum for 48 h.

### 3.3.3 Establishment of the formulation table

To prepare a series of formulations with the same composition as the LD as a function of raw materials and manufacturing variables, a formulation table was created based on the standard condition. The selected manufacturing variables included polymer supplier/ polymerization type, gelatin supplier/ bloom number, polymer concentration, $1^{st}$ homogenization speed and time, volume of primary water phase, $2^{nd}$ homogenization time, volume of secondary water phase and stirring rate. The polymers synthesized by ring-opening (RO) polymerization of cyclic $_{D,L}$-lactide and glycolide with the brand name Resomer® 752H was chosen as the second source of polymer. Another two type B gelatin products with lower bloom numbers from Sigma-Aldrich were used

in the corresponding formulations. For the other microencapsulation variables, the values in the standard condition served as medium level (level 2) and based on which low/ high levels (level 1/ level 3) were created to form the formulation table (Table 3-1). Different formulations were generated by changing one variable a time from the standard condition with the constant theoretical loading of leuprolide at 16.4% and gelatin at 1.73%. The theoretical loading was calculated by:

$$Theoretical\ loading = \frac{Mass\ of\ peptide\ or\ gelatin}{Mass\ of\ PLGA + peptide + gelatin} \times 100\% \quad (3\text{-}1)$$

*Table 3-1. Formulation table*

| # | Parameters | Level 1 | **Level 2 (Standard condition)** | Level 3 |
|---|---|---|---|---|
| *Raw materials* | | | | |
| 1 | Polymer products/ polymerization type | Resomer®/ RO | **Wako/ DC** | |
| 2 | Gelatin suppliers/ bloom number | Sigma/ 225 | **Nitta/ 300** | Sigma/ 75 |
| *Primary emulsion* | | | | |
| 3 | Concentration of PLGA in DCM (mg/mL) | 400 | **500** | 600 |
| 4 | W1/O phase volume ratio (v/v) | 100 μL/ 1mL | **120 μL/ 1mL** | 150 μL/ 1mL |
| 5 | 1st homogenization speed (rpm) | 8000 | **10000** | 12000 |
| 6 | 1st homogenization time (min) | 1 | **2** | 3 |
| *Secondary emulsion* | | | | |
| 7 | 2nd homogenization time (s) | 10 | **30** | 45 |
| 8 | O/W2 phase volume ratio (v/v) | 1/1 | **1/2** | 1/4 |
| *In-liquid drying conditions* | | | | |
| 9 | Stir rate (rpm) | 450 | **750** | 900 |

### 3.3.4 Determination of the PLGA weight average molecular weight (Mw)

Raw polymer was dissolved in dehydrated tetrahydrofuran (THF) at 4 mg/mL. The samples were subjected to gel-permeation chromatography (GPC) installed with two styragel columns (HR 1 and HR 5E columns, Waters, Milford, MA, USA) and a refractive index detector (2414 refractive index detector, Waters, Milford, MA, USA). Polystyrene standards with Mw ranging from 1,000 Da to 50,000 Da were dissolved in the dehydrated THF. Mw of PLGA was calculated by Breeze software (Waters, Milford, MA, USA).

### 3.3.5 Determination of leuprolide acetate loading

The loading of leuprolide acetate was determined by single extraction and amino acid analysis (AAA) [129]. In the single extraction method [21,54], 5 mg of formulation was dissolved in 1mL of DCM and then mixed with 2 mL of 1/30 M sodium phosphate buffer (pH 6.0) by vortex for 5 min. The supernatant of the aqueous phase was obtained after centrifugation (4000 rpm, 5 min) at room temperature. The content of leuprolide acetate in the aqueous phase was determined by UPLC. The UPLC system consisted of an Acquity Quaternary Solvent Manager, Sample Manager-FTN, Column Manager and TUV Detector (Waters, Milford, MA, USA). The separation of leuprolide was carried out using an Acquity UPLC Peptide BEH C18 column (1.7 μm, 2.1 x 100 mm, Waters, Milford, MA, USA) and a gradient elution of acetonitrile with 0.1% TFA (solvent A) and water with 0.1% TFA (solvent B) at a flow rate of 0.5 mL/min as follows: 0 min (25% A), 2 min (35% A), and 2.5 min (25% A), followed by 1 min recovery with initial conditions. The concentration of leuprolide was detected by UV absorbance at 215 nm of wavelength and its peak appeared around a retention time of 2.2 min. The loading of peptide and encapsulation efficiency (EE) were determined by the following:

$$peptide\ loading = \frac{Mass\ of\ peptide\ loaded}{Mass\ of\ microspheres} \times 100\% \quad (3\text{-}2)$$

$$EE\ (\%) = \frac{leuprolide\ loading}{theoretical\ loading} \times 100\% \quad (3\text{-}3)$$

Amino acid analysis was used as the second method to determine the content of leuprolide acetate in the microspheres [129]. Leuprolide contains 9 amino acids and tyrosine (Tyr) and histidine (His) are the specific amino acids that do not exist in the gelatin [1,117] and histidine content was used to determine the content of leuprolide as it provided reproducible results. About 25 mg of leuprolide/PLGA formulations or 5 mg of leuprolide acetate were weighed into hydrolysis tubes and 1.0 mL of 6 N constant boiling HCl (Fisher Chemical, Fair Lawn, NJ, USA) was added. The tubes were purged under nitrogen, sealed under light vacuum, and incubated at 110 °C for 24 h. After incubation, the solution was frozen with liquid nitrogen and lyophilized under vacuum at room temperature. Then, 400 μL of 20 mM HCl was added into each tube to reconstitute the samples. Standard solutions of leuprolide acetate were prepared by dilution of the hydrolyzed leuprolide samples. Derivatization and analysis were performed by using Waters AccQ•Tag Chemistry kit. Briefly, hydrolyzed amino acids were derivatized using the borate buffer (< 5% sodium tetraborate in water) with the Waters AccQ•Fluor reagent (6-aminoquinolyl-N-hydroxysuccinimidyl carbamate). Norleucine was added to the samples during the derivatization and used as the internal standard. The derivatized samples were separated by reverse phase UPLC using a C18 column (AccQ·Tag Ultra C18, 1.7 μm (Millipore Corporation, Milford, MA, USA)) and a gradient elution of solvent A (5% solution of Waters AccQ·Tag Eluent A concentrate in 19 wt% sodium acetate, 6-7 wt% phosphoric acid and 1-2% wt% triethylamine) and solvent B (2% formic acid in acetonitrile solution) at a flow rate of 0.5 mL/min as follows: 0 min (99.9% A), 1 min (98.5% A), 11.5 min (78% A), 13.5 min (40% A)

and 15 min (99.9% A), followed by a 2 min recovery with initial conditions. The urea derivatives yielded during the derivatization were detected by fluorescence (excitation-emission, 250-395 nm).

### 3.3.6 Determination of gelatin loading

Amino acid analysis was performed in the same way as described in the previous section. Standard solutions of gelatin were prepared by dilution of the hydrolyzed Nitta B 300 gelatin samples. Gelatin has several specific amino acids such as alanine (Ala), asparagine and aspartic acid (Asx), hydroxylproline (OH-Pro) and valine (Val), which do not exist in the nonapeptide sequence of leuprolide [1,117]. The second abundant amino acid in the gelatin, alanine, was used to determine the gelatin content in the formulation [129]. The experiment was performed in triplicate. The EE of gelatin was calculated in the similar way as in equation (3-3).

### 3.3.7 Particle size distribution

The median diameter of the microspheres was determined using a Malvern Mastersizer 2000 (Malvern Instruments Ltd., Worcestershire, UK). About 30-40 mg of microspheres were suspended in 1 mL of water and vortexed vigorously before added to the instrument sample dispersion unit. Three measurements were performed per sample at a stirring speed of 2500 rpm and sampling time of 15 s.

### 3.3.8 Surface morphology

The surface morphology of microspheres was examined using a TESCAN MIRA3 FEG scanning electron microscope (SEM) (Kohoutovice, Czech Republic). The microspheres were fixed on a brass stub using double-sided carbon adhesive tape and the samples were prepared electrically conductive by coating with a thin layer of gold for 60 s at 18 mamp under vacuum [123]. Images were taken at an excitation voltage of 2 kV.

### 3.3.9 Glass transition temperature

The $T_g$ of microspheres was determined with a modulated differential scanning calorimeter (mDSC) (TA Instruments, New Castle, DE, USA). Microspheres (3-5 mg) were crimped in DSC aluminum pans. Temperatures were ramped between -20 °C and 90 °C at 3 °C/min. All samples were subjected to a heat/cool/heat cycle. The results were analyzed by using TA TRIOS software and $T_g$ was taken as the midpoint of the reversing heat event.

### 3.3.10 Residual moisture

Residual water content in the microspheres was determined by Karl Fischer (KF) titration. Eighty mg of formulation was weighed into a vial and sealed with a septum cap. Anhydrous dimethyl sulfoxide (DMSO) was added to make the final concentration at 10 mg/mL and the sample was sonicated for 10 minutes before injection into the KF for titration. The moisture in the blank DMSO was also determined.

### 3.3.11 Residual solvent

Residual solvent (DCM) in the microspheres was determined by a Trace 1310 gas chromatograph (GC) (Thermo Fisher Scientific Inc., Waltham, MA, USA). The microspheres were added into a glass vial containing anhydrous DMSO to make the final concentration at ~10 mg/ mL and the vial was sealed. The samples were applied to the GC by headspace injection. The GC conditions were as follows: nitrogen gas was used as the carrier solvent at a flow of 25 mL/min; air flow was 350 mL/min and hydrogen flow was 35 mL/min; the front detector temperature was 240 °C and the front inlet pressure was a constant flow at 2 mL/min. Each sample was agitated for 20 min at 80 °C and 1 mL of the headspace sample was injected into the front inlet with the temperature of 140 °C, split flow of 40.0 ml/min, and a split ratio of 20. The GC column temperature was initially set at 40°C for 15 min, then increased at 10 °C/min to 240

°C and held at 240 °C for 2 min. A standard curve was prepared by adding methylene chloride to DMSO at 1, 10, 50, 100, 250, and 500 ppm.

3.3.12 Porosity

The porosity of microspheres was determined by mercury intrusion porosimetry (AutoPore V Series, Micromeritics, Norcross, GA, USA). About 80-150 mg of microspheres were weighed into 3 cc powder penetrometers to make the final used penetrometer stem volume in the range of 25-80%. Analysis was performed over low and high pressure ranging from 0.5 psia - 61,000 psia with an equilibration of 10 s at each pressure. The curve of the cumulative intrusion volume per gram (mL/g) vs. filling pressure was reported. Interstitial void volume between the particles was filled before the mercury intrusion into the pores and subtracted from the total intrusion volume. The completion of inter-particle space filling was indicated by an abrupt change in filling rate on the intrusion volume curve [131] and the starting point of the corrected intrusion volume used for porosity calculation was determined at the inflection point. The porosity was calculated by the percentage of intrusion volume in the bulk volume.

3.3.13 Release kinetics of leuprolide from PLGA microspheres

Drug release of microspheres was carried out using a sample-and-separate method in release medium PBST (phosphate buffered saline (PBS) + 0.02% Tween 80 + 0.02% $NaN_3$, pH 7.4). Microspheres (~10 mg) were suspended in 1 mL of medium and shaken mildly at 37 ºC. At each time point (1, 3, 7 days and weekly thereafter), the medium was completely collected after centrifugation at 8000 rpm for 5 min and replaced with fresh PBST buffer. The concentration of leuprolide in the supernatant was determined by UPLC as described in the section of determination of leuprolide acetate loading.

3.3.14 Kinetics of erosion

Microspheres (weight = $W_0$) were incubated in release medium at 37 °C under mild agitation. At each time point, the microspheres were washed by dd$H_2O$ and retrieved on 0.20 μm nylon filter paper under reduced pressure. The collected microspheres and filter paper were transferred into pre-weighed tubes and then dried under reduced pressure at room temperature for about 2 days. Dried microspheres were weighed ($W_1(t)$), and the mass loss was calculated by:

$$Mass\ loss\ (\%) = \frac{W_0 - W_1(t)}{W_0} \times 100\% \quad (3\text{-}4)$$

The mass loss after initial burst was plotted against the release after initial burst, which was calculated by:

$$\text{Release after initial burst}(\%) = \frac{A(t) - A_1}{A_L - A_1} \times 100\% \quad (3\text{-}5)$$

where $A(t)$ is the amount of peptide released at time t, $A_1$ is the amount of peptide released on day 1, $A_L$ is the amount of peptide loaded in the microspheres.

3.3.15 Statistical Analysis

All data were expressed as mean ± SEM (n=3 or specifically indicated). Statistical analyses were carried out using GraphPad Prism 8.0.2 software. An ANOVA test was performed to determine the significance. The level of significance was established at the 95% confidence interval (α = 0.05).

## 3.4 **Results**

### 3.4.1 Effect of manufacturing parameters on EE of leuprolide

In most of the formulations, the encapsulation efficiency of leuprolide was above 50% (Figure 3-10). The loading determined by one time extraction (Figure 3-1A) was slightly lower than the results determined by AAA (Figure 3-1B) due to the decreased recovery caused by

peptide-polymer interaction [118,129]. The effect of manufacturing parameters on the EE of leuprolide included: the substitution of ring-opening polymerized PLGA (Mw 15140, 75/25, acid-capped) in place of polycondensation PLGA (Mw 13887, 75/25, acid-capped) slightly increased the EE of leuprolide; when the gelatin was replaced by low bloom number gelatin, the EE was decreased while the substitution of similar bloom number gelatin did not significantly change the EE. To achieve a higher EE of leuprolide, higher polymer concentration, higher 1st homogenization speed, shorter homogenization time, lower 2nd water phase volume and higher stirring rate were preferred.

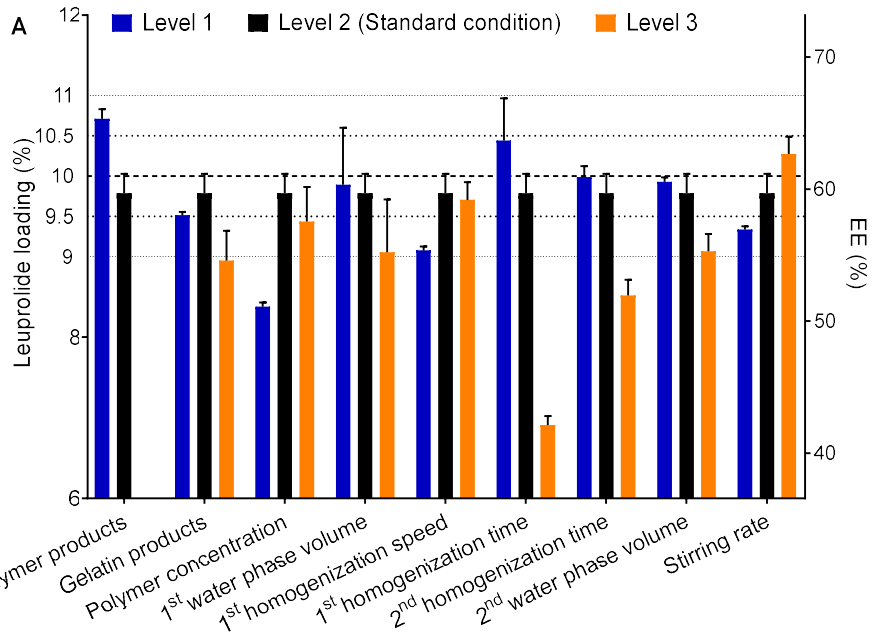

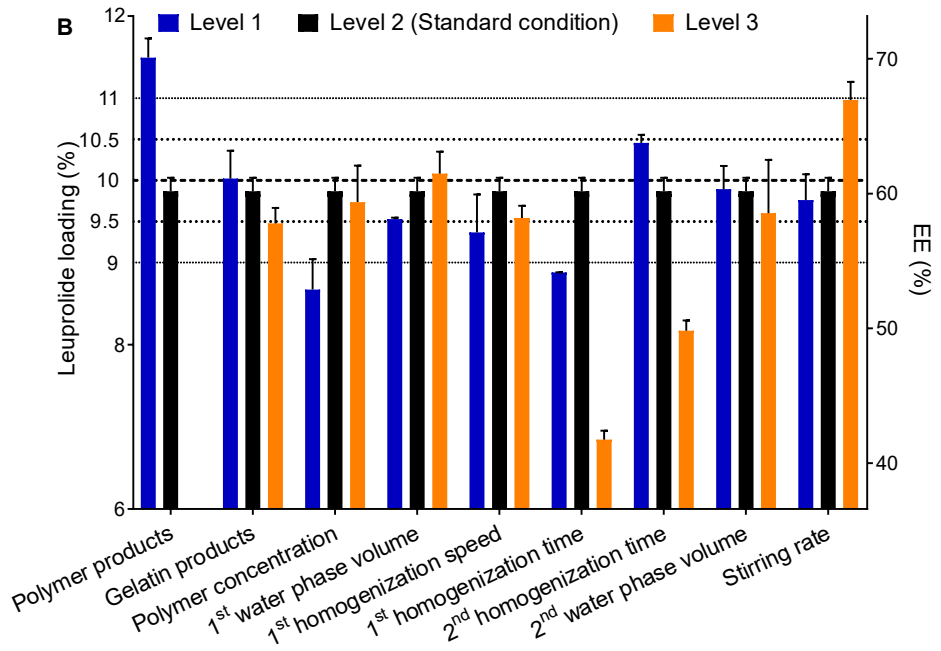


*Figure 3-1. Loading of leuprolide determined by one-time extraction (A) and AAA methods (B). All values present as mean ± SEM (n=3). The dash lines indicate the desired loading of 10% w/w ± 5% or 10% specification.*

### 3.4.2 Effect of manufacturing parameters on EE of gelatin

During development of composition equivalent formulations, the EE of gelatin (101 ± 1%) in the formulations loaded with gelatins with relative high bloom numbers (225 or 300) were observed to be much higher than the EE of LUP. The majority of formulations had desirable loading of 1.73% w/w gelatin (Figure 3-2), as in the LD. When the gelatin was replaced with Sigma 75, the EE was decreased.

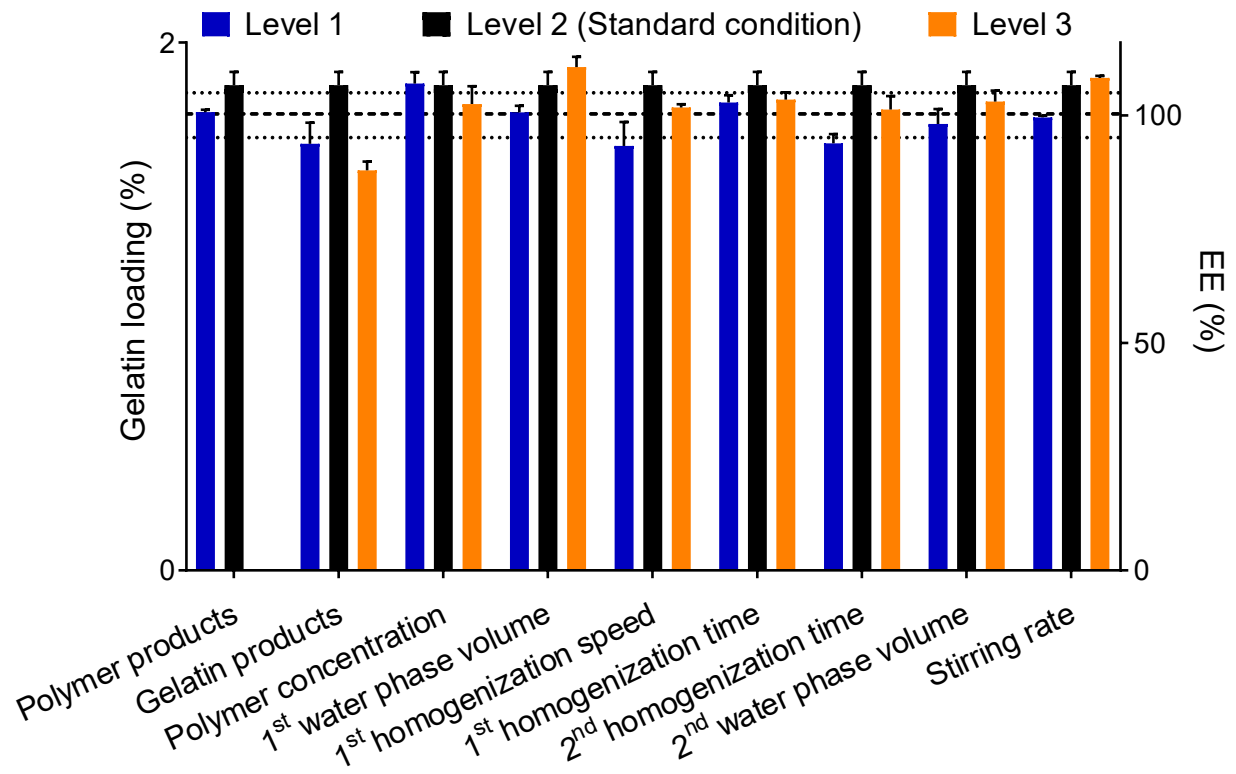


*Figure 3-2. Loading of gelatin. All values present as mean ± SEM (n=3). The dash lines indicate the desired loading of 10% w/w ± 5% specification.*

### 3.4.3 Effect of manufacturing parameters on product attributes

#### *3.4.3.1 Morphology*

SEM micrographs indicated the LD microspheres (Figure 3-3A) were fine and small particles with smooth surface. The formulation made under the standard condition (Figure 3-3B) exhibited higher surface porosity compared to the LD. The figures of sectioned microspheres showed that the LD have small pores distributed homogeneously inside of the microspheres (Figure 3-3C). The standard condition microspheres had a denser polymer core under the porous surface (Figure 3-3D).

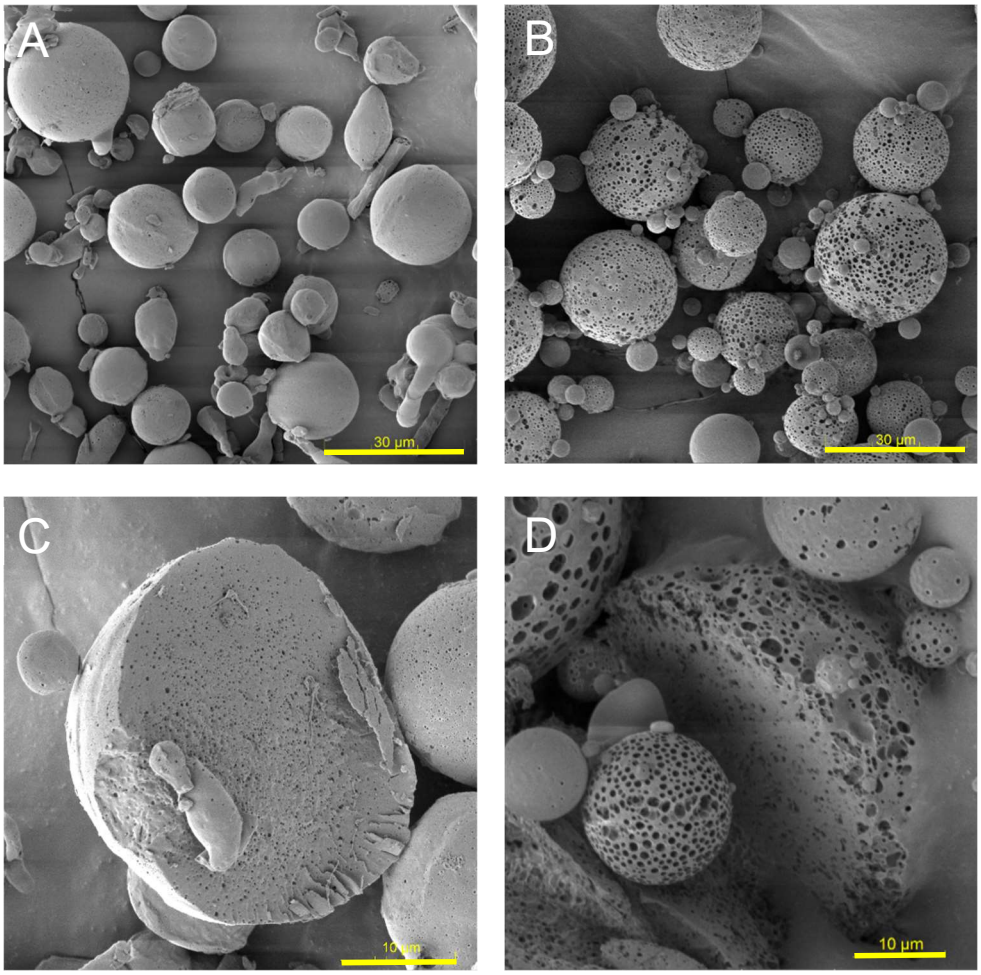


*Figure 3-3. The SEM micrographs of (A) LD microspheres, (B) standard condition microspheres, (C) sectioned LD microspheres, and (D) sectioned standard condition microspheres.*

### *3.4.3.2 Particle size distribution*

The particle size distribution of LD was narrow with a volume median diameter (D (0.5)) (13.5 ± 0.29 µm) (mean ± SEM, n=3) and the standard condition formulation showed a left skewed particle size distribution with a D (0.5) at 36.38 ± 1.95 µm (Figure 3-4A). The effect of manufacturing parameters on the particle size included (Figure 3-4B): replacement of polymer with Resomer polymer increased the particle size; using gelatin with low bloom number decreased the size; when the polymer concentration, primary water phase volume, 1$^{st}$

homogenization speed and 2nd water phase volume were decreased, the particle size was decreased; and increasing 2nd homogenization time significantly decreased the particle size.

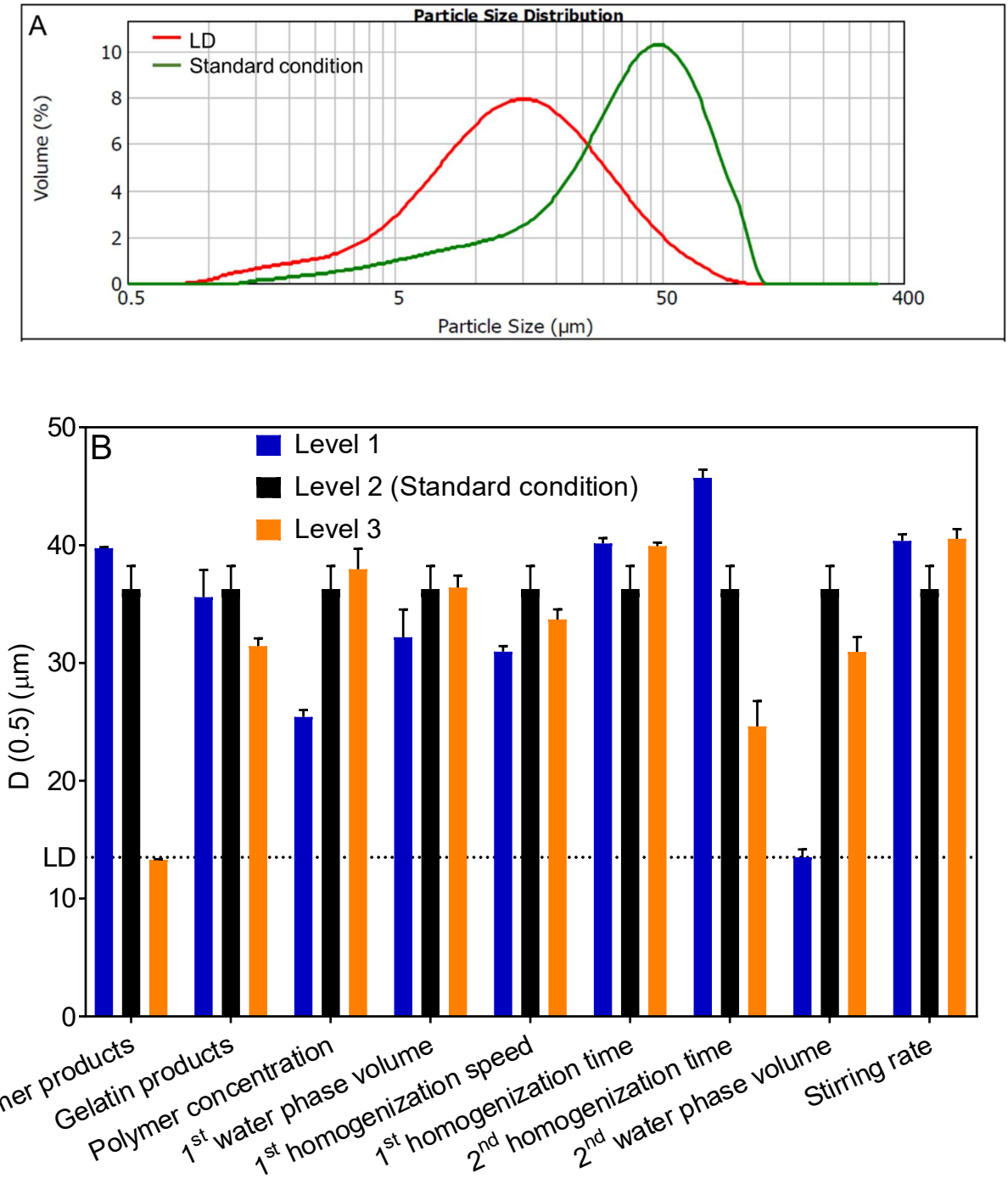


*Figure 3-4. (A) Particle size distribution of LD and standard condition formulation and (B)Median diameters (D 0.5) of the formulations. The columns indicate mean ± SEM (n=3).*

*3.4.3.3 Glass transition temperature ($T_g$)*

Figure 3-5 displays $T_g$ for raw polymer, LD and formulations. The $T_g$ of the raw Wako polymer was observed to be 39.6 ± 0.3 °C and 49.5 ± 0.1 °C for the standard condition formulation (w/ mannitol) (Figure 3-5A&B), consistent with the well-known PLGA-leuprolide interaction upon microspheres form [1]. The $T_g$ of LD microspheres (w/ mannitol) (49.4 ± 0.2 °C) and standard condition formulation (w/ mannitol) were not significantly different ($p>0.05$). The standard condition formulation (w/o mannitol) exhibited a $T_g$ of 49.4 ± 0.2 °C, indicating the presence of mannitol in the formulations did not significantly affect the $T_g$ ($p>0.05$) (Figure 3-5B). In addition, the measured $T_g$ values for all other formulations prepared with the Wako polymer were very close to that of commercial product and standard condition formulation (Figure 3-5C). The $T_g$ of raw Resomer polymer was measured as 46.2 ± 0.1 °C, and the microspheres prepared by this polymer had a $T_g$ of 51.5 ± 0.1 °C. In the formulations prepared by Wako polymer, the loading of peptide varied in a relatively narrow range and showed no significant difference from the LD. The $T_g$ of Resomer polymer was 6.6 °C higher than that of Wako but the increased $T_g$ in microspheres relative to raw polymer was only ~5°C.

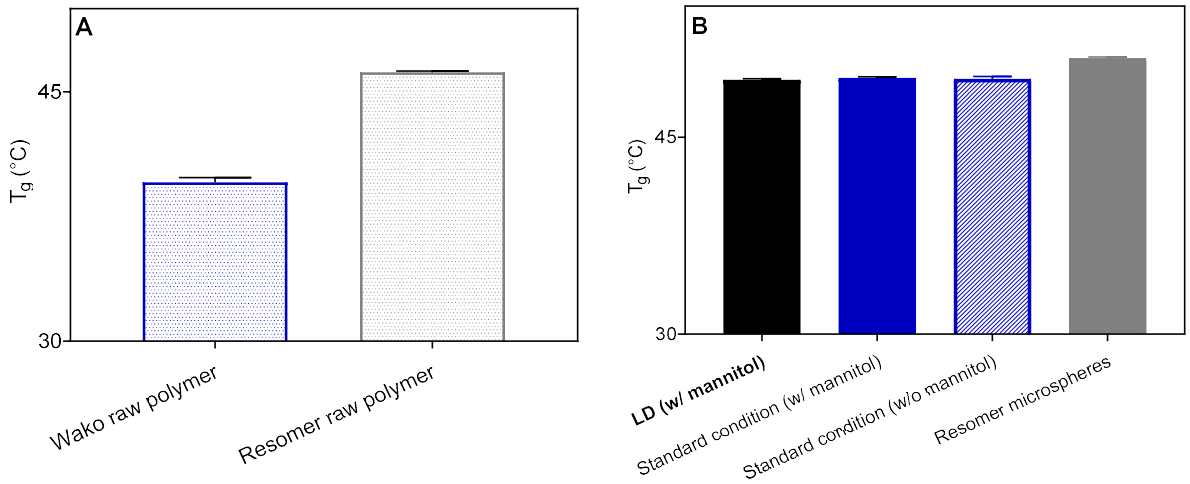

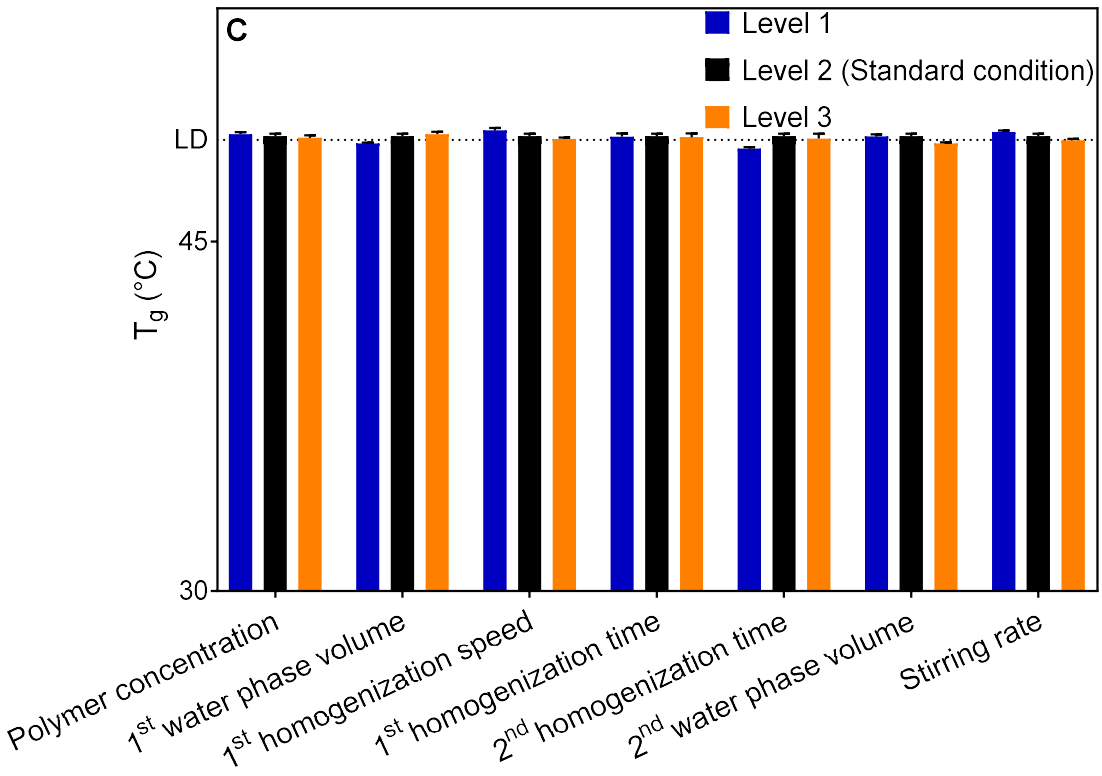


*Figure 3-5. Glass transition temperatures ($T_g$) of (A) raw polymers, (B) LD, standard condition formulation w/ or w/o mannitol and Resomer microspheres, and (C) all other formulations. Data represent mean ± SEM (n=3).*

### *3.4.3.4 Residual moisture, solvent and porosity*

The water content of the LD was determined by Karl Fischer titration to be 0.14 ± 0.06 %. The prepared formulations showed higher residual water content and the majority of them showed the values around 1-2% (Figure 3-6). The highest residual moisture was observed in the formulation prepared with low 1st water phase volume and shortest 2nd homogenization time. The residual content of DCM in LD was lower than 1 ppm. The prepared formulations showed residual DCM in the range of 0.02-0.2% (Figure 3-7). The porosity of the LD was 7.5% (n=2) while the porosity of the standard condition formulation was observed to be 47% (n=2). The other prepared formulations also showed higher level of porosity compared to LD and no significant difference was observed in the group of formulations prepared with different 2nd homogenization time (Figure 3-8).

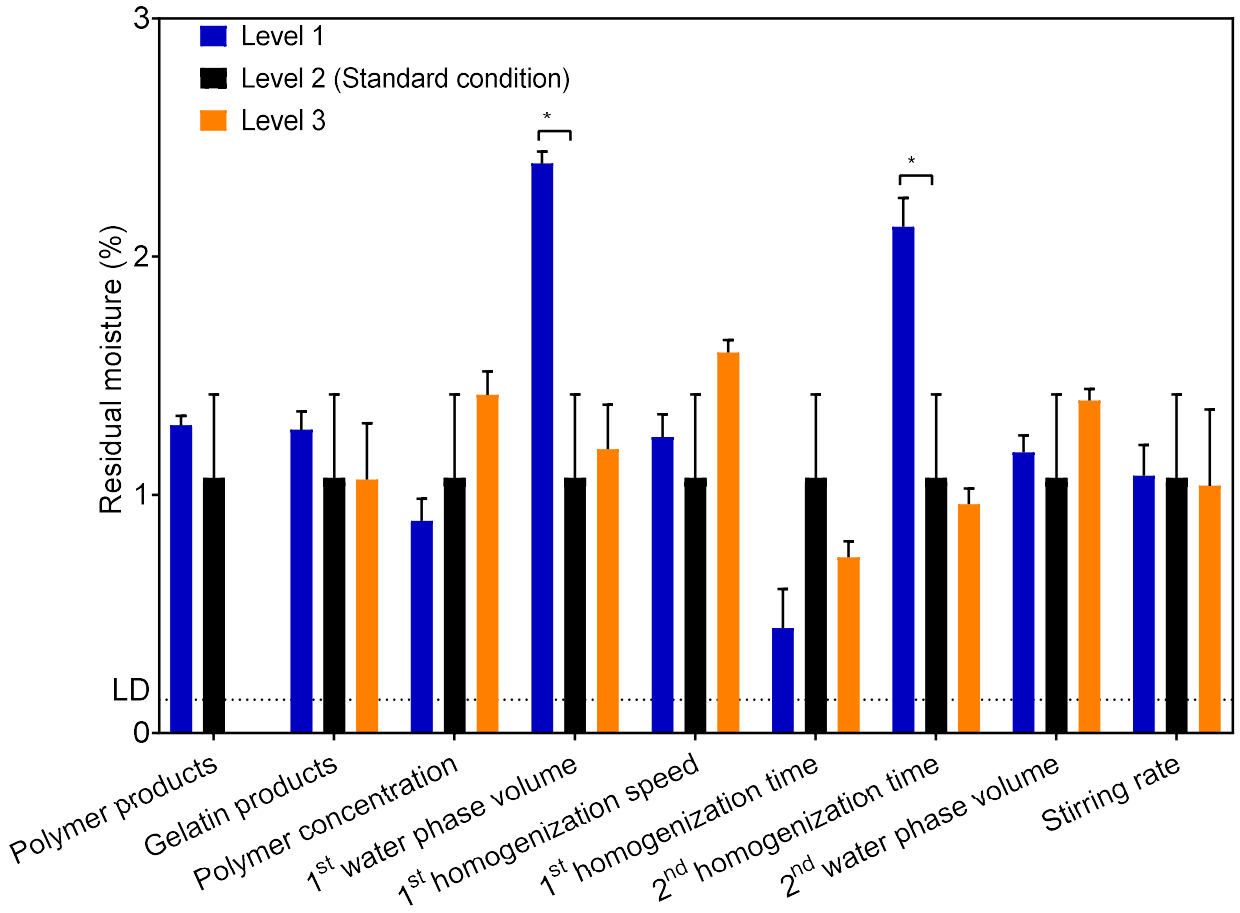


*Figure 3-6. Residual moisture of formulations. Data represent mean ± SEM (n=3). The dash line indicates the value for LD. * $p \leq 0.05$.*

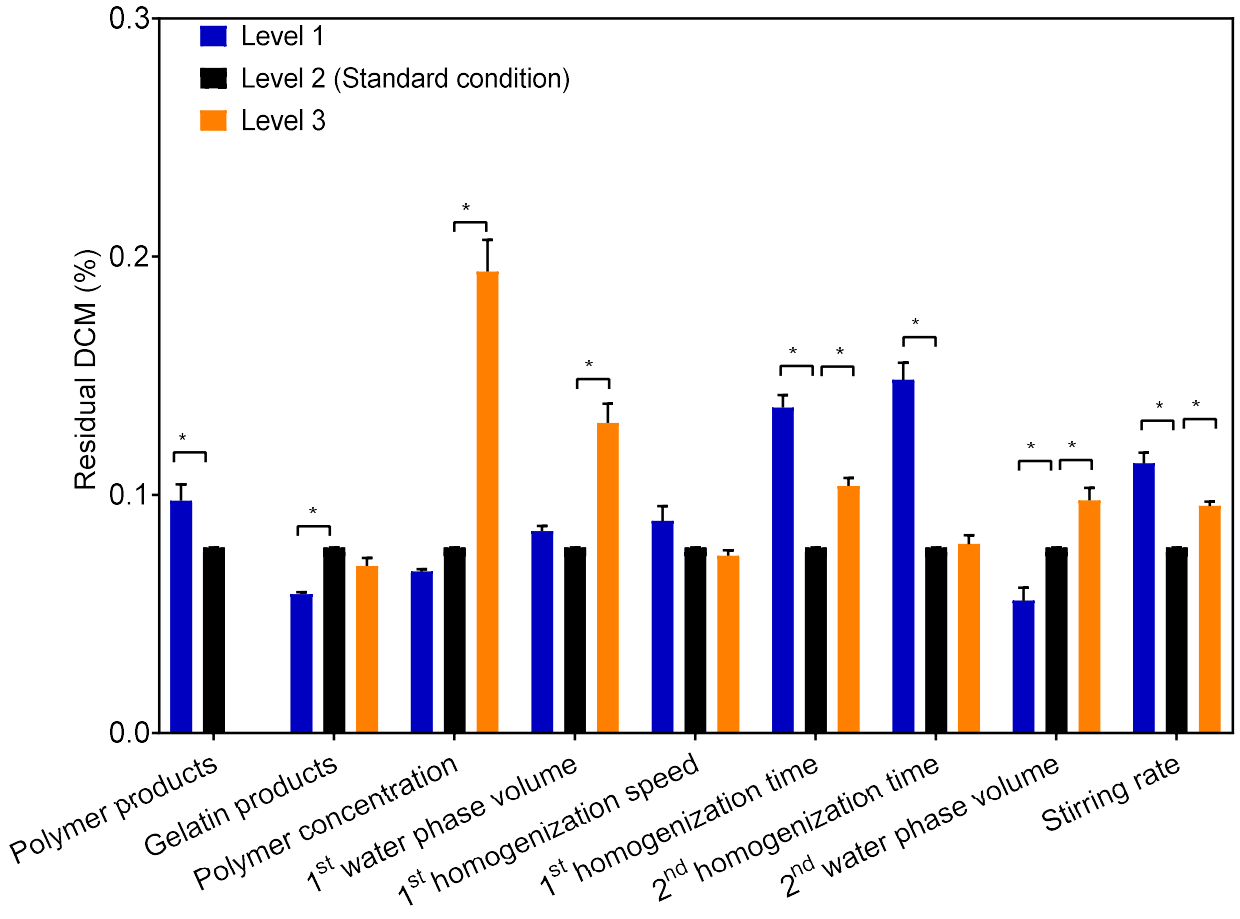


*Figure 3-7. Residual DCM of formulations. Data represent mean ± SEM (n=3). * $p \leq 0.05$.*

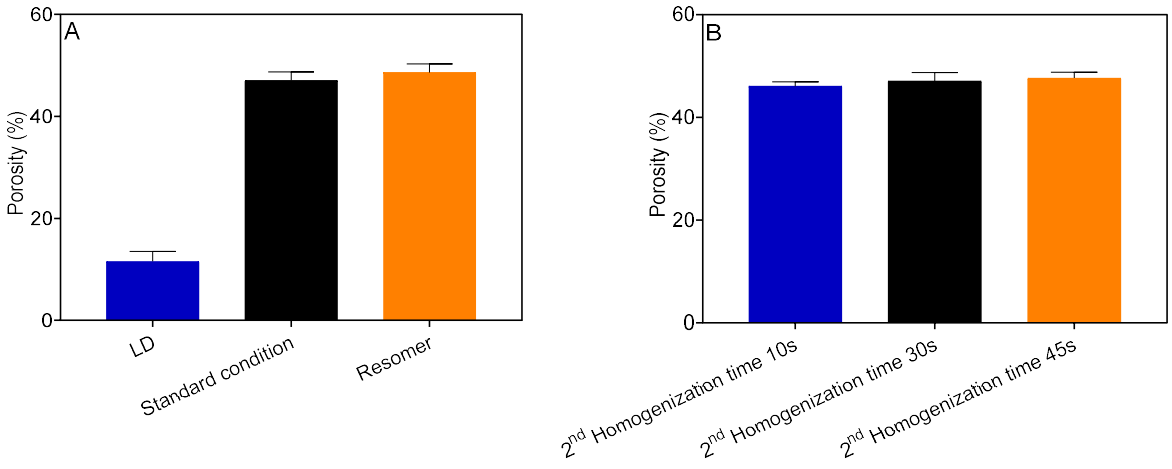


*Figure 3-8. Porosity of formulations in raw material and 2nd homogenization time groups. Data represent mean ± range (n=2).*

### 3.4.4 Release kinetics

The cumulative release of LD in PBST lasted for 7 weeks with a 22.8 ± 0.4% initial burst on day one followed by a zero-order release after day three. The release of peptide from prepared formulations showed similar release pattern (Figure 3-9). In each parameter group, when the formulation had a higher EE, it usually followed with higher initial burst. The loading and release of leuprolide in each formulation was normalized to the values of the standard condition formulation and the comparison is shown in Figure 3-10. When the formulation was prepared with the Resomer polymer, it showed a higher EE and higher initial burst but the release slowed down after 7 days and exhibited slower release compared to the standard condition formulation (0.93 %/day for Resomer formulation vs 1.12 %/day for standard condition formulation; 1.05 %/day for LD based on least squared slope for 7-63 days). The release mechanisms of standard condition formulation, Resomer formulation and LD appeared to be the same (Figure 3-11) and likely to be governed by a combination of factors (desorption and mass loss) [119]. In each case, the kinetics of peptide release was faster than mass loss. Slightly slower mass loss rate from Resomer formulation was consistent with its slower peptide release.

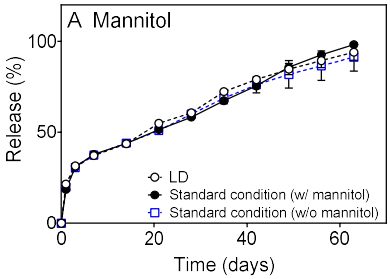
A Mannitol
Release (%)
Time (days)
LD
Standard condition (w/ mannitol)
Standard condition (w/o mannitol)

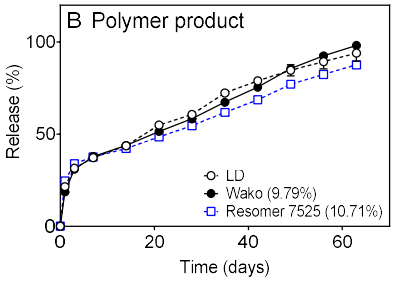
B Polymer product
Release (%)
Time (days)
LD
Wako (9.79%)
Resomer 7525 (10.71%)

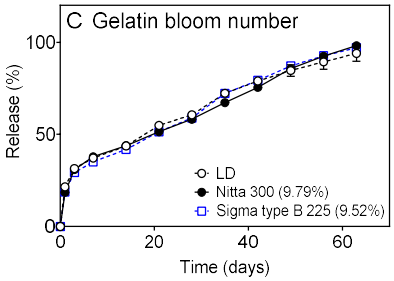
C Gelatin bloom number
Release (%)
Time (days)
LD
Nitta 300 (9.79%)
Sigma type B 225 (9.52%)

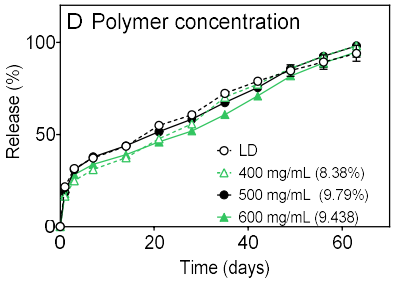
D Polymer concentration
Release (%)
Time (days)
LD
400 mg/mL (8.38%)
500 mg/mL (9.79%)
600 mg/mL (9.438)

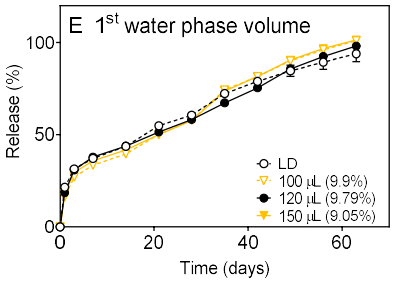
E 1st water phase volume
Release (%)
Time (days)
LD
100 µL (9.9%)
120 µL (9.79%)
150 µL (9.05%)

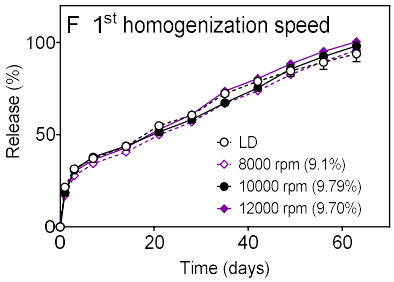
F 1st homogenization speed
Release (%)
Time (days)
LD
8000 rpm (9.1%)
10000 rpm (9.79%)
12000 rpm (9.70%)

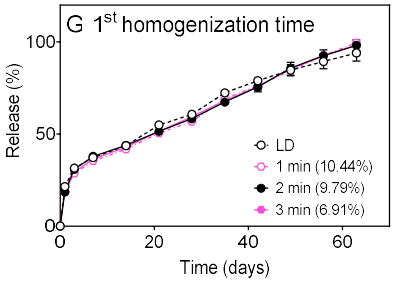
G 1st homogenization time
Release (%)
Time (days)
LD
1 min (10.44%)
2 min (9.79%)
3 min (6.91%)

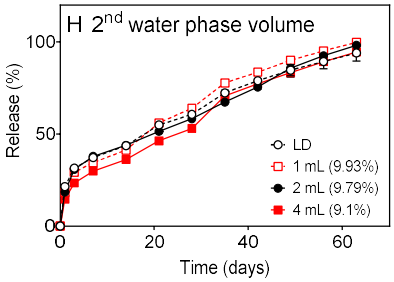
H 2nd water phase volume
Release (%)
Time (days)
LD
1 mL (9.93%)
2 mL (9.79%)
4 mL (9.1%)

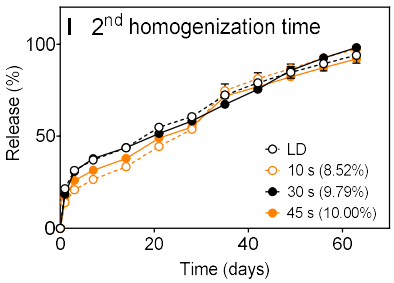
I 2nd homogenization time
Release (%)
Time (days)
LD
10 s (8.52%)
30 s (9.79%)
45 s (10.00%)

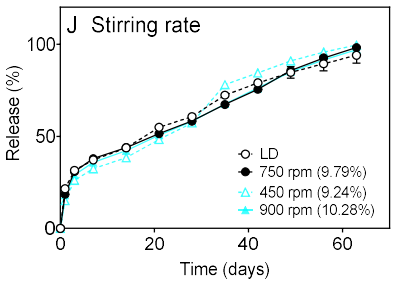
J Stirring rate
Release (%)
Time (days)
LD
750 rpm (9.79%)
450 rpm (9.24%)
900 rpm (10.28%)

*Figure 3-9. Release kinetics of formulations in different variable groups. Data represent mean ± SEM (n=3). The values in the parenthesis are the loading of peptide in each formulation.*

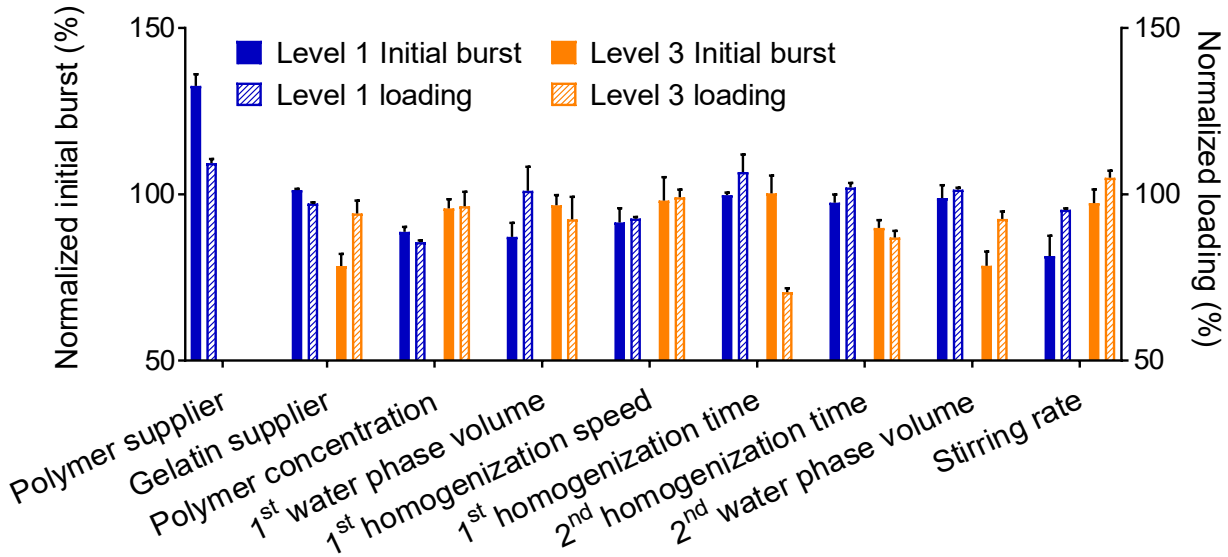


*Figure 3-10. Relationships between normalized initial burst and loading. Data represent mean ± SEM (n=3).*

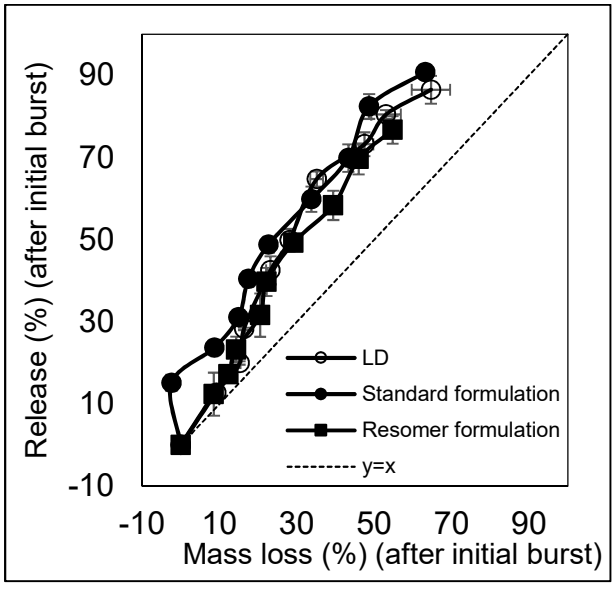


*Figure 3-11. Kinetics of release after initial burst plotted against mass loss kinetics. Data represent mean ± SEM (n=3).*

## 3.5 **Discussion**

Based on the ionic interaction between basic residual of amino acids in the leuprolide and carboxylic group in the polymer chains, Okada *et al* [83] proposed the drug core structure in the microspheres loaded with leuprolide where polymer chain served as a hydrophobic diffusion barrier. We observed ~ 60% EE of the leuprolide and ~100% EE of the gelatin (Figure 3-1 and Figure 3-2). The loss of peptide mainly occurred during the 2$^{nd}$ homogenization step and the loss content increased as homogenization intensity increased (Figure S 3-1). In our study, small microspheres were preferably prepared. Thus, a balanced protocol was established to produce microspheres with desired EE, particle size and release kinetics due to the efficiency of the homogenizer and small sample size. Both leuprolide and gelatin are considered water soluble, but gelatin is only readily dissolved at relatively high temperature [117]. Though leuprolide and gelatin were fully dissolved in the primary water phase at 60 °C, the temperature of the primary emulsion formed after homogenization was close to room temperature (see in Chapter 4, Table 4-1). It is assumed that the gelatin in the disperse phase became a rigid gel-like structure and cannot easily migrate into the outer water phase during the second homogenization.

The effect of raw materials/manufacturing variables on EE of leuprolide and D (0.5) were shown in (Figure 3-1 and Figure 3-4B) and also summarized in Table S 3-1. When the Wako PLGA was replaced with the Resomer polymer, increased EE and slightly larger particle size were obtained in the formulation. The Resomer 752H has similar average molecular weight to Wako polymer but the polymer solution of the formulation showed higher viscosity, which also raised the viscosity of the primary emulsion (*data not shown*) and finally decreased the drug loss during manufacturing. Gelatin products with bloom numbers 75, 225 and 250 were used to prepare three different microspheres. The EE of leuprolide and gelatin in microspheres loaded with gelatins with relatively high bloom numbers were comparable while the EE for both

ingredients was lower in the formulation with low bloom number gelatin (Figure 3-1 and Figure 3-2). The bloom number typically affects the gelatin molecular weight [117] and solution viscosity [132]. The low viscosity of the gelatin 75 solution might be the reason for decreased EE as the primary emulsion size would be expected to be smaller, increasing the mobility and escape of the disperse phase droplets.

When the polymer concentration was decreased from 500 and 600 mg/mL to 400 mg/mL, a drop in the EE of peptide and median diameter of microspheres were observed (Figure 3-1 and Figure 3-4B). The concentrated polymer solution is expected to shorten the evaporation time of DCM [57], and thus more strongly inhibit drug leakage from the polymer matrix to the outer water phase [53,55]. The effect of W1/O ratio on the EE of drug could be complex. Lower W1/O ratio (i.e., lower primary water phase) usually results in an efficient emulsification to form the primary emulsion with good quality and minimize the drug loss during the secondary emulsification [55–57]. But lower primary water phase may also produce smaller microspheres [37,60] with relatively low EE of peptide. Ogawa *et al* [118] observed increased EE of peptide as the particle size of microspheres increased. The water phase volume range (100, 120 and 150 μL) selected in this study did not significantly affect the EE of peptide (Figure 3-1) while slightly decrease the particle size when the smaller primary aqueous phase volume was used. The 1$^{st}$ homogenization speed range (8000, 10000 and 12000 rpm) selected in this study did not significantly affect the EE of peptide but low homogenization speed slightly decreased the EE, which was probably due to the larger emulsion droplets size that increased the chances of drug leakage. However, a significant reduction in the EE of peptide was obtained when the 1$^{st}$ homogenization time increased. Another dramatic decrease of peptide EE occurred when the 2$^{nd}$ homogenization time or secondary water phase volume was increased. The intensity of 2$^{nd}$

homogenization seems to be the critical factor that affects both EE of peptide and particle size. Particularly, when larger water phase was mixed with the primary emulsion, the emulsification efficiency was reduced and led to increased particle size [55,60]. Stirring rate is expected to affect the particle size by controlling break-up of emulsion into small droplets [54,61,63]. In our study, the dispersion of the oil phase into the water phase and separation of nascent emulsion droplets occurred during the 2$^{nd}$ emulsification by the high shear force provided by the homogenizer. Since the soft microspheres droplets already formed before the in-liquid drying step, the stirring rate mainly affected the solvent removal rate. Higher stirring rate will lead to faster evaporation of DCM [93] and solidification of microspheres, and slightly increased EE of peptide was observed in this case.

The $T_g$ of microspheres is mainly affected by the $T_g$ of raw polymer and the interaction between leuprolide and polymer chains. When leuprolide acetate was loaded into microspheres, the basic amino acid residuals in peptide interacted with the carboxylic group in the polymer chains [83] and formed salts throughout the polymer matrix, increasing the $T_g$. Okada *et al* found the $T_g$ of the leuprolide loaded microspheres increased gradually from 42 to 47 °C as the loading increased in the range of 0-8 % [1,84]. However, in our study, for all microspheres prepared with Wako polymer displayed same $\Delta T_g$ (~10 °C) independent of the peptide loading. As the loading of peptide was always ~10%, it is possible that the reported effect has a plateau at high peptide loading (> 8%). Though the Resomer polymer showed a higher $T_g$ than the Wako polymer, the $\Delta T_g$ during the encapsulation of peptide was only ~ 5 °C.

The residual moisture and residual DCM level for LD was lower than the formulations prepared. Particularly, the residual DCM in LD was lower than the lowest detection limitation 1 ppm. These results indicated the in-water drying protocol on a large scale is capable of achieving

low levels of organic solvent in the manufactured microspheres. DCM is classified as solvent to be limited in USP General Chapter <467> with the permitted daily exposure (PDE) at 6 mg/day [133]. The concentration limit could be calculated by [133]:

$$\text{Concentration (ppm)} = (1000\ \mu\text{g/mg} \times \text{PDE (mg/day)})/\ \text{Dose (g)} \quad (3\text{-}6)$$

The total amount of 1-Month LD product in a single administration is 88.2 mg. Since most of the formulations in this study were considered as composition-equivalent and similar dose was proposed to calculate the concentration of DCM exposure. The maximum concentration of DCM in the formulations was 0.19% and the corresponding amount of DCM in the formulation dosed was 0.17 mg, which was lower than the PDE. When the microspheres were prepared with shortest 2$^{nd}$ homogenization time, they displayed the high residual levels of both water and DCM. This is probably due to the relatively large particle size that increased the distance for the solvent to be transported through the polymer matrix and evaporate. When the 2$^{nd}$ water phase volume was increased, the residual DCM was also increased. The DCM close to the surface of the nascent microspheres was removed quickly, which facilitated the formation of a thick skin layer impeding further removal of solvent [58]. Since solvents, like water and DCM, affect the polymer relaxation and work as plasticizer on PLGA [134], the $T_g$ of formed microspheres might be regulated by residual solvent content. However, in this study, we did not see significant difference of $T_g$ in the formulations with different levels of residual solvents. This may indicate that the current difference of residual solvent is not large enough to induce significant changes on the microsphere $T_g$.

The release kinetics for all formulations were highly similar to LD. The biggest difference in the release curves was caused by the initial burst. The theoretical loading of leuprolide was kept constant in the formulation, but the actual loading varied based on the

different input variables. The increased loading of water-soluble drug caused a slightly higher concentration gradient that induced more drug diffusion to release medium. The microspheres prepared with Resomer polymer had a slightly larger particle size, higher loading of peptide and higher initial burst. Meanwhile, studies have shown that increased $T_g$ might decrease the long-term release rate [51,135]. The $T_g$ of both the raw Resomer polymer or the final microspheres were higher than those based on the Wako polymer. After the initial burst, Resomer microspheres showed slightly slower release rate compared the Wako microspheres consistent with the slightly slower polymer erosion. The composition-equivalent microspheres showed much higher porosity than the LD and they were expected to release the peptide more quickly. However, the release of peptide is very insensitive to the length-scale of the PLGA matrix at least when above a certain matrix size [136]. Moreover, the peptide is expected to be released by diffusion mechanisms after the initial burst [119].

## 3.6 **Conclusions**

The composition, $T_g$, and in vitro release kinetics of PLGA microspheres loaded with leuprolide can be largely replicated on the bench scale relative to the LD. The encapsulation efficiency of leuprolide was lowered than that of gelatin. The substitution of ring-opening polymerized PLGA in place of polycondensation PLGA increased $T_g$, EE and initial burst, and slightly reduced long-term release rate. Changing manufacturing variables centered at a standard formulation did not strongly affect release behavior. Changes in initial burst release mirrored changes in drug loading/encapsulation efficiency.

## 3.7 **Acknowledgments**

This research was funded by FDA contract HHSF223201510170C A0001 BAA. This paper reflects the views of the authors and should not be construed to represent FDA's views or policies.

## 3.8 **Supplementary material**

*Table S 3-1. Effect of increased variables on the EE of leuprolide and D (0.5) in formulations.*

| Parameters ↑ | Change of EE | Change of D (0.5) |
|---|---|---|
| Polymer supplier/ | Resomer ↑ | Resomer ↑ |
| Gelatin bloom number | ↑ | ↑ |
| Polymer concentration | ↑ | ↑ |
| 1st water phase volume | Not significant | ↑ |
| 1st homogenization speed | (slightly) ↑ | ↑ |
| 1st homogenization time | ↓ | Standard is the smallest |
| 2nd homogenization time | ↓ | ↓ |
| 2nd water phase volume | ↓ | ↑ |
| Stir rate (rpm) | ↑ | Not significant |

Note: ↑ and ↓ indicates upregulation and downregulation.

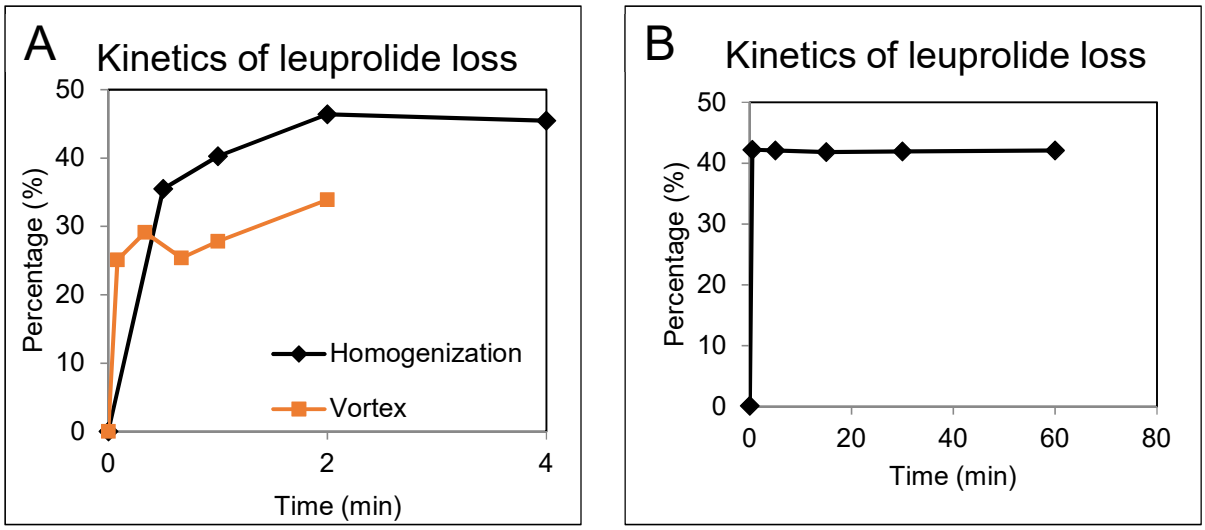


*Figure S 3-1. Kinetics of leuprolide loss during secondary homogenization process and in-liquid drying process.*

# Chapter 4 Mechanistic understanding of microsphere formation

## 4.1 **Abstract**

The emulsion-based microencapsulation method for producing PLGA microspheres suffers from batch-to-batch variation and scale-up difficulties. This study aimed to develop a detailed understanding of the effects of process variables on the complex emulsification processes during encapsulation of leuprolide in PLGA microspheres using a high-shear rotor-stator mixer. Multiple variables during the formation of primary and secondary emulsion were investigated, including: rotor speed (ω) and time (t), dispersed phase fraction (Φ) and continuous phase viscosity ($\mu_c$). The dimensionless Sauter mean diameter of primary emulsion droplet was observed to be proportional to the product of several key dimensionless groups ($\Phi_1, We, Re, \omega_1 t_1$) raised to the appropriate power indices. A new dimensionless group (total surface energy/total energy input to fluid) was used to rationalize insertion of a proportionate time dependence in the scaling of the Sauter mean diameter. The increased viscosity of primary emulsion inhibited drug loss during microencapsulation consistent with literature reports while increased droplet size enhanced drug leakage to the outer water phase. The dimensionless Sauter mean diameter of secondary emulsion was found proportional to the product of three dimensionless groups ($\Phi_2, \frac{\mu_1'}{\mu_{c_2}}, \omega_2 t_2$) raised to the appropriate power indices. The results will be useful for dimensional analysis and improving formulation and manufacturing of PLGA microspheres by the solvent evaporation method.

## 4.2 **Introduction**

Microspheres loaded with water-soluble peptide prepared by double emulsion-solvent evaporation method involves two emulsification steps: 1) emulsification of aqueous peptide phase into organic polymer phase (W1/O) and 2) further emulsification of liquid emulsion (W1/O) in aqueous phase (W2) to form a complex emulsion for microsphere formation. Both steps include key parameters that may affect the attributes of final microspheres, e.g., encapsulation efficiency (EE) of peptide, particle size, and polymer microstructure. The current emulsion-based microencapsulation process is based on trial and error and has batch-to-batch variation and scale-up difficulties [92,93]. Experimental approaches and quantitative correlations have been developed to improve the understanding of how microencapsulation process influence the final product attributes.

Multiple reports [1,137,138] have indicated that the emulsion viscosity, droplet size and stability could affect the drug loading and particle size of the microspheres. The loss of drug during the microencapsulation process has been described by different mechanisms. Alex and Bodmeier [138] indicated the drug was lost from inner water phase to the outer water phase by diffusion through polymer phase or internal water channels. They found decreasing polymer concentration or increasing inner water phase volume could decrease EE of the drug [138]. The inventors of Lupron Depot® found that decreasing the temperature of the primary emulsion dramatically increased the viscosity of the emulsion, and high EE of peptide was obtained [54,86]. Maa and Hsu [137] explained the drug loss by using hydrodynamic model [139]. The microspheres were formed by liquid drop fragmentation mechanism [137]. Turbulent flow generates eddies with different interfacial velocities on the liquid droplets which causes dynamic pressure difference across the droplet [137]. The fragmentation of drops happens when the

pressure difference is higher than the interfacial tension and other cohesive forces [137]. Low viscosity of inner water phase or large droplet size readily induce such fragmentation and the internal aqueous droplets are exposed to outer water phase during secondary emulsion and causes drug leakage [137].

Viscosity ($\mu$) and droplet size ($d$) of the emulsion have been reported to be correlated to [96,97,104–106]: continuous phase viscosity ($\mu_c$) and density ($\rho_c$), dispersed phase viscosity ($\mu_d$) and density ($\rho_d$), dispersed phase volume fraction (Φ), interfacial tension (σ), rotor speed ($\omega$), and mixing time/pass times ($t$). Krieger and Dougherty [114] proposed an empirical model for relative viscosity when the Φ is low based on Einstein equation [111,112] and Taylor [113] equations:

$$\frac{\mu}{\mu_c} = 1 + (\frac{\mu_d}{\mu_c} - 1)\Phi \tag{4-1}$$

The relationships between the geometry, rotor speed, and the energy dissipation of the homogenizer have been studied [94,97–100]. The first step is to link the energy dissipation rate to geometry and rotor speed [94]. Atiemo-Obeng [101] indicated that the definition of power number ($P_O$) and Reynolds number ($Re$) for rotor-stator mixer could be the same as those for conventional stirred tanks. When impeller type and thickness, and turbulent flow conditions are assumed to be constant, $P_O$ becomes nearly constant [102]. The Reynolds number is

$$Re = \frac{\rho\omega D^2}{\mu} = \frac{\omega D^2}{v} \tag{4-2}$$

where $\mu$ is the fluid dynamic viscosity, $\rho$ is the liquid density, $\omega$ is impeller speed and $D$ is rotor diameter. In the full turbulent regime ($Re$ is above ~$10^4$), the $P_O$ is constant of Reynolds number [94] but dependent on the geometry of rotor-stator. The concept developed by Kolmogorov has

been widely used to describe the turbulent eddies [95,103]. The Kolmogorov length scale ($\delta_K$) is expressed as:

$$\delta_K = (\frac{v^3}{\varepsilon})^{1/4} \tag{4-3}$$

where ε is the local energy dissipation rate per unit mass of fluid. For isotropic turbulence, ε can be expressed as the energy loss rate from mixer to the fluid divided by the mass of fluid ($\rho V$) [52,93]:

$$\varepsilon = \frac{\omega^3 D^5 P_O}{V} \tag{4-4}$$

Then the $\delta_K$ is

$$\delta_K = \left[\frac{V {v_c}^3}{\omega^3 D^5 P_O}\right]^{1/4} = \left[\frac{V(\frac{\mu_c}{\rho_c})^3}{\omega^3 D^5 P_O}\right]^{1/4} \tag{4-5}$$

The Sauter mean diameter ($d_{3,2}$), which is defined as the ratio of third and second moments of a particle size distribution, has been used to study the effect of processing variables on the physical properties of emulsion [95]. Based on the values of $\delta_K$ and droplet size, and the viscosity of the solution, different correlations to predict particle size from dimensionless groups have been studied and summarized by Calabrese [92], Leng [107] and Hall *et al* [95,96]. Rotor stator mixers usually produce droplets with the diameter ($d$) on the order of $\delta_K$ and smaller ($\delta_K > d$), and if the stress on drop is inertial, the following correlation exists [92]:

$$\frac{d_{3,2}}{D} \propto (WeRe)^{-\frac{1}{3}} \tag{4-6}$$

where $We$ is the Weber number and defined as

$$We = \rho\omega^2 D^3/\sigma \tag{4-7}$$

When $\delta_K >> d$, the correlations is [92]:

$$\frac{d_{3,2}}{D} \propto (WeRe^4)^{-\frac{1}{7}} \quad (4\text{-}8)$$

If the droplets are broken by turbulent viscous stress, the relationship becomes [92]:

$$\frac{d_{3,2}}{D} \propto (We^{-1}Re^{1/2}) \quad (4\text{-}9)$$

Leng and Calabrese [107] established a correlation between dispersed phase volume and droplet size in the stirred vessel system:

$$\frac{d_{3,2}}{D} = C_1(1 + C_2\Phi)We^{-0.6} \quad (4\text{-}10)$$

where $C_1$ and $C_2$ are constants related to geometry of device and coalesce characteristics of system. A generalized form of the models has been reported as [140]:

$$\frac{d_{3,2}}{D} = C_3We^a Re^b(\frac{\mu_d}{\mu_c})^c \quad (4\text{-}11)$$

where $a$ was found to be -0.6 in many studies [141].

This study aims to provide more understanding of effect of manufacturing variables on the emulsification process using a high-shear rotor-stator mixer by testing the existing correlations in the literature or identifying appropriate relationships that could be applied to a definitive dimensional analysis in the future.

## 4.3 **Materials and Methods**

### 4.3.1 Chemicals and Reagents

Leuprolide acetate with purity more than 99% by high-performance liquid chromatography (HPLC) analysis was purchased from Bachem Americas Inc. (Torrance, CA, USA). Type B gelatin derived from porcine skin with bloom number 300 (beMatrix™ Low Endotoxin Gelatin LS-W) was purchased from Nitta Gelatin Inc. (Osaka, Japan). Wako 7515 PLGA polymer was purchased from Wako Pure Chemical Industries, Ltd. (Tokyo, Japan).

Polyvinyl alcohol (PVA) (GOHSENOL$^{TM}$ EG-40P) was purchased from Soarus L.L.C. (Arlington Heights, IL, USA). All solvents used were HPLC grade and were purchased from Fisher Scientific.

### 4.3.2 Preparation of double emulsions

Double emulsions were prepared according to the solvent evaporation protocol described in Chapter 3 as a function of manufacturing variables listed in the formulation table (Table 3-1). Briefly, the standard condition is shown below and from which emulsions were prepared by changing one variable at a time. Wako PLGA (500 mg) was dissolved in 1 mL methylene chloride (DCM). Gelatin (bloom number 300) (10.6 mg) and leuprolide acetate (100 mg) were dissolved in 120 μL dd$H_2O$ at 60 °C. The oil phased was transferred to the water phase and immediately vortexed for 20 s followed by emulsification using a VirTis Tempest IQ$^2$ homogenizer (SP Scientific Inc., Warminster, PA, USA) at speed 10000 rpm for 2 min to form a W1/O emulsion. The obtained W1/O emulsion was cooled in ice bath for 2 min to increase the viscosity of the primary emulsion. Then 2 mL aqueous 0.25% PVA solution was mixed with the cooled primary emulsion by vortex for 20 s and homogenization at 15000 rpm for 30 s to form the secondary emulsion, i.e. a W1/O/W2 emulsion.

### 4.3.3 Determination of viscosity

The viscosity of primary and secondary emulsion, and other samples at room temperature were determined by *micro*VISC™ viscometer (Rheosense, Inc., San Ramon, CA, USA). The room temperature in the lab was ~23.5 °C. The sample was injected into the measuring cell that contains a rectangular slit flow channel at a constant flow rate where multiple pressure sensors monitored the pressure drop from the inlet to the outlet [142]. The pressure drop was correlated with the shear-stress and the shear rate and shear stress were related to the geometry of the

rectangular slit and the flow rate [142]. The viscosity of the primary emulsion after cooling process was determined by *m*-VROC viscometer (Rheosense, Inc., San Ramon, CA, USA) with temperature precisely controlled at 4 ± 0.15 °C.

### 4.3.4 Determination of emulsion size

The size of primary emulsion droplets was determined by a Zeiss Axio Lab light microscopy (Carl Zeiss AG, Oberkochen, Germany) equipped with 40X objectives. Briefly, the emulsion was added to the glass microscope slide and glass cover was placed over the sample. The pictures of emulsions were taken by a Cannon camera. MATLAB was used to identify the boundary of each droplet and the particle size distribution. The Sauter mean diameter was calculated by:

$$d_{3,2} = \frac{\sum_{i=1}^{n} d_i^3}{\sum_{i=1}^{n} d_i^2} \tag{4-12}$$

where $d_i$ is the diameter of the i$^{th}$ droplet.

The size of secondary emulsion droplets was determined using a Malvern Mastersizer 2000 (Malvern Instruments Ltd., Worcestershire, UK). A certain volume of the emulsion solution was added in the instrument sample dispersion unit to enable the obscuration of the sample around ~10%. Three measurements were performed per sample at a stirring speed of 2500 rpm and sampling time of 15 s. To achieve repeatable results, all samples were measured within 10-15 min after the secondary emulsions were formed.

### 4.3.5 Dimensional analysis

The number of particles ($N_p$) could be calculated by the total mass and mass of particles:

$$N_p = \frac{\rho_d V_d}{\rho_d \frac{4}{3}\pi r_{3,2}^3} = \frac{6V_d}{\pi d_{3,2}^3} \tag{4-13}$$

where $\rho_d$ is the density of the dispersed phase and $r_{3,2}$ is the radius of the particles. Then the total surface energy of particles is:

$$\gamma = N_p \cdot 4\pi r_{3,2}^2 \cdot \sigma = 6d_{3,2}^{-1}\mathrm{V}_d\sigma \tag{4-14}$$

Based on equation (4-4), the input energy on fluid could be calculated by:

$$\varepsilon \cdot \rho_c \mathrm{V} \cdot \mathrm{t} = \rho_c \omega^3 D^5 P_O t \tag{4-15}$$

Thus, the ratio of input energy and surface energy (X) is:

$$\mathrm{X} = \frac{\rho_c \omega^3 D^5 P_O d_{3,2} t}{6V_d\sigma} \propto \frac{\rho_c \omega^3 D^5 P_O d_{3,2} t}{V_d\sigma} \tag{4-16}$$

The ratio of $\delta_K$ and $d_{3,2}$ is:

$$\mathrm{Y} = \frac{\delta_K}{d_{3,2}} = \left[\frac{V(\frac{\mu_c}{\rho_c})^3}{\omega^3 D^5 P_O}\right]^{1/4} \frac{1}{d_{3,2}} \tag{4-17}$$

The dimensionless groups X and Y were used to develop non-dimensional correlations between emulsion size and process variables.

## 4.4 **Results and discussion**

### 4.4.1 Effect of manufacturing variables on primary emulsion viscosity and droplet size

The experimental conditions and parameters of primary emulsion are summarized in Table 4-1. When the concentration of polymer was increased, the viscosity of continuous phase ($\mu_{c_1}$) and $\mu_1$ both significantly increased (Figure 4-1A). When the 1st homogenization time ($t_1$) increased from 60 s to 180 s, the viscosity of primary emulsion ($\mu_1$) slightly decreased, and the correlation could be described by a linear regression (Figure 4-1B). In the series of composition-equivalent formulations used to define the emulsification conditions studied here, the theoretical loading of peptide and gelatin were controlled at constant values. When the polymer

concentration was increased, the amount of drug was also increased while the volume of water phase was not changed. Then the concentration of drug as well as the viscosity ($\mu_d$) of the dispersed phase was increased. The primary water phase is a highly concentrated solution of leuprolide and gelatin, and $\mu_d >> \mu_{c_1}$. Based on equation (4-1), it is expected the viscosity of primary emulsion #1-3 is dramatically increased. The results (Table 4-1) also indicated increasing 1st homogenization speed ($\omega_1$) or increasing water phase volume within relatively narrow ranges (8000 - 12000 rpm for $\omega_1$, and 0.10 - 0.15 for $\Phi_1$) did not significantly affect the emulsion viscosity.

*Table 4-1. Summary of characteristics of primary emulsions formed.*

| Emulsion # | $C_p$ (mg/mL) | $\mu_{c_1}{}^*$ (mPa·s) | $\Phi_1$ | $\omega_1$ (rpm) | $t_1$ (s) | $T_1$ (°C) | $d_1{}^*$ (μm) | $d_{3,2}$ (μm) | $\mu_1{}^*$ (mPa·s) | $\mu_1'{}^*$ (mPa·s) |
|---|---|---|---|---|---|---|---|---|---|---|
| 1-1 | 500 | 23.64 ± 0.03 | 0.12 | 10000 | 120 | 29.0 | 1.74 ± 0.01 | 2.62 | 122.2 ± 0.6 | 1281 ± 35 |
| 1-2 | 400 | 17.87 ± 0.01 | 0.12 | 10000 | 120 | 24.7 | 0.63 ± 0.01 | 2.23 | 62.1 ± 0.3 | 550 ± 6 |
| 1-3 | 600 | 48.62 ± 0.08 | 0.12 | 10000 | 120 | 30.3 | 5.31 ± 0.02 | 5.50 | 239.7 ± 6.1 | 3131 ± 17 |
| 1-4 | 500 | 23.64 ± 0.03 | 0.1 | 10000 | 120 | 28.7 | 1.45 ± 0.02 | 2.88 | 111.1 ± 1.1 | 787 ± 88 |
| 1-5 | 500 | 23.64 ± 0.03 | 0.15 | 10000 | 120 | 28.7 | 1.83 ± 0.02 | 2.33 | 116.5 ± 1.2 | 1768 ± 20 |
| 1-6 | 500 | 23.64 ± 0.03 | 0.12 | 8000 | 120 | 26.9 | 2.11 ± 0.02 | 4.77 | 107.2 ± 2.2 | 1032 ± 56 |
| 1-7 | 500 | 23.64 ± 0.03 | 0.12 | 12000 | 120 | 28.3 | 0.74 ± 0.01 | 1.43 | 115.3 ± 2.4 | 1098 ± 52 |
| 1-8 | 500 | 23.64 ± 0.03 | 0.12 | 10000 | 60 | 27.9 | 2.87 ± 0.07 | 4.28 | 131.4 ± 2.7 | 1444± 30 |
| 1-9 | 500 | 23.64 ± 0.03 | 0.12 | 10000 | 180 | 28.4 | 0.95 ± 0.01 | 2.11 | 99.1 ± 2.0 | 1199± 42 |

*Note: $C_p$: polymer concentration; $\mu_{c1}$: viscosity of primary continuous phase; $\Phi_1$: dispersed phase fraction in primary emulsion; $\omega_1$: 1$^s$ homogenization speed; $t_1$: 1$^{st}$ homogenization time; $T_1$: temperature after 1$^{st}$ homogenization; $d_1$: mean droplet size of primary emulsion; $d_{3,2}$:Sauter mean diameter of primary emulsion; $\mu_1$: viscosity of primary emulsion at room temperature; $\mu_1$': viscosity of primary emulsion at 4 °C. $^*$ values indicate mean ± SEM.*

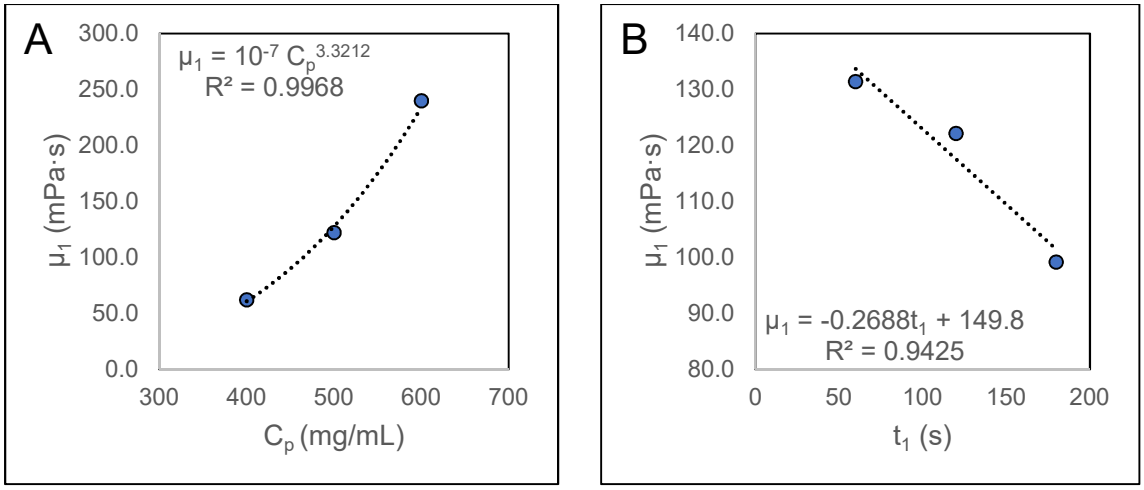


*Figure 4-1. Correlations between primary emulsion viscosity with (A) continuous phase concentration and (B) homogenization time.*

The correlations between primary emulsion droplet size ($d_{3,2}$) with (A) dispersed phase fraction, (B) 1st homogenization speed, (C) 1st homogenization time and (D) viscosity of continuous phase were fitted by power law with index -0.52, -2.96, -0.65 and 0.93, respectively (Figure 4-2). The indices allowed the establishment of a correlation between $d_{3,2}$ and independent variables:

$$d_{3,2} = f(V_d, V_c, \mu_{c_1}, \rho_c, \omega_1, t_1, \sigma, D) \tag{4-18}$$

where $V_d$ and $V_c$ are the volume of the dispersed phase and continuous phase and $\Phi_1$ could be expressed by $\frac{V_d}{V_c}$. There are nine variables in equation (4-18), then 9-3 = 6 independent dimensionless groups are needed to describe dimensionless Sauter mean diameter:

$$\frac{d_{3,2}}{D} = f(\Phi_1, We, Re, \omega_1 t_1, \frac{D^3}{V_c}) \tag{4-19}$$

where the $Re$ and $We$ could be calculated by equations (4-2) and (4-7). The interfacial tension between DCM and water has been reported at 28.3 mN/m [143,144]. In this study, both $D$ and $V_c$ were constant and the equation (4-19) was reduced to:

$$\frac{d_{3,2}}{D} \propto f(\Phi_1, We, Re, \omega_1 t_1) \tag{4-20}$$

Based on the generalized form in (4-11), the power assigned to the Weber number was -0.6. The appropriate index for the other dimensionless groups were determined by using the relationships in Figure 4-2. The dimensional correlation between $d_{3,2}$ and product of $({V_d}^{-0.5} {V_c}^{0.5} {\mu_c}^{1.13} {\rho_c}^{-1.73} {t_1}^{-0.667} {\omega_1}^{-3} \sigma^{0.6} D^{-3})$ is shown in Figure 4-3A and the correlation between $\frac{d_{3,2}}{D}$ and product of dimensionless groups (i.e., ${\Phi_1}^{-0.5} We^{-0.6}\ Re^{-1.13} (\omega_1 t_1)^{-0.667}$) is shown in the insert. Excellent linearity between the process variables and $d_{3,2}$ was found with $R^2$=0.99.

Another approach to develop the correlates included the dissipation of total input energy to the fluid and surface energy of the formed droplets. The dimensionless groups X and Y (equations (4-16) and (4-17)) were created to predict the size of the emulsion size. The product of $X^{-\frac{2}{3}}$ and $Y^{\frac{4}{3}}$ is:

$$X^{-\frac{2}{3}} Y^{\frac{4}{3}} \propto \frac{V_d^{\frac{2}{3}} V_c^{\frac{1}{3}} \sigma^{\frac{2}{3}} \mu_{c_1}}{\rho_{c_1}^{\frac{5}{3}} \omega_1^{\,3} D^5 P_O t_1^{\frac{2}{3}} d_{3,2}^2} \tag{4-21}$$

To obtain the correct power index of variables, dimensionless groups $\left(\frac{V_d}{V_c}\right)^{-7/6}$ and $\frac{D^3}{V_c}$ were also introduced, then:

$$\frac{d_{3,2}}{D} \propto X^{\frac{2}{3}} Y^{-\frac{4}{3}} \left(\frac{V_c}{D^3}\right)^1 \left(\frac{V_d}{V_c}\right)^{\frac{7}{6}} \tag{4-22}$$

$$d_{3,2} \propto {V_d}^{-\frac{1}{2}} V_c^{\frac{1}{2}} {\mu_{c_1}}^1 {\rho_{c_1}}^{-\frac{5}{3}} {t_1}^{-\frac{2}{3}} {\omega_1}^{-3} \sigma^{\frac{2}{3}} D^{-3} \tag{4-23}$$

This correlation was tested in Figure 4-3B and there is also a good linearity with $R^2$=0.97. The dimensionless correlation above could also be expressed by using the same dimensionless groups as in the previous fitting (4-20):

$$\frac{d_{3,2}}{D} \propto {\Phi_1}^{-1/2} We^{-2/3}\, Re^{-1} (\omega_1 t_1)^{-2/3} \tag{4-24}$$

However, there is a deviation from linearity for the emulsions with large particle size. The $d_{3,2}$ of primary emulsion was significantly affected by the homogenization speed while the effect of homogenization time and dispersed phase fraction was weaker.

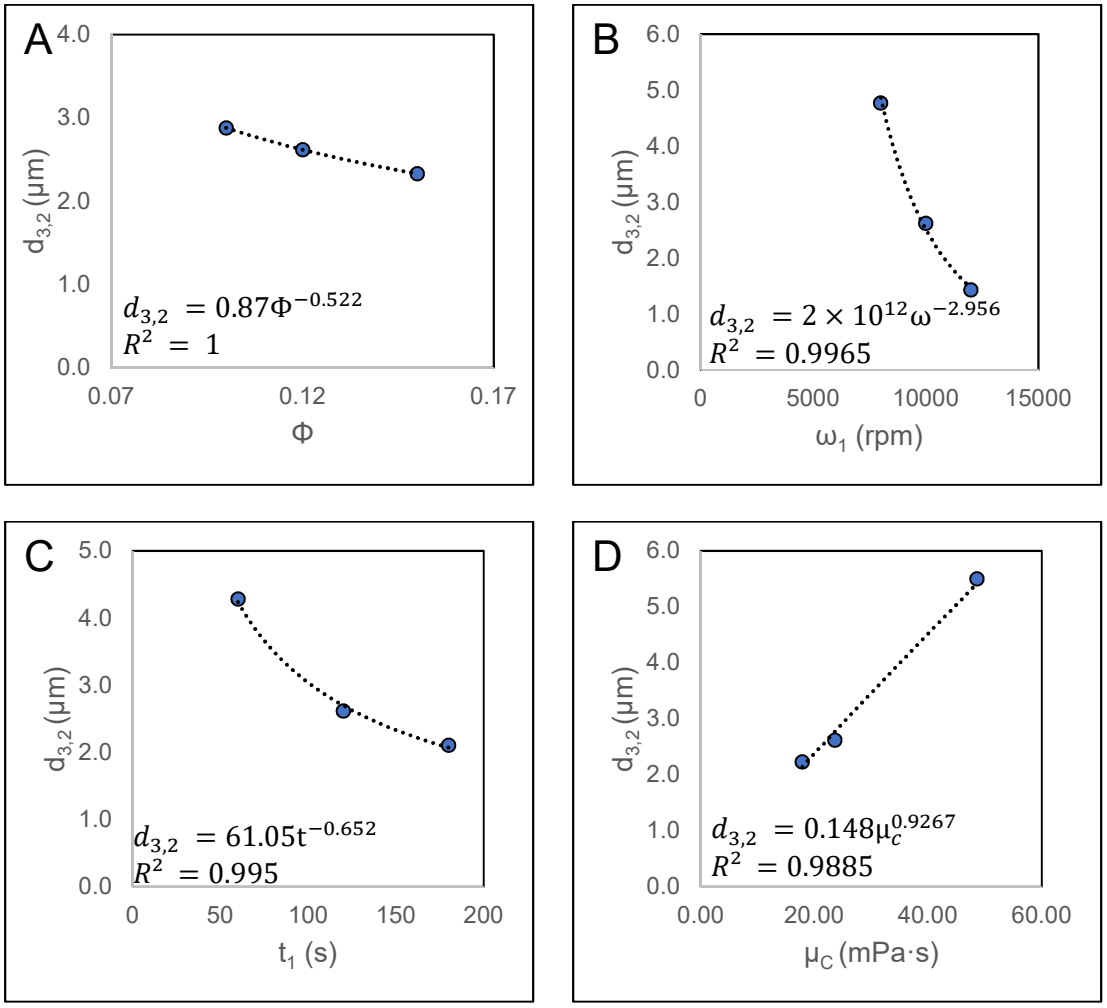


*Figure 4-2. Correlations between primary emulsion droplet size ($d_1$) with (A) dispersed phase fraction and (B) homogenization speed, (C) homogenization time and (D) polymer concentration.*

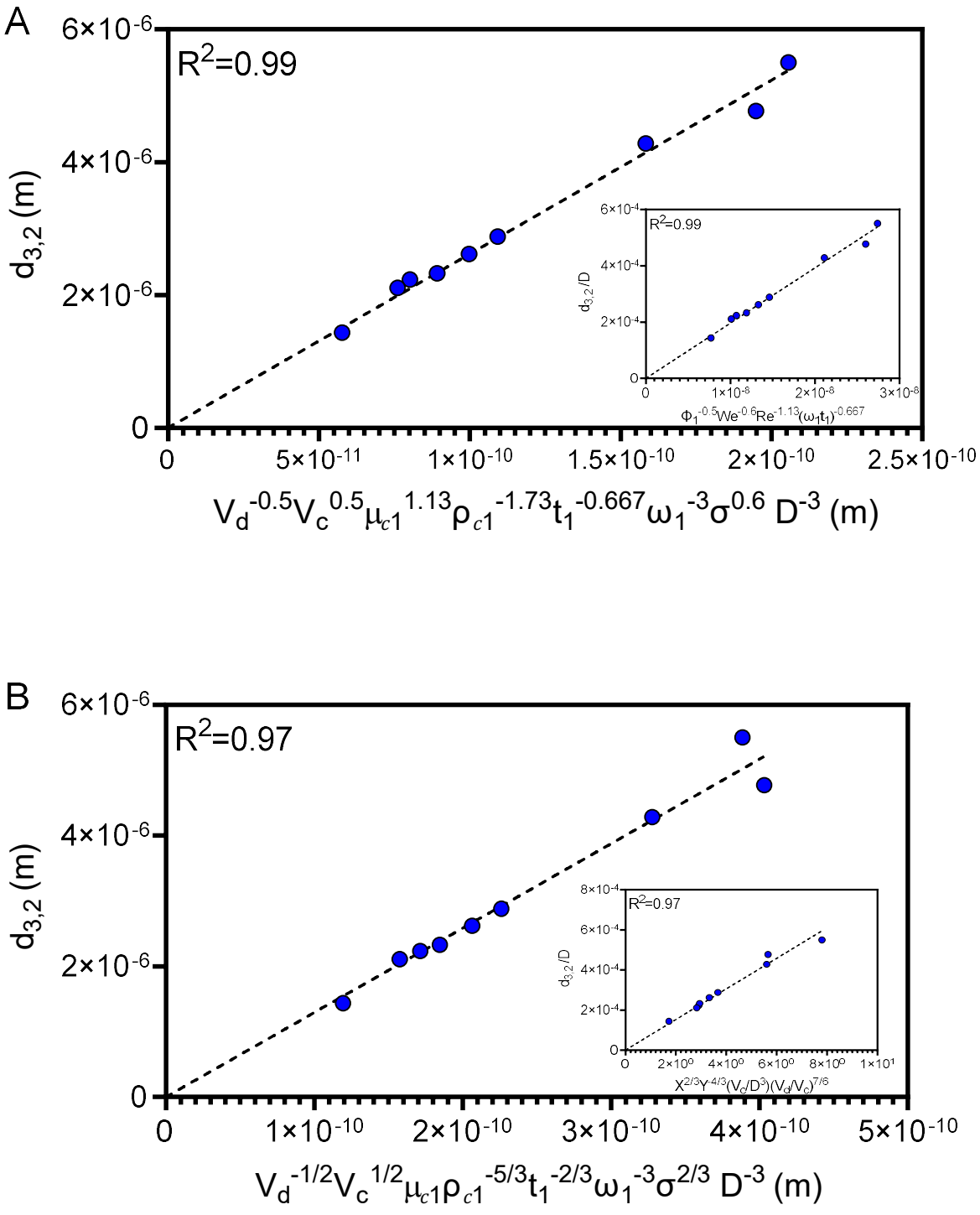


*Figure 4-3. Generation of master curve for correlations between primary emulsion size and manufacturing variables.*

### 4.4.2 Effect of primary emulsion viscosity and droplet size on EE

Primary emulsion viscosity before and after the cooling process, mean droplet size ($d_1$) and the EE of peptide in the corresponding microspheres are shown in Figures 4-4 and 4-5. The viscosity of primary emulsion or primary water phase have been shown by Takeda [54] to be a critical step to achieve high EE of peptide. The cooling step significantly increased the viscosity of primary water phase ($\mu_1'$) for all emulsions (Figure 4-4). When the polymer concentration was increased from 400 mg/mL to 500 mg/mL, the viscosity of primary emulsion was increased (Figure 4-4A) and decreased the drug leakage from inner water phase to the outer water phase. When the $C_p$ was further increased to 600 mg/mL, both the primary emulsion viscosity and the emulsion droplet size (Figure 4-5A) were increased. The later result might be an offset that prevents the EE elevation. A similar phenomenon was observed in the primary water phase volume group. The emulsion viscosity after cooling increased gradually as dispersed phase fraction was raised (Figure 4-4B) while the droplet size was also elevated (Figure 4-5B). Alex and Bodmeier [138] found that when the amount of water was increased, the thickness of polymer phase around the water phase decreased and more water droplets were connected with the continuous phase, leading to higher drug leakage. Therefore. the water phase volume range (100, 120 and 150 μL) selected in this study did not significantly affect the EE of peptide. By increasing the homogenization speed or increasing homogenization time, the droplet size was decreased (Figure 4-5 C&D). However, the viscosity of the emulsion appeared to be dominant factor that regulated the EE in these two groups (Figure 4-4 C&D).

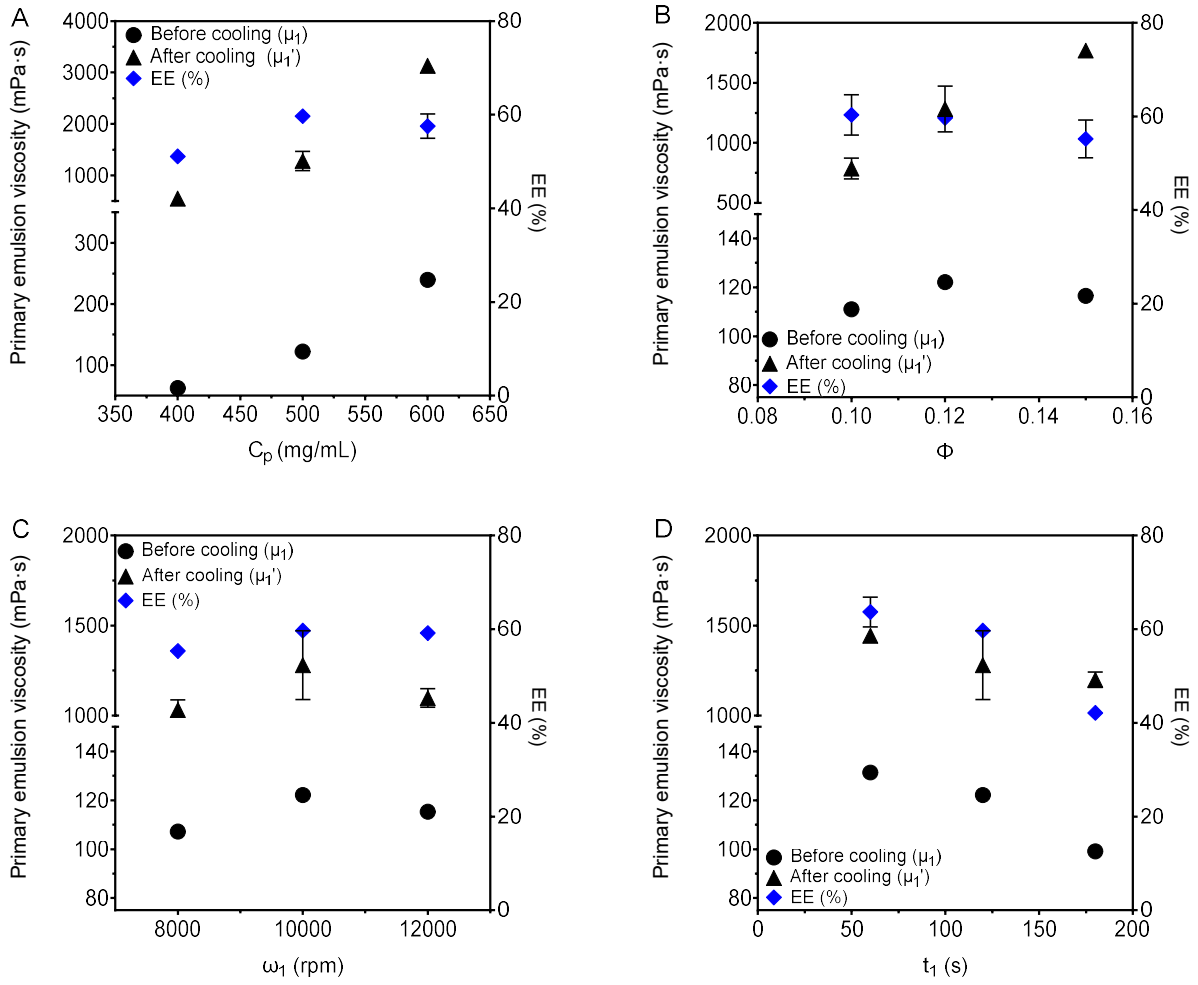


*Figure 4-4. Relationships between manufacturing variables, primary emulsion viscosity and EE of peptide.*

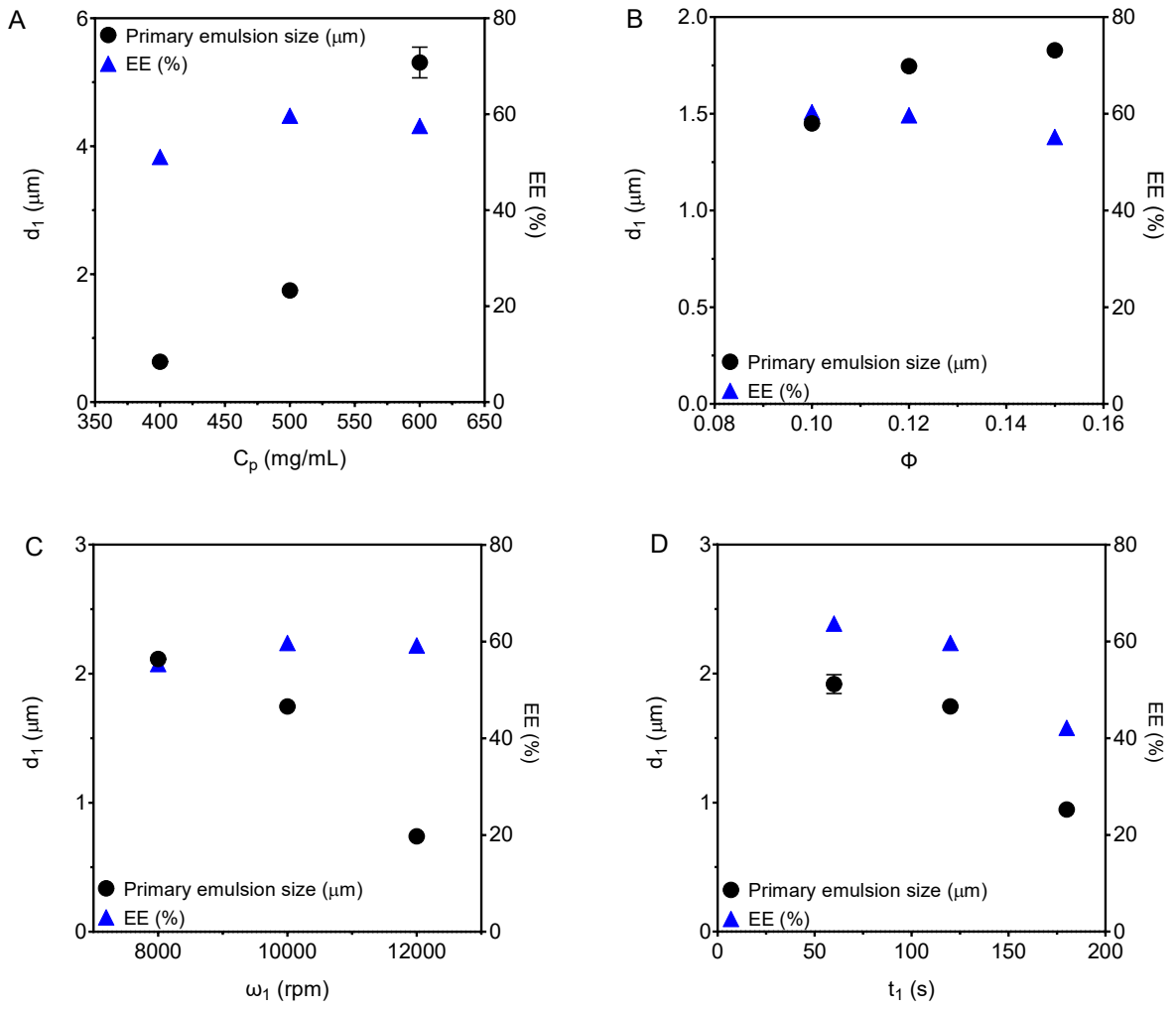


*Figure 4-5. Relationships between manufacturing variables, primary emulsion droplet size and EE of peptide*

### 4.4.3 Effect of manufacturing variables on the secondary emulsion

Secondary emulsions #2-1 - #2-9 (Table 4-2) were prepared from the primary emulsion listed in Table 4-1 with the same process variables during the 2nd homogenization step. Secondary emulsions #2-10 - #2-13 were prepared from primary emulsion #1-1 (standard condition) by changing 2nd homogenization time or 2nd water phase volume. When the secondary water phase volume was increased from 1 mL to 4 mL ($\Phi_2$ decreased from 1 to 0.25), the viscosity of secondary emulsion decreased while the droplet size increased (Figure 4-6 A&C). In

the secondary emulsion, the dispersed phase was the cooled primary emulsion, which could also be considered as an oil phase with higher viscosity ($\mu_1'$), and the continuous phase was PVA solution with a much lower viscosity ($\mu_{c_2}$) (Table 4-2). On the one hand, if the dispersed phase fraction $\Phi_2$ is high, an increase in the difficulty for the homogenizer to break up the droplet to small particle is expected [145]. On the other hand, when the ratio is controlled in an appropriate range, increased outer water phase volume is expected to reduce the emulsification efficiency and lead to increased particle size [55,60,146]. In this study, the high values of $\mu_1'$ were caused by the low temperature after cooling the primary emulsion. After the secondary homogenization process performed at room temperature, the primary emulsion was dispersed into the water phase to form a less viscous emulsion ($\mu_2$) and the temperature ($T_2$) was raised. In this case, $\Phi_2$ has a more significant effect on the droplet size (Sauter mean diameter) ($d'_{3,2}$) than on the viscosity. Based on the equation (4-10) developed by Leng and Calabrese [107], the data fit the correlation in equation (4-25) with a regression coefficient $R^2$ =0.99:

$$\frac{d'_{3,2}}{D} = 0.8(1 - 0.8\Phi_2)We^{-0.6} \quad (4\text{-}25)$$

The correlation between homogenization time ($t_2$) and viscosity was described by a power law with index of -1.15 (Figure 4-6B). The droplet size of secondary emulsion was correlated to homogenization time $t_2$ by a power law fitting with index of -1.25 (Figure 4-6D). The dimensionless correlation between secondary emulsion size and process variables could be expressed by equation (4-26) with excellent $R^2$ 0.99 (Figure 4-7).

$$\frac{d'_{3,2}}{D} \propto (1 - 0.8\Phi_2)(\omega_2 t_2)^{-1.25} \quad (4\text{-}26)$$

Secondary emulsions #2-1 - #2-9 were prepared using the primary emulsions generated in section 4.4.1 with constant 2nd emulsification process variables (i.e., $\Phi_2$=0.5, $\omega_2$ =15000 rpm

and $t_2$=30 s). Thus, the droplet size of these secondary emulsions is expected to be highly dependent on the dispersed phase viscosity, i.e., $\mu_1'$. The dimensionless group, $\frac{\mu'_1}{\mu_{c_2}}$, was included to establish the correlation:

$$\frac{d'_{3,2}}{D} \propto (1 - 0.8\Phi_2)\left(\frac{\mu'_1}{\mu_{c_2}}\right)^{0.5} (\omega_2 t_2)^{-1.25} \quad (4\text{-}27)$$

This correlate was tested in Figure 4-8 with a regression coefficient $R^2 = 0.98$. The secondary emulsion size was significantly affected by homogenization time and secondary water phase volume while the viscosity of primary emulsion had a weaker effect.

*Table 4-2. Summary of characteristics of secondary emulsions formed.*

| Emulsion # | $\mu_1'^*$ (mPa·s) | $\mu_{c_2}{}^*$ (mPa·s) | $\Phi_2$ | $\omega_2$ (rpm) | $t_2$ (s) | $T_2$ (°C) | $d_2{}^*$ (μm) | $d'_{3,2}{}^*$ (μm) | $\mu_2{}^*$ (mPa·s) |
|---|---|---|---|---|---|---|---|---|---|
| 2-1 | 1281 ± 35 | 2.3 ± 0.1 | 0.50 | 15000 | 30.00 | 20.50 | 58.4 ± 0.4 | 20.9 ± 0.2 | 9.1 ± 0.6 |
| 2-2 | 550 ± 6 | 2.3 ± 0.1 | 0.50 | 15000 | 30.00 | 18.60 | 28.6 ± 0.1 | 12.6 ± 0.1 | 7.1 ± 0.4 |
| 2-3 | 3131 ± 17 | 2.3 ± 0.1 | 0.50 | 15000 | 30.00 | 18.60 | 83.7 ± 1.7 | 38.9 ± 0.8 | 18.5 ± 0.6 |
| 2-4 | 787 ± 88 | 2.3 ± 0.1 | 0.50 | 15000 | 30.00 | 18.80 | 59.4 ± 1.0 | 20.8 ± 0.2 | 10.2 ± 0.4 |
| 2-5 | 1768 ± 20 | 2.3 ± 0.1 | 0.50 | 15000 | 30.00 | 18.70 | 59.4 ± 0.6 | 23.9 ± 0.4 | 9.9 ± 0.5 |
| 2-6 | 1032 ± 56 | 2.3 ± 0.1 | 0.50 | 15000 | 30.00 | 19.70 | 66.2 ± 0.3 | 27.8 ± 0.1 | 10.1 ± 0.8 |
| 2-7 | 1098 ± 52 | 2.3 ± 0.1 | 0.50 | 15000 | 30.00 | 19.60 | 58.8 ± 0.9 | 19.4 ± 0.3 | 7.6 ± 0.5 |
| 2-8 | 1444 ± 30 | 2.3 ± 0.1 | 0.50 | 15000 | 30.00 | 20.60 | 73.4 ± 1.6 | 26.6 ± 0.7 | 8.7 ± 0.1 |
| 2-9 | 1199 ± 42 | 2.3 ± 0.1 | 0.50 | 15000 | 30.00 | 17.70 | 64.1 ± 1.4 | 18.6 ± 0.3 | 7.2 ± 0.4 |
| 2-10 | 1281 ± 35 | 2.3 ± 0.1 | 0.50 | 15000 | 10.00 | 16.70 | 133.3 ± 4.1 | 87.4 ± 2.6 | 47.0 ± 2.1 |
| 2-11 | 1281 ± 35 | 2.3 ± 0.1 | 0.50 | 15000 | 45.00 | 19.10 | 43.4 ± 3.2 | 13.7 ± 0.7 | 9.6 ± 0.5 |
| 2-12 | 1281 ± 35 | 2.3 ± 0.1 | 1.00 | 15000 | 30.00 | 19.60 | 14.3± 0.3 | 7.2 ± 0.1 | 11.1 ± 0.4 |
| 2-13 | 1281 ± 35 | 2.3 ± 0.1 | 0.25 | 15000 | 30.00 | 18.70 | 68.8 ± 0.5 | 28.7 ± 0.2 | 5.00 ± 0.8 |

*Note:$\mu_1'$: viscosity of primary emulsion at 4 °C; $\mu_{c2}$: viscosity of secondary continuous phase; $\Phi_2$: dispersed phase fraction in secondary emulsion; $\omega_2$: 2nd homogenization speed; $t_2$: 2nd homogenization time; $T_2$: temperature after 2nd homogenization; $d_2$: volume median droplet size of secondary emulsion; $d'_{3,2}$: Sauter mean diameter of the secondary emulsion; $\mu_2$: viscosity of secondary emulsion at room temperature. * values indicate mean ± SEM.*

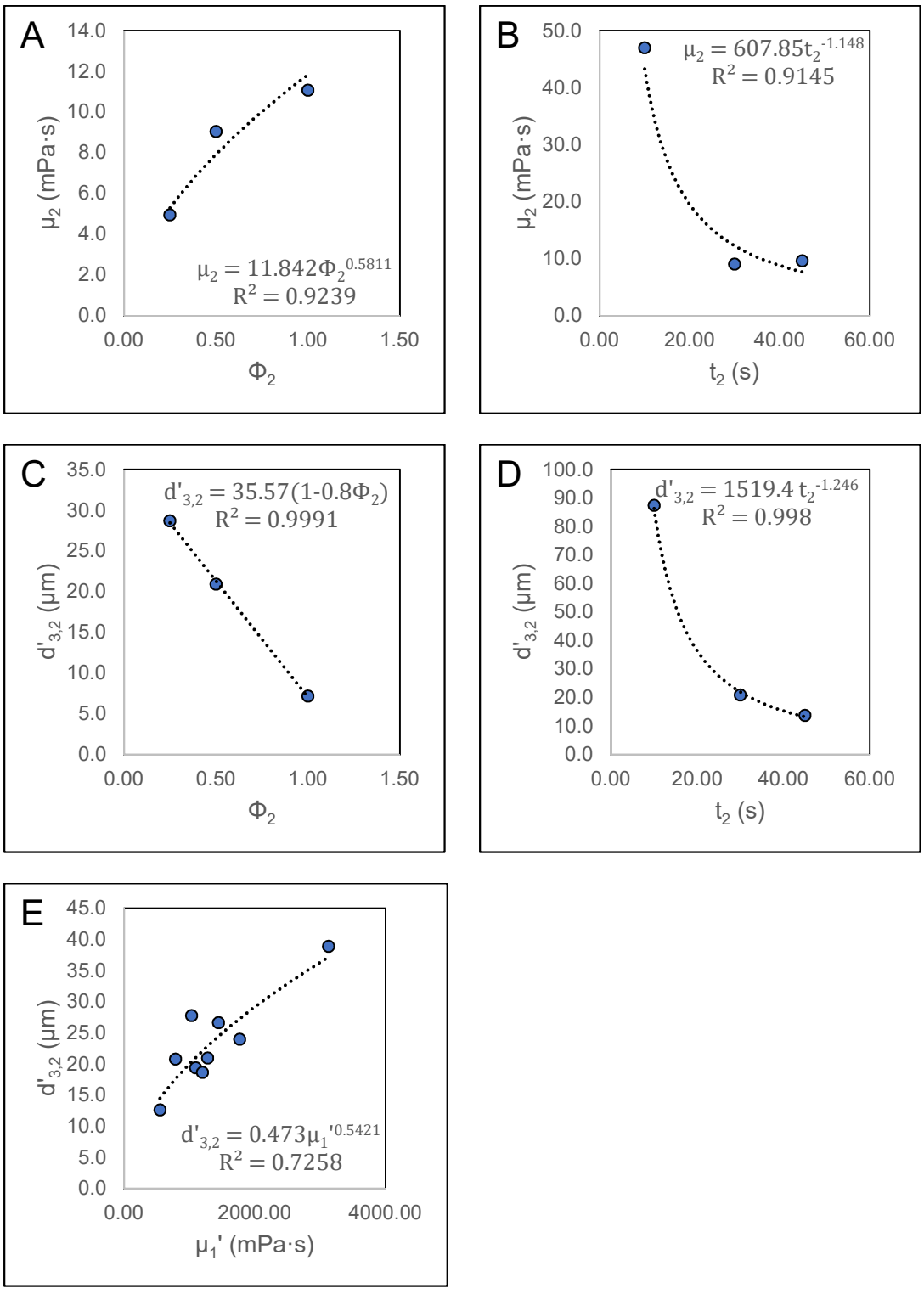


*Figure 4-6. Effect of dispersed phase fraction ($\Phi_2$) and homogenization time ($t_2$) on secondary emulsion viscosity ($\mu_2$) (A&B), and Sauter mean diameter ($d'_{3,2}$) (C&D).*

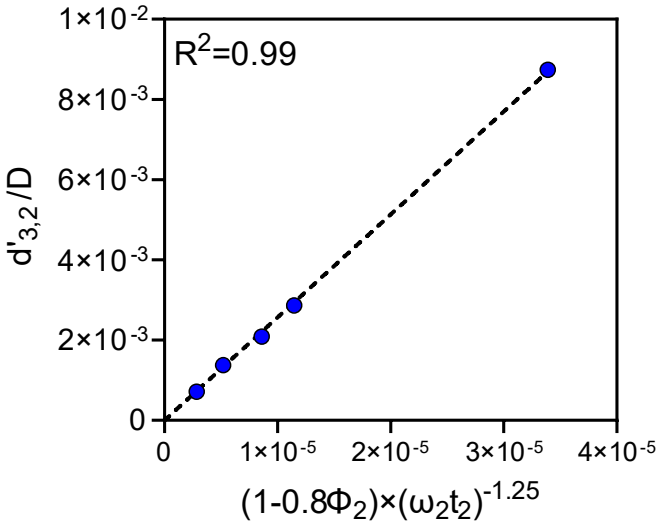


*Figure 4-7. Effect of process variables during secondary emulsification step on the droplet size.*

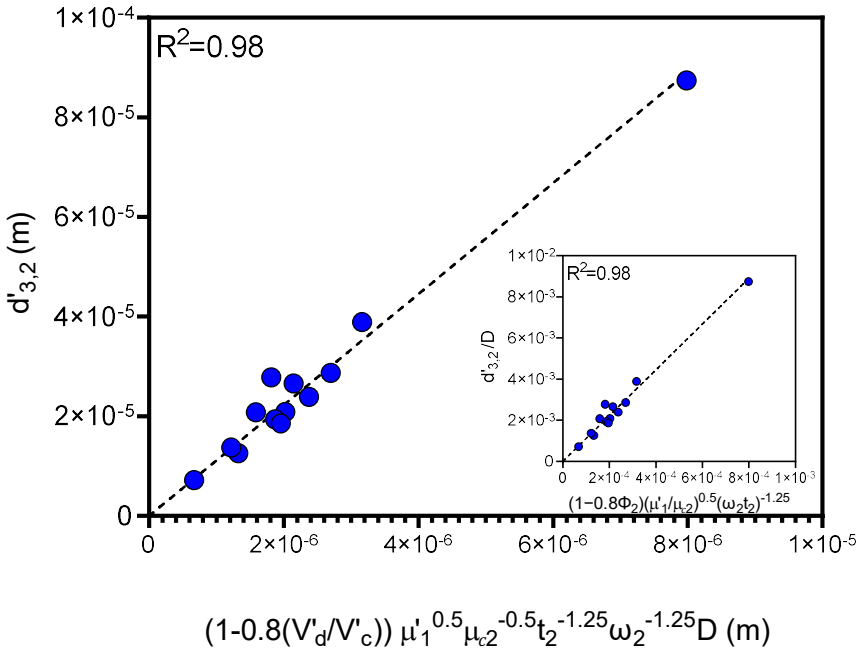


*Figure 4-8. Generation of master curve for correlations between secondary emulsion size and manufacturing variables.*

### 4.4.4 Effect of secondary emulsion viscosity and droplet size on EE

Relationships between manufacturing variables, secondary emulsion droplet size and EE of peptide are shown in Figure 4-9. The intensity of 2$^{nd}$ homogenization seems to be the critical factor that affects both EE of peptide and particle size. Another dramatic decrease of peptide EE happened when the 2$^{nd}$ homogenization time or secondary water phase volume increased. When the secondary water phase volume was increased from 1 mL to 4 mL ($\Phi_2$ decreased from 1 to 0.25), there was a faster solvent removal rate due to the sink condition facilitating the DCM to dissolve in the outer aqueous phase [58]. In this case, solidification of periphery microspheres occurs quickly and a thick skin layer is formed [58] inducing the diffusion of peptide through the polymer phase to outer water phase [138]. It was previously shown in a pilot study that the drug loss increased as a function of homogenization time (Figure S 3-1). This result could be explained by the assumption that drug diffuses through the polymer matrix gradually as time is extended as well as the drop fragmentation theory [137] suggesting more drug leakage in the small droplets after exposure to the outer water phase.

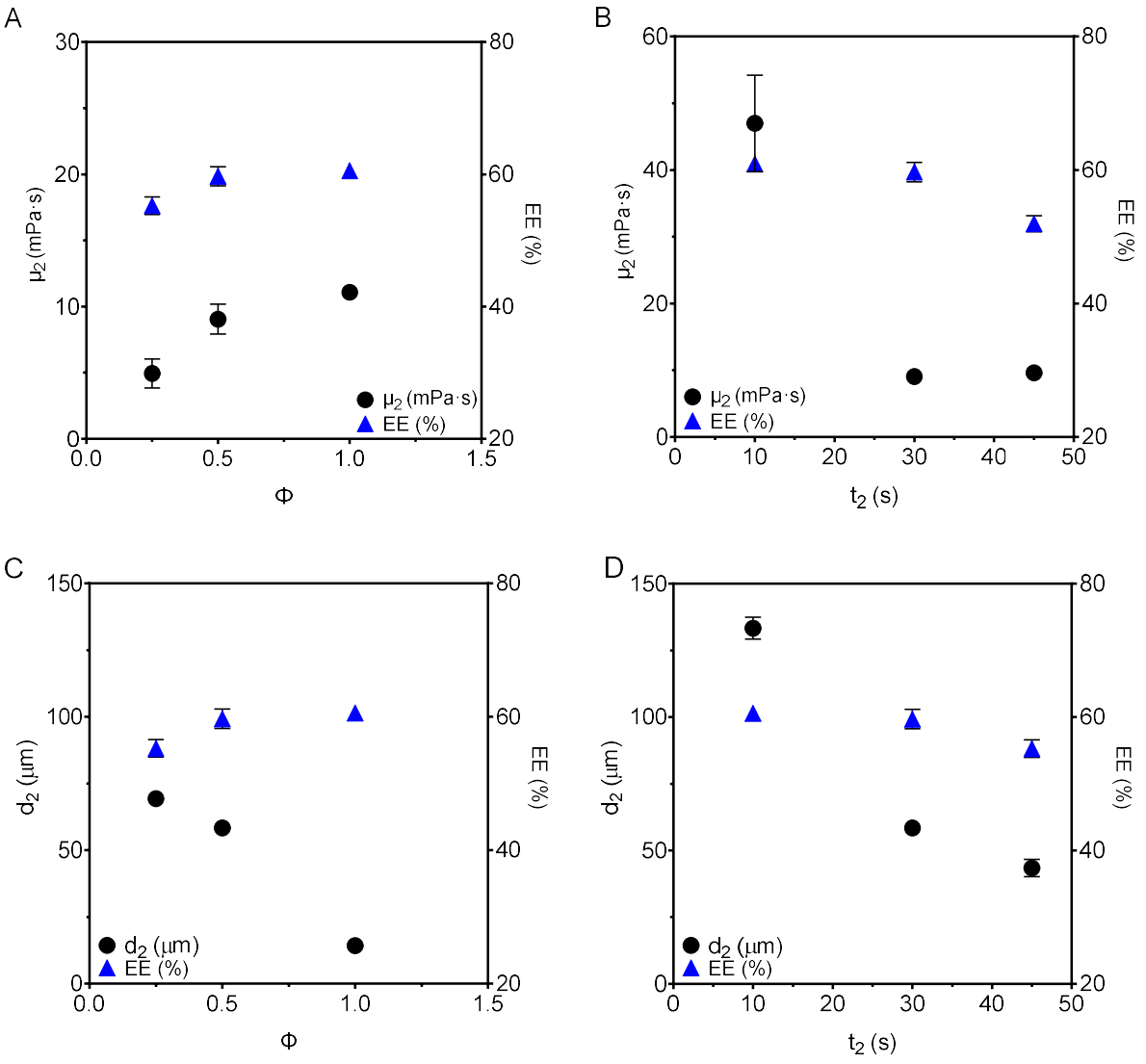


*Figure 4-9. Relationships between manufacturing variables, secondary emulsion droplet size and EE of peptide*

As shown in Table 4-2, the secondary emulsion droplet size in some emulsions was larger than the final particle size (Figure 3-4 B) indicating a significant shrinkage occurred after homogenization and in the in-liquid drying process. The correlation between the ratio of secondary emulsion droplet size/final particle size with secondary emulsion size was established

(Figure 4-10). The emulsions with large size appeared to shrink more than the smaller ones. However, this shrinkage did not significantly affect the EE of peptide.

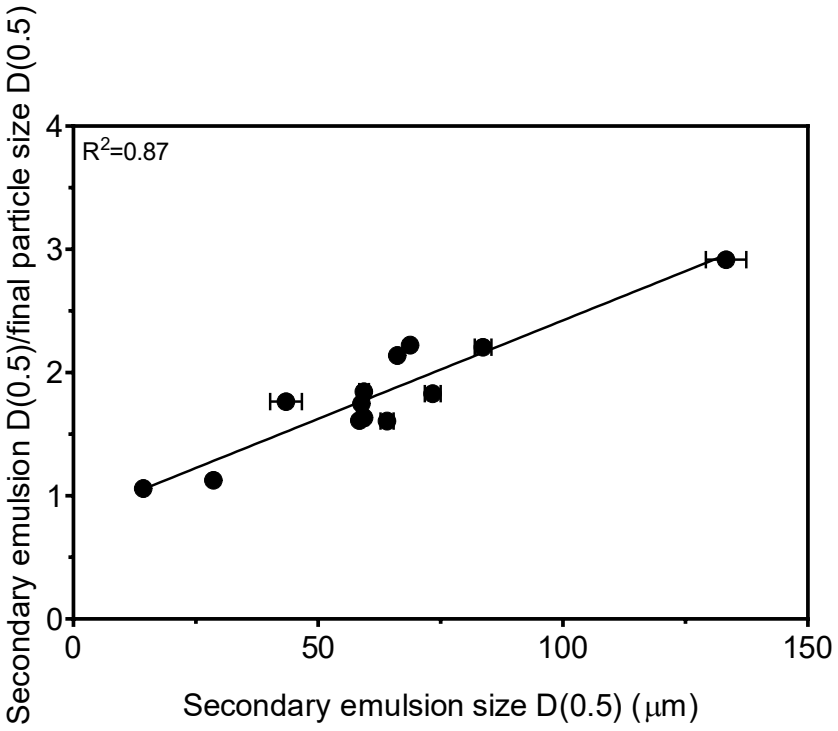


*Figure 4-10. Correlation between the ratio of secondary emulsion droplet size/final particle size with secondary emulsion size.*

## 4.5 **Conclusions**

The viscosity of primary emulsion increases when polymer concentration increases, or homogenization time decreases. The Sauter mean diameter of primary emulsion droplet size is proportional to the product of $(\Phi_1,\ We, Re, \omega_1 t_1)$ with appropriate power index. A new dimensionless group (total surface energy/total energy input to fluid) was used to rationalize insertion of a proportionate time dependence in the scaling of the Sauter mean diameter. Increasing the viscosity of primary inhibits drug loss during microencapsulation while increasing droplet size enhances drug leakage to the outer water phase. The viscosity of secondary emulsion increases when dispersed phase fraction is increased or when homogenization time is decreased.

The Sauter mean diameter of secondary emulsion is proportional to the product of $\left(\Phi_2, \frac{\mu_1'}{\mu_{c_2}}, \omega_2 t_2\right)$ with each dimensionless group raised to appropriate power index. The final microspheres size is related to the secondary emulsion. The correlations identified in this study could be used in the further dimensional analysis.

## 4.6 **Acknowledgments**

This research was funded by FDA contract HHSF223201510170C A0001 BAA. This paper reflects the views of the authors and should not be construed to represent FDA's views or policies.

## 4.7 **Nomenclature**

| *Symbols* | Definition | Unit |
|---|---|---|
| $C_p$ | polymer concentration | mg/mL |
| $D$ | rotor diameter | m |
| $d_{0.5}$ | volume median diameter | m |
| $d_{3,2}$ | Sauter mean diameter | m |
| $N_p$ | particle number | - |
| $r_{3,2}$ | Sauter mean radius | m |
| $P$ | power | W |
| $T_1$ | temperature of primary emulsion | °C |
| $T_2$ | temperature of secondary emulsion | °C |
| $t$ | homogenization time | s |
| $t_1$ | 1st homogenization time | s |
| $t_2$ | 2nd homogenization time | s |
| $V$ | volume of fluid | mL |
| $V_c$ | volume of continuous phase in primary emulsion | mL |
| $V'_c$ | volume of continuous phase in secondary emulsion | mL |
| $V_d$ | volume of disperse phase in primary emulsion | mL |
| $V'_d$ | volume of disperse phase in secondary emulsion | mL |

| *Greek letters* | Definition | Unit |
|---|---|---|
| $\gamma$ | surface energy | J |
| $\delta_K$ | Kolmogorov length scale of turbulence | m |
| $\varepsilon$ | energy dissipation rate per unit mass of fluid | J/kg |
| $\mu$ | dynamic viscosity | mPa·s |

| | | |
|---|---|---|
| $\mu_1$ | viscosity of primary emulsion | mPa·s |
| $\mu'_1$ | viscosity of primary emulsion after cooling | mPa·s |
| $\mu_2$ | viscosity of secondary emulsion | mPa·s |
| $\mu_{c_1}$ | viscosity of continuous phase in primary emulsion | mPa·s |
| $\mu_{c_2}$ | viscosity of continuous phase in secondary emulsion | mPa·s |
| $\mu_d$ | viscosity of dispersed phase in primary emulsion | mPa·s |
| $\rho$ | liquid density | $kg \cdot m^{-3}$ |
| $\rho_c$ | continuous phase density | $kg \cdot m^{-3}$ |
| $\rho_{c_1}$ | polymer phase density | $kg \cdot m^{-3}$ |
| $\rho_d$ | dispersed phase density | $kg \cdot m^{-3}$ |
| $\sigma$ | interfacial tension (water/DCM) | N/m |
| $\sigma'$ | interfacial tension (DCM/PVA) | N/m |
| $\Phi_1$ | dispersed phase volume fraction in primary emulsion | - |
| $\Phi_2$ | dispersed phase volume fraction in secondary emulsion | - |
| $v$ | kinematic viscosity | $m^2/s$ |
| $v_c$ | continuous phase kinematic viscosity | $m^2/s$ |
| $\omega$ | rotor speed | $s^{-1}$ |
| $\omega_1$ | 1st homogenization speed | $s^{-1}$ |
| $\omega_2$ | 2nd homogenization speed | $s^{-1}$ |

| *Dimensionless group* | Definition | Equation |
|---|---|---|
| $P_O$ | Power number | $P_O = \frac{P}{\rho\omega^3 D^5}$ |
| $R_e$ | Reynolds number | $R_e = \frac{\rho\omega D^2}{\mu}$ |
| $W_e$ | Weber number | $W_e = \rho_c\omega^2 D^3/\sigma$ |

## Chapter 5 Conclusions, Significance, and Future Directions

The work presented in this thesis begins to fill in the knowledge gap between raw materials/manufacturing parameters and product attributes/release performance/mechanisms in composition-equivalent PLGA microsphere formulations for controlled release of leuprolide. The knowledge gap was addressed by: 1) developing a series of composition-equivalent leuprolide/PLGA microsphere formulations, 2) developing correlates between the input variables, product attributes and release performance, 3) identifying the correlations between manufacturing variables with characteristics of emulsions.

In the reverse engineering of LD, we established comprehensive analytical methods for analyzing the specific components of the commercial product, identifying and quantifying the ingredients. The results are consistent with the values reported in the drug label and literature, and we found the leuprolide content by rigorous AAA and multiple extraction protocols to be slightly higher than listed in the drug label, although the difference is not statistically significant. The gelatin in LD appears to be Type B with Bloom 300. From the composition-equivalent formulations, we observe higher EE of gelatin (101 ± 1%) compared to the EE of leuprolide (42-63%). The composition, $T_g$, and in vitro release kinetics of the microspheres loaded with leuprolide can be largely replicated on the bench scale. Changing manufacturing variables centered at a standard formulation does not strongly affect release behavior. Changes in initial burst release reflect changes in drug loading/encapsulation efficiency. The substitution of ring-opening polymerized PLGA in place of polycondensation PLGA increases $T_g$ and initial burst,

and slightly reduces long-term release rate and mass loss rate. The release mechanisms of standard condition formulation, Resomer formulation and LD appear to be the same and requires more than just mass loss to explain release. Indeed, the release may have a desorption component. Nondimensional correlations are established based on the literature, and the dimensionless Sauter mean diameter of primary emulsion droplet size is proportional to the product of dimensionless groups ($\Phi_1,\ We, Re, \omega_1 t_1$) raised to appropriate power indices. A new dimensionless group (total surface energy/total energy input to fluid) is used to rationalize insertion of a proportionate time dependence in the scaling of the Sauter mean diameter. The Sauter mean diameter of secondary emulsion is proportional to the product of dimensionless groups $\left(\Phi_2, \frac{\mu\prime_1}{\mu_{c_2}}, \omega_2 t_2\right)$ raised to appropriate power indices. Increasing the viscosity of the primary emulsion inhibits drug loss during microencapsulation while increasing droplet size enhances drug leakage to the outer water phase.

Future studies will determine the equivalence of composition-equivalent formulations to LD *in vivo*. This could be achieved by dosing selected formulations to rats subcutaneously and determining the pharmacokinetics of formulations for up to 35 days. The critical pharmacokinetic parameters, $AUC_{0\text{-}t}$, $AUC_{0\text{-}\infty}$, $C_{max}$ and $T_{max}$ would be obtained to determine the bioequivalence. It may also be of interest to more definitively establish the dimensional analysis based on the correlations in Chapter 4. This could be achieved by expanding the range of variable values and involving confounding variables to prepare emulsions.

This research has significant applications in the development of new and generic peptide loaded microsphere products. Particularly, the analytical methods that were developed in Chapter 2 could be used to reverse engineer other peptide loaded microsphere commercial products. The effects identified in Chapter 3 could be used to optimize the manufacturing variables to prepare

formulations with desirable EE, particle size and release kinetics during pilot studies. The correlations established in Chapter 4 could be helpful to predict characteristics of emulsions and determine the initial values of parameter before experiments. The correlates in Chapter 3 and 4 could greatly shorten development time and cost. These approaches may offer an aid in future FDA regulation development for generic drug of long acting release products.

## BIBLIOGRAPHY


[1] H. Okada, One- and three-month release injectable microspheres of the LH-RH superagonist leuprorelin acetate, Adv. Drug Deliv. Rev. 28 (1997) 43–70. doi:Doi 10.1016/S0169-409x(97)00050-1.

[2] G.L. Plosker, R.N. Brogden, Leuprorelin: A Review of its Pharmacology and Therapeutic Use in Prostatic Cancer, Endometriosis and Other Sex Hormone-Related Disorders, Drugs. 48 (1994) 930–967. doi:10.2165/00003495-199448060-00008.

[3] D.J. Craik, D.P. Fairlie, S. Liras, D. Price, The Future of Peptide-based Drugs, Chem. Biol. Drug Des. (2013). doi:10.1111/cbdd.12055.

[4] I. Tuncer Degim, N. Celebi, Controlled Delivery of Peptides and Proteins, Curr. Pharm. Des. 13 (2007) 99–117. doi:10.2174/138161207779313795.

[5] K. Fosgerau, T. Hoffmann, Peptide therapeutics: current status and future directions, Drug Discov. Today. 20 (2015) 122–128. doi:10.1016/j.drudis.2014.10.003.

[6] Y. Wang, Q. Wen, S.H. Choi, FDA's regulatory science program for generic PLA/PLGA-based drug products, Am. Pharm. Rev. 19 (2016) 5–9. https://www.americanpharmaceuticalreview.com/Featured-Articles/188841-FDA-s-Regulatory-Science-Program-for-Generic-PLA-PLGA-Based-Drug-Products/.

[7] S. Benita, Microencapsulation: Methods and Industrial Applications, Second Edi, CRC Press, 2005.

[8] R.A. Jain, The manufacturing techniques of various drug loaded biodegradable poly(lactide-co-glycolide) (PLGA) devices, Biomaterials. 21 (2000) 2475–2490. doi:10.1016/S0142-9612(00)00115-0.

[9] E. Marin, M.I. Briceño, C. Caballero-George, Critical evaluation of biodegradable polymers used in nanodrugs, Int. J. Nanomedicine. (2013). doi:10.2147/IJN.S47186.

[10] R.C. Mundargi, V.R. Babu, V. Rangaswamy, P. Patel, T.M. Aminabhavi, Nano/micro technologies for delivering macromolecular therapeutics using poly(D,L-lactide-co-glycolide) and its derivatives, J. Control. Release. 125 (2008) 193–209. doi:10.1016/j.jconrel.2007.09.013.

[11] D.S. Pisal, M.P. Kosloski, S. V Balu-Iyer, Delivery of Therapeutic Proteins, J. Pharm. Sci. 99 (2010) 2557–2575. doi:10.1002/jps.22054.

[12] K. Avgoustakis, Polylactic-Co-Glycolic Acid (PLGA), in: G.E. Wnek, G.L. Bowlin

(Eds.), Encycl. Biomater. Biomed. Eng., CRC Press, 2008. doi:10.3109/E-EBBE-120013950.

[13] H. Fukuzaki, M. Yoshida, M. Asano, M. Kumakura, Synthesis of copoly(d,l-lactic acid) with relatively low molecular weight and in vitro degradation, Eur. Polym. J. (1989). doi:10.1016/0014-3057(89)90131-6.

[14] C. Jérôme, P. Lecomte, Recent advances in the synthesis of aliphatic polyesters by ring-opening polymerization, Adv. Drug Deliv. Rev. (2008). doi:10.1016/j.addr.2008.02.008.

[15] A.C. Albertsson, I.K. Varma, Recent developments in ring opening polymerization of lactones for biomedical applications, Biomacromolecules. (2003). doi:10.1021/bm034247a.

[16] I. Vroman, L. Tighzert, Biodegradable Polymers, Materials (Basel). 2 (2009) 307–344. doi:Doi 10.3390/Ma2020307.

[17] O. Dechy-Cabaret, B. Martin-Vaca, D. Bourissou, Controlled ring-opening polymerization of lactide and glycolide, Chem. Rev. (2004). doi:10.1021/cr040002s.

[18] L. Xiao, B. Wang, G. Yang, M. Gauthier, Poly (lactic acid)-based biomaterials: synthesis, modification and applications, in: Biomed. Sci. Eng. Technol., InTechOpen, 2012.

[19] B. Bittner, M. Morlock, H. Koll, G. Winter, T. Kissel, Recombinant human erythropoietin (rhEPO) loaded poly(lactide-co-glycolide) microspheres: influence of the encapsulation technique and polymer purity on microsphere characteristics, Eur. J. Pharm. Biopharm. 45 (1998) 295–305. doi:Doi 10.1016/S0939-6411(98)00012-5.

[20] C. Wischke, S.P. Schwendeman, Principles of encapsulating hydrophobic drugs in PLA/PLGA microparticles, Int J Pharm. 364 (2008) 298–327. doi:10.1016/j.ijpharm.2008.04.042.

[21] Y. Ogawa, M. Yamamoto, S. Takada, H. Okada, T. Shimamoto, Controlled-release of leuprolide acetate from polylactic acid or copoly(lactic/glycolic) acid microcapsules: influence of molecular weight and copolymer ratio of polymer, Chem Pharm Bull. 36 (1988) 1502–1507. doi:10.1248/cpb.36.1502.

[22] H. Okada, Y. Inoue, T. Heya, H. Ueno, Y. Ogawa, H. Toguchi, Pharmacokinetics of once-a-month injectable microspheres of leuprolide acetate, Pharm Res. 8 (1991) 787–791. doi:10.1023/A:1015818504906.

[23] P. Gentile, V. Chiono, I. Carmagnola, P. V Hatton, An Overview of Poly(lactic-co-glycolic) Acid (PLGA)-Based Biomaterials for Bone Tissue Engineering, Int. J. Mol. Sci. 15 (2014) 3640–3659. doi:10.3390/ijms15033640.

[24] X.S. Wu, N. Wang, Synthesis, characterization, biodegradation, and drug delivery application of biodegradable lactic/glycolic acid polymers. Part II: Biodegradation, J. Biomater. Sci. Polym. Ed. 12 (2001) 21–34. doi:10.1163/156856201744425.

[25] J.P. Kitchell, D.L. Wise, [32] Poly(lactic/glycolic acid) biodegradable drug—polymer matrix systems, Methods Enzymol. 112 (1985) 436–448. doi:10.1016/S0076-6879(85)12034-3.

[26] M. Yamada, S. Ishiguro, Y. Ogawa, Prolonged release preparation and polymers thereof, US5304377, 1994.

[27] S. Cohen, M.J. Alonso, R. Langer, Novel Approaches to Controlled-Release Antigen Delivery, Int. J. Technol. Assess. Health Care. 10 (1994) 121–130. doi:10.1017/S0266462300014045.

[28] K.E. Uhrich, S.M. Cannizzaro, R.S. Langer, K.M. Shakesheff, Polymeric Systems for Controlled Drug Release, Chem. Rev. 99 (1999) 3181–3198. doi:10.1021/cr940351u.

[29] P.I.P. Park, S. Jonnalagadda, Predictors of glass transition in the biodegradable polylactide and poly-lactide-co-glycolide polymers, J. Appl. Polym. Sci. (2006). doi:10.1002/app.22135.

[30] F. von Burkersroda, L. Schedl, A. Göpferich, Why degradable polymers undergo surface erosion or bulk erosion, Biomaterials. 23 (2002) 4221–4231. doi:10.1016/S0142-9612(02)00170-9.

[31] Y. Zhang, A.M. Sophocleous, S.P. Schwendeman, Inhibition of peptide acylation in PLGA microspheres with water-soluble divalent cationic salts, Pharm Res. 26 (2009) 1986–1994. doi:10.1007/s11095-009-9914-2.

[32] X. Chen, C.P. Ooi, T.H. Lim, Effect of ganciclovir on the hydrolytic degradation of poly(lactide-co-glycolide) microspheres, J. Biomater. Appl. 20 (2006) 287–302. doi:10.1177/0885328206054265.

[33] J. Wang, B.M. Wang, S.P. Schwendeman, Characterization of the initial burst release of a model peptide from poly(d,l-lactide-co-glycolide) microspheres, J. Control. Release. 82 (2002) 289–307. doi:10.1016/S0168-3659(02)00137-2.

[34] E. Sah, H. Sah, Recent Trends in Preparation of Poly(lactide- *co* -glycolide) Nanoparticles by Mixing Polymeric Organic Solution with Antisolvent, J. Nanomater. 2015 (2015) 1–22. doi:10.1155/2015/794601.

[35] N.K. Varde, D.W. Pack, Microspheres for controlled release drug delivery, Expert Opin. Biol. Ther. 4 (2004) 35–51. doi:10.1517/14712598.4.1.35.

[36] F.-J.J. Wang, C.-H.H. Wang, Sustained release of etanidazole from spray dried microspheres prepared by non-halogenated solvents, J. Control. Release. 81 (2002) 263–280. doi:10.1016/S0168-3659(02)00066-4.

[37] U. Bilati, E. Allémann, E. Doelker, Poly(D,L-lactide-co-glycolide) protein-loaded nanoparticles prepared by the double emulsion method—processing and formulation issues for enhanced entrapment efficiency, J. Microencapsul. 22 (2005) 205–214.

doi:10.1080/02652040400026442.

[38] E. Toorisaka, K. Watanabe, M. Hirata, Development of Fine Poly(D,L-Lactic-Co-Glycolic Acid) Particles for Hydrophilic Drug Using a Solid-in-Oil-in-Water Emulsion, J. Encapsulation Adsorpt. Sci. 8 (2018) 58–66. doi:10.4236/jeas.2018.82004.

[39] P. Giunchedi, B. Conti, I. Genta, U. Conte, G. Puglisi, Emulsion Spray-Drying for the Preparation of Albumin-Loaded PLGA Microspheres, Drug Dev. Ind. Pharm. 27 (2001) 745–750. doi:10.1081/DDC-100107331.

[40] R. Alcock, J.. Blair, D.. O'Mahony, A. Raoof, A.. Quirk, Modifying the release of leuprolide from spray dried OED microparticles, J. Control. Release. 82 (2002) 429–440. doi:10.1016/S0168-3659(02)00165-7.

[41] E. Gavini, P. Chetoni, M. Cossu, M.G. Alvarez, M.F. Saettone, P. Giunchedi, PLGA microspheres for the ocular delivery of a peptide drug, vancomycin using emulsification/spray-drying as the preparation method: in vitro/in vivo studies, Eur. J. Pharm. Biopharm. 57 (2004) 207–212. doi:10.1016/je.jpb.2003.10.018.

[42] J.M. Newton, Spray drying and its application in pharmaceuticals, Manuf. Chem. Aerosol News. 37 (1966) 33–36. http://discovery.ucl.ac.uk/id/eprint/1419655.

[43] J. Schäfer, G. Lee, Spray-Drying of Enzymes on the Bench-Top Scale with lengthened Chamber Retention Time, 2015.

[44] P.D. Hede, P. Bach, A.D. Jensen, Two-fluid spray atomisation and pneumatic nozzles for fluid bed coating/agglomeration purposes: A review, Chem. Eng. Sci. 63 (2008) 3821–3842. doi:10.1016/j.ces.2008.04.014.

[45] J. Broadhead, S.K. Edmond Rouan, C.T. Rhodes, The spray drying of pharmaceuticals, Drug Dev. Ind. Pharm. 18 (1992) 1169–1206. doi:10.3109/03639049209046327.

[46] C. Anish, A.K. Upadhyay, D. Sehgal, A.K. Panda, Influences of process and formulation parameters on powder flow properties and immunogenicity of spray dried polymer particles entrapping recombinant pneumococcal surface protein A, Int. J. Pharm. 466 (2014) 198–210. doi:10.1016/j.ijpharm.2014.03.025.

[47] K. Thoma, B. Schlutermann, Relationships between manufacturing parameters and pharmaceutical-technological requirements on biodegradable microparticles. Part 6. In vitro release characteristics of cinchocaine and bubivacaine from biodegradable microparticles, Pharmazie. 47 (1992) 436–438.

[48] M. Mumenthaler, C.C. Hsu, R. Pearlman, Feasibility study on spray-drying protein pharmaceuticals: recombinant human growth hormone and tissue-type plasminogen activator, Pharm Res. 11 (1994) 12–20. doi:10.1023/A:1018929224005.

[49] K. Masters, Understanding and applying spray-dryers in chemical processing, Powder Bulk Eng. Apr (1990) 36–44.

[50] S.G. Wright, T. Christenson, T.Y. Yeah, M.E. Rickey, J.M. Hotz, R. Kumar, H.R. Costantino, Polymer-based sustained release device, 2008.

[51] H.K. Makadia, S.J. Siegel, Poly Lactic-co-Glycolic Acid (PLGA) as biodegradable controlled drug delivery carrier, Polymers (Basel). 3 (2011) 1377–1397. doi:10.3390/polym3031377.

[52] J. Wang, B.M. Wang, S.P. Schwendeman, Mechanistic evaluation of the glucose-induced reduction in initial burst release of octreotide acetate from poly(d,l-lactide-co-glycolide) microspheres, Biomaterials. 25 (2004) 1919–1927. doi:10.1016/j.biomaterials.2003.08.019.

[53] Y.Y. Yang, T.S. Chung, X.L. Bai, W.K. Chan, Effect of preparation conditions on morphology and release profiles of biodegradable polymeric microspheres containing protein fabricated by double-emulsion method, Chem. Eng. Sci. 55 (2000) 2223–2236. doi:10.1016/S0009-2509(99)00503-5.

[54] Y. Ogawa, M. Yamamoto, H. Okada, T. Yashiki, T. Shimamoto, A New Technique to Efficiently Entrap Leuprolide Acetate into Microcapsules of Polylactic Acid or Copoly(Lactic Glycolic) Acid, Chem. Pharm. Bull. (Tokyo). 36 (1988) 1095–1103.

[55] S. Mao, J. Xu, C. Cai, O. Germershaus, A. Schaper, T. Kissel, Effect of WOW process parameters on morphology and burst release of FITC-dextran loaded PLGA microspheres, Int. J. Pharm. 334 (2007) 137–148. doi:10.1016/j.ijpharm.2006.10.036.

[56] E.J.A.M. Schlicher, N.S. Postma, J. Zuidema, H. Talsma, W.E. Hennink, Preparation and characterisation of Poly (D,L-lactic-co-glycolic acid) microspheres containing desferrioxamine, Int. J. Pharm. 153 (1997) 235–245. doi:10.1016/S0378-5173(97)00116-6.

[57] H. Yushu, S. Venkatraman, The effect of process variables on the morphology and release characteristics of protein-loaded PLGA particles, J. Appl. Polym. Sci. 101 (2006) 3053–3061. doi:10.1002/app.23933.

[58] W.-I.I. Li, K.W. Anderson, R.C. Mehta, P.P. Deluca, Prediction of solvent removal profile and effect on properties for peptide-loaded PLGA microspheres prepared by solvent extraction/ evaporation method, J. Control. Release. 37 (1995) 199–214. doi:10.1016/0168-3659(95)00076-3.

[59] M.J. BlancoPrieto, E. Leo, F. Delie, A. Gulik, P. Couvreur, E. Fattal, Study of the influence of several stabilizing agents on the entrapment and in vitro release of pBC 264 from poly(lactide-co-glycolide) microspheres prepared by a W/O/W solvent evaporation method, Pharm. Res. 13 (1996) 1127–1129. doi:10.1023/A:1016087530812.

[60] H. Jeffery, S.S. Davis, D.T. O'Hagan, The Preparation and Characterization of Poly(lactide-co-glycolide) Microparticles. II. The Entrapment of a Model Protein Using a (Water-in-Oil)-in-Water Emulsion Solvent Evaporation Technique, Pharm. Res. An Off. J. Am. Assoc. Pharm. Sci. 10 (1993) 362–368. doi:10.1023/A:1018980020506.

[61] Y. Yang, Morphology, drug distribution, and in vitro release profiles of biodegradable polymeric microspheres containing protein fabricated by double-emulsion solvent extraction/evaporation method, Biomaterials. 22 (2001) 231–241. doi:10.1016/S0142-9612(00)00178-2.

[62] S. Freitas, H.P. Merkle, B. Gander, Microencapsulation by solvent extraction/evaporation: Reviewing the state of the art of microsphere preparation process technology, J. Control. Release. 102 (2005) 313–332. doi:10.1016/j.jconrel.2004.10.015.

[63] T. Uchida, S. Goto, Oral delivery of poly(lactide-co-glycolide) microspheres containing ovalbumin as vaccine formulation: particle size study., Biol. Pharm. Bull. 17 (1994) 1272–1276. doi:10.1248/bpb.17.1272.

[64] C. Witschi, E. Doelker, Influence of the microencapsulation method and peptide loading on poly(lactic acid) and poly(lactic-co-glycolic acid) degradation during in vitro testing, J. Control. Release. 51 (1998) 327–341. doi:10.1016/S0168-3659(97)00188-0.

[65] G.F. Blehn, M.L. Ernsberger, Polyvinyl Alcohol as an Emulsifying Agent, Ind. Eng. Chem. 40 (2005) 1449–1453. doi:10.1021/ie50464a024.

[66] M. Jobmann, G. Rafler, Controlled release systems of biodegradable polymers: 6th communication: Control of particle size and size distribution of microparticles produced by the solvent evaporation technique, Pharm. Ind. 60 (1998) 979–982.

[67] R. Jain, N.H. Shah, A.W. Malick, C.T. Rhodes, Controlled Drug Delivery by Biodegradable Poly(Ester) Devices: Different Preparative Approaches, Drug Dev. Ind. Pharm. 24 (1998) 703–727. doi:10.3109/03639049809082719.

[68] Q. Yang, G. Owusu-Ababio, Biodegradable progesterone microsphere delivery system for osteoporosis therapy, Drug Dev. Ind. Pharm. 26 (2000) 61–70. doi:10.1081/DDC-100100328.

[69] T.M.C. Maria, R.A. de Carvalho, P.J.A. Sobral, A.M.B.Q. Habitante, J. Solorza-Feria, The effect of the degree of hydrolysis of the PVA and the plasticizer concentration on the color, opacity, and thermal and mechanical properties of films based on PVA and gelatin blends, J. Food Eng. 87 (2008) 191–199. doi:10.1016/J.JFOODENG.2007.11.026.

[70] M.B. DeYoung, L. MacConell, V. Sarin, M. Trautmann, P. Herbert, Encapsulation of exenatide in poly-(D,L-lactide-co-glycolide) microspheres produced an investigational long-acting once-weekly formulation for type 2 diabetes, Diabetes Technol Ther. 13 (2011) 1145–1154. doi:10.1089/dia.2011.0050.

[71] J.L. Cleland, Solvent evaporation processes for the production of controlled release biodegradable microsphere formulations for therapeutics and vaccines, Biotechnol. Prog. 14 (1998) 102–107. doi:10.1021/bp970128t.

[72] R.P. Batycky, J. Hanes, R. Langer, D.A. Edwards, A theoretical model of erosion and macromolecular drug release from biodegrading microspheres, J. Pharm. Sci. 86 (1997)

1464–1477. doi:Doi 10.1021/Js9604117.

[73] K. Mäder, RESOMER® - Biodegradable polymers for sutures, medical devices, drug delivery systems and tissue engineering, (n.d.). http://www.sigmaaldrich.com/technical-documents/articles/material-matters/resomer-biodegradeable-polymers.html.

[74] A. Göpferich, Polymer bulk erosion, Macromolecules. 30 (1997) 2598–2604. doi:10.1021/ma961627y.

[75] S. Fredenberg, M. Wahlgren, M. Reslow, A. Axelsson, The mechanisms of drug release in poly(lactic-co-glycolic acid)-based drug delivery systems—A review, Int. J. Pharm. 415 (2011) 34–52. doi:10.1016/j.ijpharm.2011.05.049.

[76] S.D. Allison, Analysis of initial burst in PLGA microparticles, Expert Opin Drug Deliv. 5 (2008) 615–628. doi:10.1517/17425247.5.6.615.

[77] Lupron Depot® package insert., (2019). http://www.rxabbvie.com/pdf/lupronuro_pi.pdf.

[78] A.C. Wilson, S. Vadakkadath Meethal, R.L. Bowen, C.S. Atwood, Leuprolide acetate: a drug of diverse clinical applications, Expert Opin. Investig. Drugs. (2007). doi:10.1517/13543784.16.11.1851.

[79] A.S. Merseburger, T. Björk, J. Whitehouse, D. Meani, Treatment costs for advanced prostate cancer using luteinizing hormone-releasing hormone agonists: A solid biodegradable leuprorelin implant versus other formulations, J. Comp. Eff. Res. (2015). doi:10.2217/cer.14.82.

[80] T. Uhlig, T. Kyprianou, F.G. Martinelli, C.A. Oppici, D. Heiligers, D. Hills, X.R. Calvo, P. Verhaert, The emergence of peptides in the pharmaceutical business: From exploration to exploitation, EuPA Open Proteomics. 4 (2014) 58–69. doi:10.1016/j.euprot.2014.05.003.

[81] P. Periti, T. Mazzei, E. Mini, Clinical Pharmacokinetics of Depot Leuprorelin, Clin. Pharmacokinet. 41 (2002) 485–504. doi:10.2165/00003088-200241070-00003.

[82] FDA, LUPRON DEPOT (leuprolide acetate for depot suspension), (2013). https://www.accessdata.fda.gov/drugsatfda_docs/label/2014/020517s036_019732s041lbl.pdf.

[83] H. Okada, M. Yamamoto, T. Heya, Y. Inoue, S. Kamei, Y. Ogawa, H. Toguchi, Drug delivery using biodegradable microspheres, J. Control. Release. 28 (1994) 121–129. doi:10.1016/0168-3659(94)90159-7.

[84] H. Okada, Y. Doken, Y. Ogawa, H. Toguchi, Preparation of three-month depot injectable microspheres of leuprorelin acetate using biodegradable polymers, Pharm. Res. 11 (1994) 1143–1147. doi:Doi 10.1023/A:1018936815654.

[85] H. Okada, Y. Ogawa, T. Yashiki, Prolonged release microcapsule and its production,

US4652441, 1987. http://www.google.com/patents/US4652441.

[86] H. Okada, Y. Inoue, Y. Ogawa, Prolonged release microcapsules, US5643607, 1997. https://www.google.com/patents/US5643607.

[87] M. Yamamoto, H. Okada, Y. Ogawa, T. Miyagawa, Polymer, production and use thereof, US4728721, 1988. https://patents.google.com/patent/US4728721.

[88] S. Kamei, M. Yamada, Y. Ogawa, Method of producing sustained-release microcapsules, US5716640, 1996. http://www.google.com/patents/US5716640.

[89] Y. Igari, Y. Yamagata, Sustained-release preparation, US6087324, 2000. https://patents.google.com/patent/US6087324A.

[90] A.M. Sophocleous, Mechanistic Investigation of Peptide Sorption and Acylation in Poly(lactic-co-glycolic acid), 2009. https://deepblue.lib.umich.edu/handle/2027.42/64668 (accessed February 23, 2019).

[91] N. Rizkalla, C. Range, F.-X. Lacasse, P. Hildgen, Effect of various formulation parameters on the properties of polymeric nanoparticles prepared by multiple emulsion method, J. Microencapsul. 23 (2006) 39–57. doi:10.1080/02652040500286185.

[92] R. V. Calabrese, M.K. Francis, V.P. Mishra, S. Phongikaroon, Measurement and Analysis of Drop Size in a Batch Rotor-Stator Mixer, 10th Eur. Conf. Mix. (2000) 149–156. doi:10.1016/B978-044450476-0/50020-0.

[93] J. Wang, S.P. Schwendeman, Mechanisms of solvent evaporation encapsulation processes: prediction of solvent evaporation rate, J Pharm Sci. 88 (1999) 1090–1099. doi:10.1021/js980169z.

[94] M. Cooke, T.L. Rodgers, A.J. Kowalski, Power consumption characteristics of an in-line silverson high shear mixer, AIChE J. 58 (2012) 1683–1692. doi:10.1002/aic.12703.

[95] S. Hall, M. Cooke, A. El-Hamouz, A.J. Kowalski, Droplet break-up by in-line Silverson rotor-stator mixer, Chem. Eng. Sci. 66 (2011) 2068–2079. doi:10.1016/j.ces.2011.01.054.

[96] S.; Hall, A.; Pacek, A.J.; Kowalski, M.; Cooke, D. Rothman, The effect of scale and interfacial tension on liquid-liquid dispersion in in-line Silverson rotor-stator mixers, (2013). doi:10.1016/j.cherd.2013.04.021.

[97] T. Rodgers, M. Cooke, S. Hall, A. Pacek, A. Kowalski, S. Pierucci, Rotor-Stator Mixers, Icheap-10 10th Int. Conf. Chem. Process Eng. Pts 1-3. 24 (2011) 6. doi:10.3303/CET1124236.

[98] S. Hall, A. Pacek, A. Kowalski, M. Cooke, Emulsification by in-line rotor-stator mixers, (2010).

[99] J. James, M. Cooke, L. Trinh, R. Hou, P. Martin, A. Kowalski, T.L. Rodgers, Scale-up of

batch rotor–stator mixers. Part 1—power constants, Chem. Eng. Res. Des. 124 (2017) 313–320. doi:10.1016/J.CHERD.2017.06.020.

[100] A. Utomo, M. Baker, A.W. Pacek, The effect of stator geometry on the flow pattern and energy dissipation rate in a rotor–stator mixer, Chem. Eng. Res. Des. 87 (2009) 533–542. doi:10.1016/J.CHERD.2008.12.011.

[101] V.A. Atiemo-Obeng, R. V. Calabrese, Rotor–Stator Mixing Devices, in: Handb. Ind. Mix., John Wiley & Sons, Inc., Hoboken, NJ, USA, 2004: pp. 479–505. doi:10.1002/0471451452.ch8.

[102] R.H. Perry, D.W. Green, J.O. Maloney, Perry's chemical engineers' handbook, McGraw-Hill New York, 1984.

[103] E.L. Paul, and S.M.K. Victor A. Atiemo-Obeng, Handbook of Industrial Mixing, 2004. doi:10.1002/0471451452.

[104] U. Teipel, N. Aksel, Rheologically identical behavior of emulsions and suspensions in steady shear flow: Dimensional analysis and experimental evidence, Chem. Eng. Technol. 26 (2003) 947–951. doi:10.1002/ceat.200303035.

[105] R. Pal, Scaling of relative viscosity of emulsions, Cit. J. Rheol. 41 (1997) 141. doi:10.1122/1.550852.

[106] T. Delmas, H. Piraux, A.C. Couffin, I. Texier, F. Vinet, P. Poulin, M.E. Cates, J. Bibette, How to prepare and stabilize very small nanoemulsions, Langmuir. 27 (2011) 1683–1692. doi:10.1021/la104221q.

[107] D.E. Leng, R. V Calabrese, Immiscible liquid–liquid systems, in: Handb. Ind. Mix. Sci. Pract., John Wiley and Sons: Hoboken, NJ, USA, 2004: pp. 639–753.

[108] K. Arai, M. Konno, Y. Matunaga, S. Saito, Effect of dispersed-phase viscosity on the maximum stable drop size for breakup in turbulent flow, J. Chem. Eng. JAPAN. (1977). doi:10.1252/jcej.10.325.

[109] A. Gupta, H.B. Eral, T.A. Hatton, P.S. Doyle, Controlling and predicting droplet size of nanoemulsions: scaling relations with experimental validation, Soft Matter. 12 (2016) 1452–1458. doi:10.1039/C5SM02051D.

[110] A. Gupta, V. Narsimhan, T.A. Hatton, P.S. Doyle, Kinetics of the Change in Droplet Size during Nanoemulsion Formation, Langmuir. 32 (2016) 11551–11559. doi:10.1021/acs.langmuir.6b01862.

[111] A. Einstein, Zur Theorie der Brownschen Bewegung, Ann. Phys. 324 (1906) 371–381. doi:10.1002/andp.19063240208.

[112] A. Einstein, Elementary consideration of the thermal conductivity of dielectric solids, Ann. Phys. 339 (1911) 591–592. doi:10.1002/andp.19113390313.

[113] G.I. Taylor, The viscosity of a fluid containing small drops of another fluid, Proc. R. Soc. A Math. Phys. Eng. Sci. 138 (1932) 41–48. doi:10.1098/rspa.1932.0169.

[114] I.M. Krieger, T.J. Dougherty, A mechanism for non-newtonian flow in suspensions of rigid spheres, Trans. Soc. Rheol. 3 (1959) 137–152. doi:10.1122/1.548848.

[115] Annual reports pursuant to Section 13 or 15(d) of the Securities Exchange Act of 1934, United States Secur. Exch. Comm. (n.d.).

[116] 21 CFR 314.94(a)(9)(iii), 2017.

[117] Gelatin Handbook, (2012). http://www.gelatin-gmia.com/.

[118] A.M. Sophocleous, K.-G.H.G. Desai, J.M. Mazzara, L. Tong, J.-X.X. Cheng, K.F. Olsen, S.P. Schwendeman, The nature of peptide interactions with acid end-group PLGAs and facile aqueous-based microencapsulation of therapeutic peptides, J. Control. Release. 172 (2013) 662–670. doi:10.1016/j.jconrel.2013.08.295.

[119] K. Hirota, A.C. Doty, R. Ackermann, J. Zhou, K.F. Olsen, M.R. Feng, Y. Wang, S. Choi, W. Qu, A.S. Schwendeman, S.P. Schwendeman, Characterizing release mechanisms of leuprolide acetate-loaded PLGA microspheres for IVIVC development I: In vitro evaluation, J Control Release. 244 (2016) 302–313. doi:10.1016/j.jconrel.2016.08.023.

[120] T. Rundlof, M. Mathiasson, S. Bekiroglu, B. Hakkarainen, T. Bowden, T. Arvidsson, Survey and qualification of internal standards for quantification by 1H NMR spectroscopy, J Pharm Biomed Anal. 52 (2010) 645–651. doi:10.1016/j.jpba.2010.02.007.

[121] Rolling-ball viscometer Lovis 2000 M/ME product website, (n.d.). http://www.anton-paar.com/us-en/products/details/rolling-ball-viscometer-lovis-2000-mme/.

[122] S. Zheng, P. Smith, L. Burton, M.L. Adams, Sensitive fluorescence-based method for the rapid determination of polysorbate-80 content in therapeutic monoclonal antibody products, Pharm Dev Technol. (2014) 1–5. doi:10.3109/10837450.2014.930490.

[123] B.A. Bailey, K.G.H. Desai, L.J. Ochyl, S.M. Ciotti, J.J. Moon, S.P. Schwendeman, Self-encapsulating Poly(lactic-co-glycolic acid) (PLGA) Microspheres for Intranasal Vaccine Delivery, Mol. Pharm. 14 (2017) 3228–3237. doi:10.1021/acs.molpharmaceut.7b00586.

[124] A.G. Ding, A. Shenderova, S.P. Schwendeman, Prediction of Microclimate pH in Poly(lactic- c o -glycolic Acid) Films, J. Am. Chem. Soc. 128 (2006) 5384–5390. doi:10.1021/ja055287k.

[125] J.A. Schrier, P.P. DeLuca, Recombinant Human Bone Morphogenetic Protein-2 Binding and Incorporation in PLGA Microsphere Delivery Systems, Pharm. Dev. Technol. 4 (1999) 611–621. doi:10.1081/PDT-100101400.

[126] R.M.C. Dawson, D.C. Elliott, W.H. Elliott, K.M. Jones, Data for Biochemical Research, Oxford University Press, New York, 1989.

[127] E.L.V. Harris, S. Angal, Protein Purification Methods: A Practical Approach (The Practical Approach Series), Oxford University Press, New York, 1990.

[128] Y. Ogawa, H. Okada, Y. Yamamoto, T. Shimamoto, In vivo release profiles of leuprolide acetate from microcapsules prepared with polylactic acids or copoly(lactic/glycolic) acids and in vivo degradation of these polymers, Chem. Pharm. Bull. (Tokyo). 36 (1988) 2576–2581. doi:10.1248/cpb.36.2576.

[129] J. Zhou, K. Hirota, R. Ackermann, J. Walker, Y. Wang, S. Choi, A. Schwendeman, S.P. Schwendeman, Reverse Engineering the 1-Month Lupron Depot®, AAPS J. 20 (2018) 105. doi:10.1208/s12248-018-0253-2.

[130] M. Yamamoto, S. Takada, Y. Ogawa, Method for producing microcapsule, US4954298, 1990. https://patents.google.com/patent/US4954298.

[131] P.A. Webb, Mercury Intrusion Porosimetry method, Norcross, Georgia, 2001. https://www.micromeritics.com/pdf/app_articles/mercury_paper.pdf (accessed October 16, 2018).

[132] B.H. Leuenberger, F. Hoffmann, Investigation of viscosity and gelation properties of different mammalian and fish gelatins, 1991. doi:10.1016/S0268-005X(09)80047-7.

[133] U. S. Pharmacopeia, USP General Chapters: <467> Residual Solvents, in: USP Gen. Chapters, 2016: pp. 1–9. https://hmc.usp.org/sites/default/files/documents/HMC/GCs-Pdfs/c467.pdf.

[134] W. Friess, M. Schlapp, Release mechanisms from gentamicin loaded poly(lactic-co-glycolic acid) (PLGA) microparticles, J. Pharm. Sci. 91 (2002) 845–855. doi:10.1002/jps.10012.

[135] Y. Xu, C.-S. Kim, D.M. Saylor, D. Koo, Review Article Polymer degradation and drug delivery in PLGA-based drug-polymer applications: A review of experiments and theories, J Biomed Mater Res Part B Appl Biomater. 105 (2016) 1692–1716. doi:10.1002/jbm.b.33648.

[136] F.G. Hutchinson, Continuous release pharmaceutical compositions, EP58481, 1986.

[137] Y.F. Maa, C.C. Hsu, Effect of primary emulsions on microsphere size and protein-loading in the double emulsion process, J. Microencapsul. (1997). doi:10.3109/02652049709015335.

[138] R. Alex, R. Bodmeier, Encapsulation of water-soluble drugs by a modified solvent evaporation Method. I. Effect of process and formulation variables on drug entrapment, J. Microencapsul. (1990). doi:10.3109/02652049009021845.

[139] V.G. LEVICH, Physicochemical hydrodynamics. Prentice-Hall, (1962). https://www.worldcat.org/title/physicochemical-hydrodynamics/oclc/1378432 (accessed March 3, 2019).

[140] K.K. Singh, S.M. Mahajani, K.T. Shenoy, S.K. Ghosh, Representative drop sizes and drop size distributions in A/O dispersions in continuous flow stirred tank, Hydrometallurgy. 90 (2008) 121–136. doi:10.1016/J.HYDROMET.2007.10.003.

[141] H. Salimi-Kenari, M. Imani, A. Nodehi, H. Abedini, An engineering approach to design of dextran microgels size fabricated by water/oil emulsification, J. Microencapsul. 33 (2016) 511–523. doi:10.1080/02652048.2016.1216188.

[142] RheoSense, Microvisc viscometer technology page, (n.d.). http://www.rheosense.com/products/viscometers/microvisc/how-it-works.

[143] P. Ghosh, Interfacial tension, NPTEL Chem. Eng. Interfacial Eng. Modul. 2 Lect. 1. (2012).

[144] W. Apostoluk, J. Drzymała, An improved estimation of water–organic liquid interfacial tension based on linear solvation energy relationship approach, J. Colloid Interface Sci. 262 (2003) 483–488. doi:10.1016/S0021-9797(03)00115-2.

[145] S. Saeidy, J. Keramat, A. Nasirpour, Microencapsulation of calcium using water-in-oil-in-water double emulsion method, J. Dispers. Sci. Technol. 35 (2014) 370–379. doi:10.1080/01932691.2013.788453.

[146] M. Yildirim, G. Sumnu, S. Sahin, The effects of emulsifier type, phase ratio, and homogenization methods on stability of the double emulsion, J. Dispers. Sci. Technol. 38 (2017) 807–814. doi:10.1080/01932691.2016.1201768.